

„Dunărea de Jos” University of Galați  
Doctoral School of Mechanical and Industrial Engineering



# **Ph.D. THESIS**

## **(ABSTRACT)**

### **UTILIZATION OF THE DIFFERENTIAL OPTICAL ABSORPTION SPECTROSCOPY IN QUANTIFICATION OF ATMOSPHERIC POLLUTION WITH NITROGEN DIOXIDE**

**Ph.D. Student:**  
ROȘU Adrian

**Scientific Coordinator:**  
Prof. Ph.D. Eng. GEORGESCU P. Lucian

**Series I4 Industrial Engineering Nr. 53**  
**GALAȚI**  
**2018**

„Dunărea de Jos” University of Galați  
Doctoral School of Mechanical and Industrial Engineering



# Ph.D. THESIS (ABSTRACT)

## UTILIZATION OF THE DIFFERENTIAL OPTICAL ABSORPTION SPECTROSCOPY IN QUANTIFICATION OF ATMOSPHERIC POLLUTION WITH NITROGEN DIOXIDE

**Ph.D. Student:** ROȘU Adrian

**Scientific Coordinator:** Prof. Ph.D. Eng. GEORGESCU Puiu Lucian -  
University „Dunarea de Jos” of Galați

**President:** Prof. Ph.D. Eng. RUSU Eugen-Victor-Cristian -  
University „Dunarea de Jos” of Galați

**Scientific Referent:** Conf. Ph.D. Eng. PREDA Ciprian Ion - West  
University of Timișoara  
Prof. Ph.D. Fiz. VOICULESCU Mirela - University  
„Dunarea de Jos” of Galați  
SR I Ph.D. Fiz. NICOLAE Doina - National Institute  
of Research and Development for Optoelectronic

Series I4 Industrial Engineering Nr. 53  
GALAȚI  
2018

The series of PhD thesis that were publicly presented in DJUG starting with October 1st, 2013:

The Domain of STUDIES in ENGINEERING (DSE)

Series I 1: **Biotechnologies**

Series I 2: **Computers and information technology**

Series I 3: **Electrical engineering**

Series I 4: **Industrial engineering**

Series I 5: **Material engineering**

Series I 6: **Mechanical engineering**

Series I 7: **Food products engineering**

Series I 8: **System engineering**

The Domain of STUDIES in ECONOMICS

Series E 1: **Economics**

Series E 2: **Management**

The Domain of HMAN SCIENCES

Series U 1: **Philology – English**

Series U 2: **Philology – Romanian**

Series U 3: **History**

## ACKNOWLEDGEMENT

With the completion of the studies and research presented in this paper, I wish to express sincere thanks to all those who have contributed to the elaboration of this thesis through advice, an idea, a discussion of encouragement or guidance in the direction of the pursued research.

First of all, I would like to extend my thanks to Prof. Ph.D. Eng. Lucian P. Georgescu, under whose guidance this thesis was completed. Sincere appreciation for the scientific support, for the involvement offered during the master and bachelor studies which formed me personally and professionally. At the same time, I thank Prof. Ph.D. Eng. Lucian P. Georgescu for instilling the desire to know and find more about the field of exact sciences contrary to the artistic inclinations developed during high school.

I would like to express my special thanks to my colleagues Ph.D. Eng Constantin Daniel-Eduard (UGAL) and Ph.D. Alexis Merlaud (BIRA-IASB) for their courtesy through scientific advice and discussions to acquire and develop knowledge in the field of differential optical absorption spectroscopy (DOAS). I also thank them for their support and opportunity to participate in numerous research projects, conferences, workshops and studies in this field in the country and abroad.

Sincere thanks, I would like to address Prof. Ph.D. Fiz. Mirela Voiculescu for her kindness and involvement with helping me to acquire the knowledge necessary to approach scientific topics.

Thanks to the entire group of researchers at BIRA-IASB, especially Dr. Michel Van Roozandael, Dr. François Hendrick, Caroline Fayt, Dr. Frederik Tack and Gaia Pinardi, for help in acquiring knowledge in DOAS technique I also want to thank for their courtesy, advice and scientific support provided during conferences, measurement campaigns and during the internship at BIRA - IASB.

I would like to especially thank my colleague Eng. Arseni Maxim for the advice and moral and scientific support offered for the research carried out during the last three years of doctoral studies. I also thank my colleague Lect. Ph.D. Cătălina Țopa and lect. Ph.D. Corina Bocăneală for the ideas and moral support offered.

In this way, I would like to thank the whole team of teachers from the Faculty of Science and Environment of Galati under the guidance of whom I formed over the last years of studies in order to pursue this path of exact sciences. Among them, I would like to remember especially: Prof. Ph.D. Chem. Cătălina Iticescu, P.C. Ph.D. Eng. Dumitru Dima, Prof. Ph.D. habil. Phys. Gabriel Murariu, Prof. Ph.D. Chem. Rodica Dinică, Assoc. Prof. Ph.D. Bianca Furdui, lect. Ph.D. Chem. Mihaela Timofti.

Finally, I want to thank my family and friends who showed moral and emotional support throughout the period of doctoral studies, a support that has had a very important impact in the elaboration of this doctoral thesis.

The research and experiments included in this thesis have been funded through the project "Determination of Spatial Distribution and Atmospheric composition using DOAS technology on mobile platforms" (DEDICAT-DOAS) PN-II-RU-TE-2014-4-2584 and co-financed by the Government of Romania and "Dunarea de Jos" University of Galati.

## **RESEARCH RESULTS\***

### **PAPERS PUBLISHED IN ISI WEB OF KNOWLEDGE JOURNALS**

- L1.** Roșu, A., D. E. Constantin, L. Georgescu. "Air pollution level in Europe caused by energy consumption and transportation" Journal of Environmental Protection and Ecology no 17.1, pg 1-8, 2016, (FI=0.774).
- L2.** Constantin, Daniel-Eduard, Alexis Merlaud, Mirela Voiculescu, Michel Van Roozendaal, Maxim Arseni, **Adrian Roșu**, Lucian Georgescu. "NO<sub>2</sub> AND SO<sub>2</sub> observations in SouthEast Europe using mobile DOAS observations" Carpathian Journal of Earth and Environmental Sciences 12, no. 2, 323-328, 2017, (FI=0.886)
- L3.** M. Arseni, **A. Roșu**, D.E. Constantin, C. Bocaneală, L. P. Georgescu, „Flood hazard monitoring using the geographic information systems and remotely sensed data”, Carpathian Journal of Earth and Environmental Sciences 12, no. 2, 329-334, 2017, (FI=0.886)

### **ARTICLES PUBLISHED IN ISI INDEXED JOURNALS (PROCEEDINGS ISI WEB OF KNOWLEDGE**

- P1.** Lucian Dimitrievici, Daniel-Eduard Constantin, **Adrian Rosu**, Luminita Moraru, „A perspective view of O<sub>3</sub> and NO<sub>2</sub> evolution above several important cities during 2005-2016 using UV-Vis observations from space”, RAD Conference Proceedings, vol. 2, pp. 191–194, 2017.

### **PUBLISHED PAPERS IN BDI/B JOURNALS**

- B1.** Roșu, A., Roșu, B., Arseni, M., Constantin, D. E., Voiculescu, M., Georgescu, L. P., Van Roozendaal, M., „Tropospheric nitrogen dioxide measurements in South-East of Romania using zenith-sky mobile DOAS observations”, TEHNOMUS - New Technologies and Products in Machine Manufacturing Technologies, No. 24, pp 189-194, 2017.
- B2.** **A. Roșu**, D.E. Constantin, C. Bocaneala, M. Arseni, L. P. Georgescu, „Corelation between O<sub>3</sub>, NO<sub>2</sub> and UV index in Romania” Annals Of “Dunarea De Jos” University of Galati Mathematics, Physics, Theoretical Mechanics Fascicle II, Year VIII (XXXIX), No. 1, pp.61-65, 2016.
- B3.** **A. Roșu**, D.E. Constantin, C. Bocaneala, M. Arseni, L. P. Georgescu „Evolution of NO<sub>2</sub> in five major cities in Europe using remote satellite observations and in situ measurements” Annals Of “Dunarea De Jos” University of Galati Mathematics, Physics, Theoretical Mechanics Fascicle II, Year VIII (XXXIX), No. 1, pp.66-70, 2016.
- B4.** **Adrian Rosu**, Daniel-Eduard Constantin, Corina Bocaneala, Mirela Voiculescu, and Lucian Puiu Georgescu, ”NO<sub>2</sub> evolution at global level using the space instruments SCIAMACHY, OMI and GOME-2”, Geophysical Research Abstracts Vol. 18, EGU2016-pp.8281, 2016.
- B5.** **Roșu, A.**, Roșu, B., Constantin, D. E., Bocăneală, C., Arseni, M., Georgescu, L. P., ”Overview of NO<sub>2</sub> ambient concentrations trends in Europe”, Annals of the University Dunarea de Jos of Galati: Fascicle II, Mathematics, Physics, Theoretical Mechanics, No.2, pp 248-253, 2016.
- B6.** M. Arseni, **A. Roșu**, D.E. Constantin, C. Bocaneala and L. P. Georgescu, „Photogrammetric Applications using UAV Systems”, Annals Of “Dunarea De Jos” University of Galati Mathematics, Physics, Theoretical Mechanics Fascicle II, Year VIII (XXXIX) No. 1, pp.37-43, 2016.

- B7.** Maxim Arseni, **Adrian Roșu**, Lucian Puiu Georgescu, Gabriel Murariu „*Single beam acoustic depth measurement techniques and bathymetric mapping for Catusa Lake from Galati*” Annals Of “Dunarea De Jos” University of Galati Mathematics, Physics, Theoretical Mechanics Fascicle II, Year VIII (XXXIX), No. 2, pp.281-285, 2016.
- B8.** **Roșu, A.**, Voiculescu, M., Georgescu, L. P., Constantin, D. E., „*Assessment of emissions from vehicles based on IOA analisys*”, Annals of the University Dunarea de Jos of Galati: Fascicle II, Mathematics, Physics, Theoretical Mechanics, Vol. 38 Issue 2, p177-182, 2015,
- B9.** **Adrian Roșu**, Mirela Voiculescu, Lucian Puiu Georgescu, Daniel Eduard Constantin, „*Influence of meteorological parameters on energy efficiency of buildings*”, TEHNOMUS - New Technologies and Products in Machine Manufacturing Technologies No 22, pg 291-296, 2015.

## **PRESENTED PAPERS AT CONFERENCES**

### **ORAL PRESENTATIONS**

- PO1.** **Roșu, A.**, Roșu, B., Arseni, M., Constantin, D. E., Voiculescu, M., Georgescu, L. P., Van Roozendaal, M.: „*Tropospheric nitrogen dioxide measurements in South-East of Romania using zenith-sky mobile DOAS observations*”, prezentare orală în cadrul conferinței internaționale The 19th International Conference New Technologies and Products in Machine Manufacturing Technologies, Mai 2017.
- PO2.** **Rosu A.**: „*Măsurători ale gazelor din atmosfera utilizând tehnica DOAS*”, Natural versus anthropogenic causes of climate variability and feedback from bio-geo-chemical processes – prezentare orală în cadrul conferinței naționale NatClimVAR, Bucuresti, Romania, 18 Oct. 2016.
- PO3.** **Adrian Roșu**, Daniel-Eduard Constantin, Mirela Voiculescu, Corina Bocăneală, Lucian Georgescu, „*Health and Quality of Life in Europe Related to NO<sub>2</sub> pollution from the perspective of remote satellite-based and in situ observations*”, prezentare orală în cadrul conferinței internaționale 11th International Conference ELSEDDIMA Mai 27, 2016.
- PO4.** D.E. Constantin, A. Merlaud, M. Voiculescu, M. van Roozendaal, M. Arseni, **A. Roșu** and L. Georgescu, „*NO<sub>2</sub> and SO<sub>2</sub> observations in South-East Europe using mobile DOAS measurements*” prezentare orală în cadrul conferinței internaționale 11th International Conference ELSEDDIMA Mai 26, 2016.
- PO5.** **Adrian Roșu**, Mirela Voiculescu, Lucian Puiu Georgescu, Daniel Eduard Constantin, „*Influence of meteorological parameters on energy efficiency of buildings*”, prezentare orală în cadrul conferinței internaționale The 17th International Conference New Technologies and Products in Machine Manufacturing Technologies, Mai 2015.

### **POSTER PRESENTATIONS**

- PP1.** Merlaud, A., Tack, F., Van Roozendaal, M., Constantin, D., **Rosu, A.**, Riffel, K., Donner, S., Wagner, T., Schreier, S., Richter, A., Eskes, H., Douros, J.: „*Synergetic use of the Mobile-DOAS measurements during Cindi-2*”, AS3.14/GI2.14, EGU2018-18038, 2018
- PP2.** **Adrian Roșu**, Bogdan Roșu, Maxim Arseni, Corina Bocăneală, Daniel-Eduard Constantin, Mirela Voiculescu, Lucian Puiu Georgescu, „*Determination of Nitrogen Dioxide using a new DOAS Instrument with two Dimensional Axes*” prezentare în format poster în cadrul conferinței naționale 5th Edition of CSSD-UDJG, Galați, 8-9 June 2017.

- PP3.** **Adrian Roșu**, Bogdan Roșu, Daniel Eduard Constantin, Maxim Arseni, Corina Bocaneală, and Lucian Puiu Georgescu, " *Estimation of NO<sub>2</sub> concentrations derived from DOAS mobile measurement in South-East of Romania*", prezentare tip poster în cadrul conferinței internaționale INTERNATIONAL U.A.B. – B.EN.A. Conference Environmental Engineering and Sustainable Development, Alba Iulia, Romania, May 26, 2017.
- PP4.** **Adrian Roșu**, Daniel-Eduard Constantin, Corina Bocaneala, Mirela Voiculescu, and Lucian Puiu Georgescu, "NO<sub>2</sub> evolution at global level using the space instruments SCIAMACHY, OMI and GOME-2", prezentare tip poster în cadrul conferinței internaționale EGU2016, 18 Apr. 2016.
- PP5.** **A.Roșu**, D.E. Constantin, C. Bocaneala, M. Arseni and L. P. Georgescu: „*Evolution of NO<sub>2</sub> in five major cities in Europe using remote satellite observations and in situ measurements*” prezentare tip poster în cadrul conferinței internaționale Scientific Conference of Doctoral Schools of „Dunarea de Jos” University, Galati (CSSD-UDJG 2016), 3 June, 2016.
- PP6.** **A. Roșu**, D.E. Constantin, C. Bocaneala, M. Arseni and L. P. Georgescu, „*Corelation between O<sub>3</sub>, NO<sub>2</sub> and UV index in Romania*”, prezentare tip poster în cadrul conferinței internaționale Scientific Conference of Doctoral Schools of „Dunarea de Jos” University, Galati (CSSD-UDJG 2016), 3 June, 2016.
- PP7.** Arseni, M., **Roșu, A.**, Nicolae A. F. , Georgescu L. P., Constantin, D. E.: Comparison of models and volumetric determination for Catusa lake, Galati. THE 19th INTERNATIONAL CONFERENCE “NEW TECHNOLOGIES AND PRODUCTS IN MACHINE MANUFACTURING TECHNOLOGIES” TEHNOMUS XIX, Suceava – ROMANIA, May 12-13, 2017
- PP8.** M. Arseni, **A. Roșu**, D.E. Constantin, C.Bocaneală and L. P. Georgescu, „*Flood hazard monitoring using the Geographic Information Systems and remotly sensed data*” prezentare tip poster în cadrul conferinței internaționale 11th International Conference ELSEDIMA, May 27, 2016.
- PP9.** Arseni Maxim, **Roșu Adrian**, Georgescu Lucian, Murariu Gabriel, „*Assessing flooded surface area Using Landsat satellite data on Siret River downstream of lower Danube*”. Conferința International U.A.B. – B.EN.A. Conference Environmental Engineering And Sustainable Development Alba Iulia, Romania May 25 - 27th, 2017.
- PP10.** Maxim Arseni, **Adrian Roșu**, Lucian Puiu Georgescu, Gabriel Murariu „*Single beam acoustic depth measurement techniques and bathymetric mapping for Catusa Lake from Galati*” prezentare tip poster în cadrul conferinței internaționale Scientific Conference of Doctoral Schools of „Dunarea de Jos” University, Galati (CSSD-UDJG 2016), 3 June, 2016.
- PP11.** M. Arseni, **A. Roșu**, D.E. Constantin, C. Bocaneala and L. P. Georgescu, „*Photogrammetric Aplications using UAV Systems*”, prezentare tip poster în cadrul conferinței internaționale Scientific Conference of Doctoral Schools of „Dunarea de Jos” University, Galati (CSSD-UDJG 2016), 3 June, 2016.

#### **PARTICIPATION IN NATIONAL RESEARCH PROJECTS**

- PN 1.** Proiectul „DEterminarea Distribuției spațiale a Compoziției ATmosferice folosind tehnica DOAS pe platforme mobile” (DEDICAT-DOAS), PN-II-RU-TE-2014-4-2584, coordonator: Universitatea Dunărea de Jos Galați, angajat în calitate de webmaster și expert domeniul tehnicii DOAS domeniul tehnicii DOAS domeniul tehnicii DOAS.
- PN 2.** Proiectul Mobilitate Cercetători (MC 1001) 4 – 18 Decembrie 2017, Finanțarea stagiului la institutul BIRA-IASB, finanțat de Guvernul României, partener Dunarea de Jos, subsemnatul angajat în calitate de director de proiect.

### **PARTICIPATION IN INTERNATIONAL RESEARCH PROJECTS**

- PI 1.** Proiectul „The Airborne Romanian Measurements of Aerosols and Trace gases” (AROMAT-2), ESA Contract No.4000113511/NL/FF/gp, partener Universitatea Dunărea de Jos Galați, subsemnatul angajat în calitate de cercetător în domeniul tehnicii DOAS.
- PI 2.** Proiectul „Cabauw Intercomparison of Nitrogen Dioxide Measuring Instruments” (CINDI-2), contractul ESA 4000118533/16/I-Sbo, partener Universitatea Dunărea de Jos Galați, subsemnatul angajat în calitate de cercetător în domeniul tehnicii DOAS.
- PI 3.** Proiectul Technical Assistance For A Romanian Atmospheric Observation System (RAMOS) proiect finanțat de ESA-ESTEC prin contractul 4000118115/16/NL/FF/GP/2016, coordonator Institutul National de Cercetare Dezvoltare pentru Optoelectronica (INOE), partener Universitatea Dunărea de Jos Galați, subsemnatul angajat în calitate de cercetător în domeniul tehnicii DOAS.
- PI 4.** Proiectul Atmospheric studies in support of ESA's sentinel 4 and 5 products (ASSES), finanțat de ESA (505/2017) , coordonator Institutul National de Cercetare Dezvoltare Aerospaciala "Elie Carafoli" - INCAS (INCAS), partener Universitatea Dunărea de Jos Galați, subsemnatul angajat în calitate de webmaster și cercetător în domeniul tehnicii DOAS.

***\* The publications and research activity presented above will be quoted in the thesis with the indicative and related number.***



## CONTENTS

<b>ACKNOWLEDGEMENT</b> .....	<b>iv</b>
<b>CONTENTS</b> .....	<b>ix</b>
<b>Introduction</b> .....	<b>xi</b>
<b>CHAPTER 1 Earth atmosphere, NO<sub>2</sub> pollution, atmospheric composition measurement techniques</b> .....	<b>1 -</b>
1.1 Characterization and dynamics of the atmosphere.....	1 -
1.2 Nitrogen compounds.....	2 -
1.3 Legislation in force to set the limit values for NO <sub>2</sub> in ambient air.....	2 -
1.4 Current state of knowledge in the field of techniques for determining atmospheric composition.....	3 -
<b>CHAPTER 2 DOAS technique and instruments used in remote sensing of NO<sub>2</sub></b> .....	<b>5 -</b>
2.1 Interaction of solar radiation with the atmosphere.....	5 -
2.2 Principle of optical absorption spectroscopy. The Lambert - Beer Law.....	5 -
2.3 Principle of DOAS technique.....	6 -
2.4 DOAS applications.....	7 -
2.5 Radiation transfer model used.....	9 -
2.6 Composition of the spectrophotometer and external optical system used...-	9 -
2.7 The software used in spectral analysis.....	11 -
<b>CHAPTER 3 Research on the level of NO<sub>2</sub> pollution in Europe</b> .....	<b>13 -</b>
3.1 Research on the evolution of NO <sub>2</sub> concentrations in Europe.....	13 -
3.1.1 Method and data used.....	13 -
3.1.2 Results and discussions.....	14 -
3.1.3 Conclusions.....	16 -
<b>CHAPTER 4 Comparison of DOAS measurements at ground level with satellite observations used for NO<sub>2</sub> determination</b> .....	<b>17 -</b>
4.1 State of the art of satellite observations for NO <sub>2</sub> determination.....	17 -
4.2 Observing the evolution of tropospheric NO <sub>2</sub> content in five major European cities using DOAS satellite instruments.....	18 -
4.2.1 Methods and data used.....	18 -
4.2.2 Results and discussions.....	19 -
4.2.3 Conclusions.....	21 -
4.3 Observations of NO <sub>2</sub> in the South Eastern Region of Romania using the DOAS mobile technique in zenith geometry.....	21 -
4.3.1 Method and data used.....	21 -
4.3.2 Results and discussions.....	24 -
4.3.3 Conclusions.....	27 -
4.4 Determination of the tropospheric NO <sub>2</sub> densities using DOAS technique on board of a vehicle in Eastern Europe.....	27 -
4.4.1 Methodology.....	27 -

4.4.2	Comparison of ZSL - DOAS mobile observations with satellite observations of the sensor OMI in Eastern Europe.....	- 29 -
4.4.3	Conclusions.....	- 31 -
4.5	ZSL - DOAS observations made on board a vehicle for the determination of NO <sub>2</sub> tropospheric VCD in Europe .....	- 31 -
4.5.1	Comparison with observations of the OMI satellite instrument.....	- 33 -
4.5.2	Conclusions.....	- 39 -
4.6	DOAS international measurement campaigns.....	- 40 -
4.6.1	AROMAT - 2 measurement campaign.....	- 40 -
4.6.2	CINDI 2 measurement campaign.....	- 43 -
4.6.3	Conclusions.....	- 45 -
<b>CHAPTER 5 Development and use of an innovative MAX - DOAS „UGAL 2D – DOAS” system in NO<sub>2</sub> detection .....</b>		<b>- 46 -</b>
5.1	Characteristics of the UGAL 2D - DOAS instrument.....	- 46 -
5.2	Experimental methodology used for NO <sub>2</sub> detection .....	- 47 -
5.3	Experimental results and discussions.....	- 48 -
5.4	Comparison between MAX - DOAS observations and ZSL - DOAS mobile observations.....	- 49 -
5.5	Conclusions.....	- 51 -
<b>CHAPTER 6 Personal contributions and research directions .....</b>		<b>- 53 -</b>
<b>References .....</b>		<b>- 55 -</b>

Keywords:

DOAS, ZSL-DOAS, MAX - DOAS, spectral analysis, QDOAS, AMF,  $VCD_{\text{tropo}}$   $\text{NO}_2$ , ZSL-DOAS mobile observations, satellite observations, OMI,  $\text{NO}_2$  pollution quantification, prediction maps of  $\text{NO}_2$  pollution dispersion, interpolation methods, GIS, identifying sources of  $\text{NO}_2$  pollution, validating satellite observations.

## Introduction

Terrestrial atmosphere is the planetary layer with a very important role in maintaining the life and balance of the geographic envelope. The atmospheric shell of the planet is composed of  $\text{N}_2$  (78%),  $\text{O}_2$  (21%), Ar (1%), and other gases that represent less than 0.1 of its composition at a lower concentration, called minor atmospheric constituents. The abundance of these gases is controlled by the interactions and processes between the biosphere, the hydrosphere and the geosphere. Although these minor constituents have a small proportion of the atmosphere, they play an important role in the radiation equilibrium and the chemical properties of the atmosphere. Among these minor constituents of the atmosphere we can list:  $\text{O}_3$ ,  $\text{NO}_2$ ,  $\text{CO}_2$ ,  $\text{SO}_2$ ,  $\text{N}_2\text{O}$ ,  $\text{H}_2\text{O}$ ,  $\text{CH}_4$ , BrO etc.

The notion of "atmospheric pollution" is nowadays a very common term, being circulated throughout the globe. According to the Romanian legislation (Law No 278/2013) pollution is defined as: "Direct or indirect introduction of substances, vibrations, heat or noise into the air, water or soil as a result of human activity, liable to cause harm to human health or the quality of the environment, cause deterioration of material goods, or impair or impede the recreational use of the environment and / or other legitimate uses of the environment ": It is known today that this concept includes both pollution from anthropogenic and natural sources . Natural sources are those such as forest fires, volcanic eruptions, pollen dispersion, wind erosion, VOC evaporation, etc., and artificial ones are associated with anthropogenic activity and industrial revolution, considered to be the main causes of atmospheric pollution.

The study of air pollution has become increasingly important due to phenomena that are produced directly by concentration of pollutant gases in certain regions of the globe or indirectly by phenomena such as acid rain, photochemical smog, thinning of ozone layer, etc.

Currently, the spatial distribution of these pollutants is monitored by various methods and techniques. These methods of measurement include in situ methods for local monitoring and quantification of variations in gas concentrations, or are used as remote monitoring networks that provide a quasi-continuous image of spatial variation of pollutant gases on extended surfaces. The magnitude and complexity of pollution phenomena today require relatively inexpensive and non-invasive studies that can lead to remote determinations, determinations that show accuracy in quantification of pollution sources on extended surfaces and on relatively small surfaces.

In 1924, Gordon Dobson performed the first observations of  $\text{O}_3$  in the free troposphere using the DOAS (Dobson and Harrison, 1926) technique.

Passive DOAS involves the use of solar radiation as a vector for collecting information about the composition of the atmosphere. This remote sensing method is current and involves relatively small costs for the determination of gaseous pollutants in the atmosphere. This technique allows to determine the number of molecules of integrated gaseous pollutants on vertical columns in the lower atmospheric layers. The method of determination has been used since 1990 on board satellites, so it is possible, through global coverage, to determine the spatio-temporal distribution of atmospheric pollutants.

The miniaturization and the development of the spectrometers used in the observations made with DOAS technique made possible mounting these instruments on board a number of mobile platforms such as: motor vehicles, bicycles, airplanes, motorcycles, UAVs, boats, satellites, etc. Each of the listed platforms has advantages and disadvantages in determining air pollution. Thus, satellite instruments are today able to provide global daily coverage at a spatial resolution of tens of square kilometers (van Geffen et al., 2017), making it unlikely to detect small sources (road traffic, small industrial platforms, small towns, etc.). Other mobile platforms can determine the distribution of pollution at local and even street level, but the limitations of these platforms are related to their track (bicycle, vehicle) or overflight tracks (airplane, motodeltaplan, UAV).

The current development of the DOAS technique involves the measurement of tropospheric profiles of pollutant gases by determinations taken at different angles of observation from the horizontal. This new approach of the technique, called MAX-DOAS (Multi AXis Differential Optical Absorption Spectroscopy), can be used to estimate the concentration of pollutants at different tropospheric altitudes by coupling with radiation transfer simulation models.

The thesis is structured in 6 chapters:

Chapter 1 presents the current state of knowledge in the field of DOAS techniques. This chapter also includes information on the characteristics and dynamics of the atmosphere in the transport of minor atmospheric constituents.

Chapter 2 describes how solar radiation interacts with the atmosphere. At the same time, the principles of the DOAS technique and the instruments used are highlighted.

Chapter 3 presents two studies for assessing the current NO<sub>2</sub> pollution level in Europe in order to prepare for future DOAS observation campaigns.

Chapter 4 focuses on a series of studies showing correlations and similarities between satellite DOAS observations, measurements of European air quality monitoring networks, mobile ground DOAS observations made from a car on NO<sub>2</sub> pollution at local, regional and European level. Also here are presented the results of DOAS measurement campaigns carried out in Romania (AROMAT - 2) and the Netherlands (CINDI - 2) in 2015 and 2016 respectively. These campaigns show how atmospheric pollution with NO<sub>2</sub> is synergistically and complementarily determined through mobile DOAS observations made from ground and air.

Chapter 5 describes the development of a new MAX - DOAS instrument used in making local MAX - DOAS observations. Validation of the scanning sequence of the instrument was determined by synergistic comparisons with ZSL - DOAS mobile observations.

Chapter 6 sets out and underline the conclusions of the researches conducted as well as the perspectives of future studies in the field of differential optical absorption spectroscopy.

The overall research direction presented in the Ph.D. thesis was focused on the determination of the nitrogen dioxide content in the troposphere at local, regional and European level by means of DOAS applications onboard ground mobile platforms, airborne and space platforms. The main subject of the research was the determination of correlations and similarities in the determination of the tropospheric NO<sub>2</sub> columns between the observations made from ground with the ones made from space which subsequently led to the successful approach of the development of new tools and algorithms for determining the tropospheric content of NO<sub>2</sub>. The thesis was based on topical references, considering that the results of the researches are of local, national and international interest, bringing a scientific contribution to the determination of atmospheric pollution with nitrogen dioxide by using a wide range of applications of the DOAS technique.

## CHAPTER 1

### Earth atmosphere, NO<sub>2</sub> pollution, atmospheric composition measurement techniques

#### 1.1 Characterization and dynamics of the atmosphere

Air dynamics interferes with atmospheric energy and substance exchange processes, so atmospheric circulation is an important factor in global energy and transport balance (IPCC, 2007).

Earth's atmosphere is the gaseous shell that surrounds the planet, which allows the transfer of energy between the sun and the planet from one region of the globe to another. (Gugiuman, 1975).

The stratification of the atmospheric coating is given by temperature and pressure variation according to altitude. The atmosphere is composed of five layers: the troposphere, the stratosphere, the mesosphere, the thermosphere (also called the ionosphere due to the phenomena of the boreal auras), the exosphere. The stratification of the atmosphere according to the vertical variation of temperature and pressure can be seen in Figure 1.1.

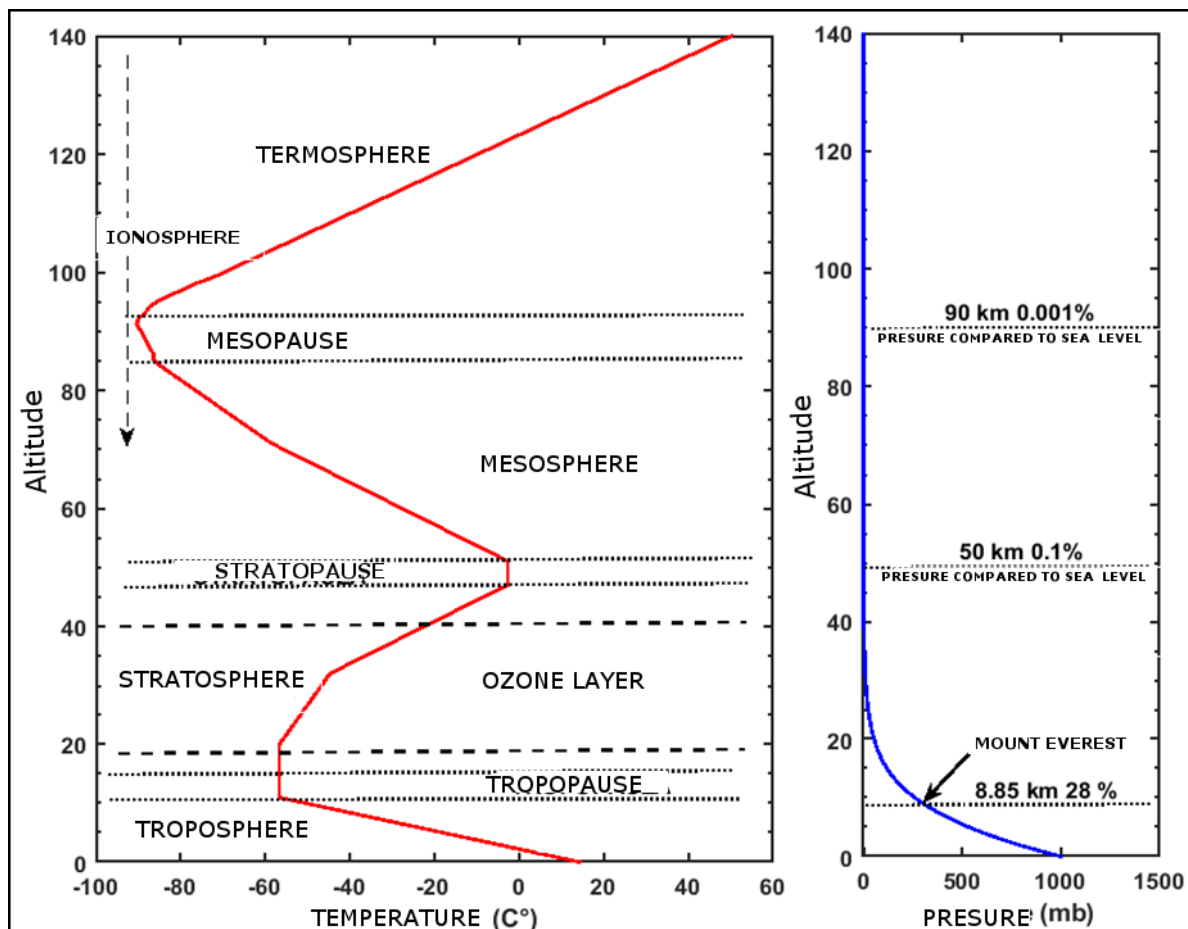


Figure 1.1: Atmospheric layers, vertical variation of temperature and pressure (adapted from Brasseur and Solomon, 1986)



1997). The European Union (EU) uses the same values proposed by WHO as limits for NO<sub>2</sub> concentration. The legislation for NO<sub>2</sub> pollution entered into force through Directive 2008/50/EC in 2010 (EU, 2008). This directive admits a number of 18 exceedances per year of the limit value per hour. Romania as an EU Member State is subject to these regulations by implementing the same values through Legea 104/2011 on ambient air quality.

In the US, the threshold limit values have been set by the National Environmental Standards (NAAQS) by the Environmental Protection Agency (EPA) of 100 µg/m<sup>3</sup> for the maximum permissible hourly and 53 µg/m<sup>3</sup> for the annual mean value ([https : //www3.epa.gov/airnow/no2.pdf](https://www3.epa.gov/airnow/no2.pdf)).

#### **1.4 Current state of knowledge in the field of techniques for determining atmospheric composition**

Knowledge of the atmosphere consists of understanding the physical and chemical processes taking place at its level. These phenomena are understood throughout studies and intense measurements of some parameters relevant to them.

When we talk about pollution, we mean the process by which products or gaseous pollutants with oxidising properties are expelled to the atmosphere as a result of an industrial process stream. These gaseous pollutants called the "minor constituents" of the atmosphere have a lifetime of minutes (Platt and Stutz, 2008). The accurate determination of the spatial distribution of the concentration of minor constituents of the atmosphere using analytical analysis methods is an objective necessity due to the need for faster results and better resolution.

At present there is a wide variety of techniques developed and specialized in the observation of atmospheric minor constituents, some examples of observation techniques being presented below:

- Gas Chromatography (GC) - a universal measurement method used in-situ or in laboratory;
- Optical spectroscopy - universal analysis method used in-situ or at distance based on using light radiation;
- Mass Spectrometry (MS) - a universal method used in-situ or in laboratory using electron or atom guns;
- Chemiluminescence - used in observing the profiles of O<sub>3</sub>, NO, NO<sub>2</sub> (Sluis et al., 2010).

The optical spectroscopy technique has a number of advantages in making atmospheric observations, ie it has a high sensitivity, is selective, universal, can be used remotely and the results can be rendered in resolutions up to 0.7 nm (Platt and Stutz, 2008) .

Absorption spectroscopy plays a prominent role in discovering the physical and chemical properties of the atmosphere. The absorption spectrometry technique can be graded according to the band of wavelengths at which observations are made.

The main remote applications of UV / Vis spectrometry are:

- Variable laser intensity diode spectroscopy (TDLS);
- Photo Acoustic Spectroscopy (PAS);
- Light Detection And Ranging (LIDAR);
- Differential Absorption by LIDAR (DIAL);
- Optical Differential Absorption Spectroscopy (DOAS).

UTILIZATION OF THE DIFFERENTIAL OPTICAL ABSORPTION SPECTROSCOPY IN QUANTIFICATION OF  
ATMOSPHERIC POLLUTION WITH NITROGEN DIOXIDE

---

DOAS (Optical Differential Absorption Spectroscopy) technique is used to rapidly demonstrate the spatial distribution of gaseous pollutants in lower atmosphere layers. It is a rapid method because it uses light radiation as a channel for collecting information about the abundance of atmospheric constituents: O<sub>3</sub>, NO<sub>2</sub>, BrO, OCIO and O<sub>4</sub> (Solomon et al., 1987, Johnston et al., 1989, Van Roozendaal et al. , 1994, Richter et al., 1999, Wittrock, 2000). DOAS method is generally used in passive applications (using natural sources: Sun, Moon and Stars) and active (artificial sources: lamps).

The historical evolution of the DOAS technique is presented in Table 1.1 where is clasified acording to the polutant gase and the geometry of observation. The first observations made in zenith geometry have demonstrated the presence of pollutant gases in the stratosphere and troposphere. Measurement in "Off Axis" geometry (observation made at angles other than zenith) by Sanders (Sanders et al., 1993). The research of Sanders represents the first step in the development and use of a new technique used today called MAX - DOAS (Multi AXis Differential Optical Absorption Spectroscopy). This technique can be used in observation at different angles of observation, as well as in sun tracking (watching the sun on the sky vault).

The development of the DOAS technique made possible performing measurements on various mobile platforms (satellites, cars, UAVs, ships, airplanes, etc.), which offers the possibility of measurements of atmospheric pollution on more extensive surfaces in different atmospheric layers.

**Table 1.1:** History of the DOAS technique. Applications of DOAS for troposphere and stratosphere using different platforms and observation angles. Range of atmospheric pollutants detected with DOAS tehniqe (adaptation after Platt and Stutz, 2008)

Applied tehniqe	Analyzed polutant species	Number of observation axes	References
COSPEC	NO <sub>2</sub> , SO <sub>2</sub> , I <sub>2</sub> - Stratosphere	1, (S)	Millan et al. (1969), Davies (1970), Stoiber și Jepsen(1973), Hoff (1992)
Zenith DOAS (ZSL - DOAS) using scattered sunlight	NO <sub>2</sub> , O <sub>3</sub> , OCIO, BrO, IO Stratosphere and Troposphere	1	Noxon (1975), Noxon et al. (1979), Harrison (1979), McKenzie și Johnston (1982), Solomon et al. (1987a, b, 1988, 1989, 1993), McKenzie et al. (1991), Fiedler et al. (1993); Pommereau și Piquard (1994); Eisinger et al. (1997); Wittrock et al. (2000)
Off-Axis DOAS and Zenith DOAS	Stratosphere OCIO	2	Sanders et al. (1993)
Off-Axis DOAS	Stratosphere BrO	1	Arpaç et al. (1994)
Zenith DOAS	Troposphere IO, BrO	1	Kreher et al. (1997); Friess et al. (2001, 2004), Wittrock et al. (2000)
Off axis DOAS	Troposphere BrO	1	Miller et al. (1997)
Off-Axis DOAS at sunset direct DOAS moonlight	Profiles NO <sub>3</sub>	2, S	Weaver et al. (1996), Solomon (1993), Smith et al. (1990, 1993)
Off Axis DOAS at sunset	Tropospheric profiles NO <sub>3</sub>	1	Kaiser (1997), von Friedeburg et al. (2002)
DOAS airborne	Stratosphere NO <sub>2</sub>	1	Wahner et al. (1989)
DOAS airbourne	Troposphere BrO	2	McElroy et al. (1999)
DOAS airbourne, Off Axis, Zenith DOAS	Ground based Stratospheric measurements	3	Petritoli et al. (2002)
MAX-DOAS	Profiles of minor atmospheric constituents	8+, M	Wagner et al. (2002), Wang et al. (2003), Wagner et al. (2010, 2012), Heue et al. (2003)
MAX-DOAS	Tropospheric profiles of BrO	4, S	Hönninger și Platt (2002), Hönninger et al. (2004a,b,c)
MAX-DOAS	Profiles of minor atmospheric constituents	2-4, M	Löwe et al. (2002), Oetjen (2002), Heckel (2003), Wittrock et al. (2003, 2004)
MAX-DOAS	NO <sub>2</sub> pollution plume	8, M	von Friedeburg (2003)
MAX-DOAS	BrO in boundary layer	6, S/M	Leser et al. (2001, 2003)
MAX-DOAS	Vulcanic emission fluxes of BrO and SO <sub>2</sub>	10, S	Bobrowski et al. (2003)
MAX-DOAS	Emissions of BrO from salted lakes	4, S	Hönninger et al. (2004b)



## CHAPTER 2

# DOAS technique and instruments used in remote sensing of NO<sub>2</sub>

### 2.1 Interaction of solar radiation with the atmosphere

There is a wide range of processes and phenomena that underlie the interactions between electromagnetic radiation and earth's atmosphere, including: absorption, elastic diffusion, inelastic diffusion, thermal emissivity, aerosol fluorescence.

In the atmosphere, solar radiation is absorbed by atoms and molecules. The energy of these particles increases from an initial energy state to a higher energy state equal to the energy of the photon absorbed.

The total spectrum of a molecule is determined by the difference between two pairs of energy transitions at which the molecule can be analyzed (Petty, 2006).

In the atmosphere, the incident photon can be scattered once (single diffusion) or multiple times (multiple diffusion). The two types of spreading are shown in Figure 2.2. Multiple diffusion usually occurs in lower layers of the atmosphere where particle density increase.

The light diffusion phenomena that occur in the earth's atmosphere are: Rayleigh, Mie and Raman. They are governed by different radiation scattering regimes as shown in Figure 2.1.

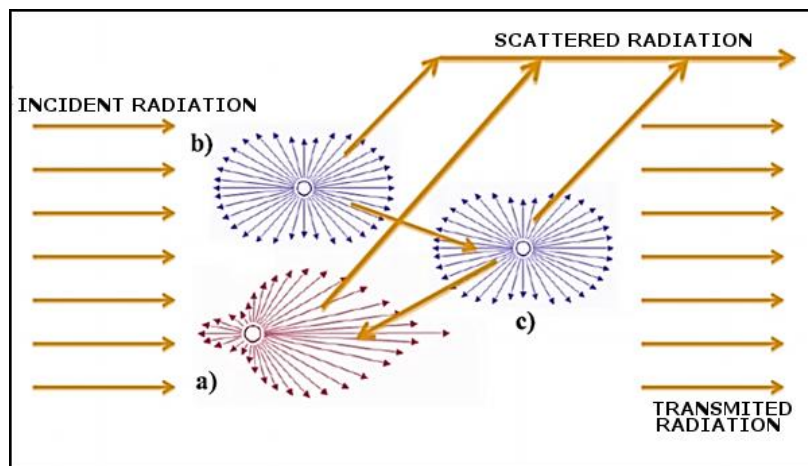


**Figure 2.1:** Schematic of the multiple scattering process in the atmosphere. a) Diffusion Mie b) c) Rayleigh diffusion

### 2.2 Principle of optical absorption spectroscopy. The Lambert - Beer Law

At the basis of the theoretical background of optical absorption spectroscopy stands the Lambert- Beer law which states that the intensity of light radiation when passing through an optical medium decreases with the length and concentration of the particles of the environment being spectrally represented by a Voigt profile (presented Figure 2.2) (Seinfeld and Padis, 2016):

$$I(\lambda) = I_0(\lambda) \exp(-\sigma(\lambda)cL) \quad (2.1)$$

Where  $I_0(\lambda)$  represents the initial intensity of the light beam emitted by a radiation source,  $I(\lambda)$  is the intensity of the beam radiation after it passes through a layer with  $L$  as thickness in which the absorbent particles are in a concentration  $c$  and  $\sigma(\lambda)$  represents the absorption cross section at wavelength  $\lambda$ .

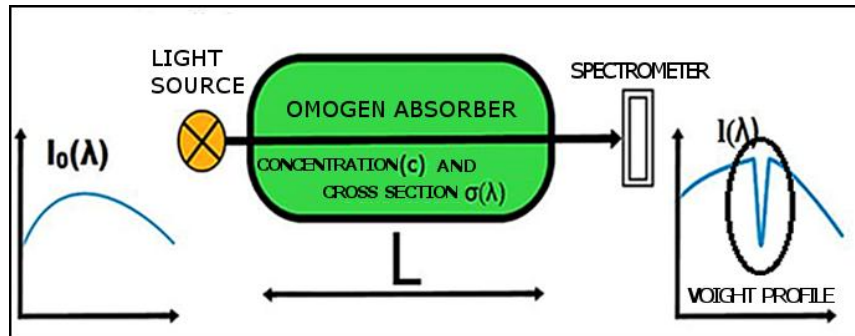


Figure 2.2: Principiul de funcționare al spectroscopiei de absorbție în laborator (adaptată după Merlaud, 2013)

### 2.3 Principle of DOAS technique

DOAS technique introduces a calculus artifice known as "differential" absorption consisting of the difference between two spectral structures of different intensities recorded at the same wavelengths (<http://home.elka.pw.edu.pl/rgraczyk/DOAS.pdf>). The difference between the reference spectrum (the incident radiation spectrum) and the spectrum measured at the passage of the radiation throughout the atmosphere is the basic principle of the optical absorption differential spectroscopy (Figure 2.3).

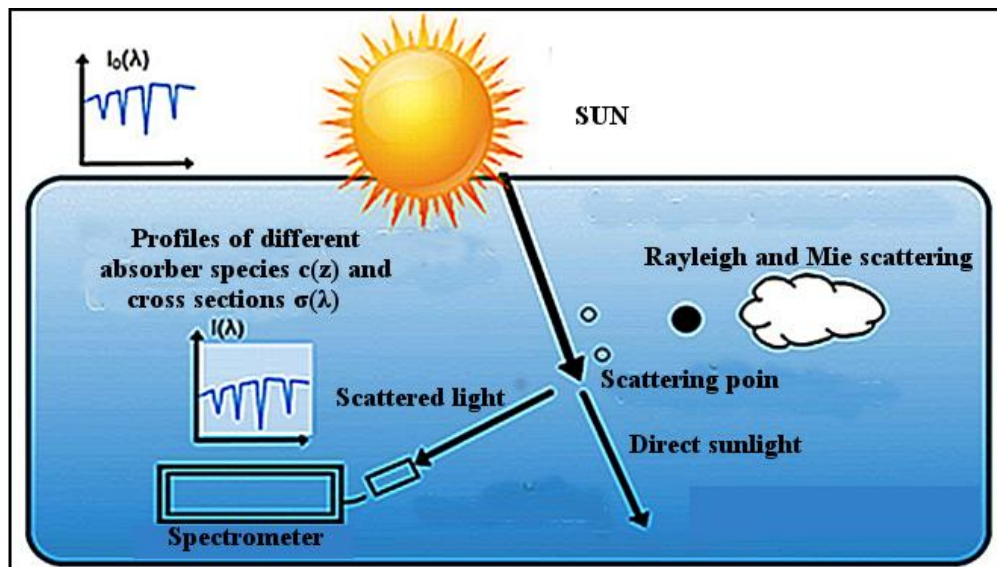
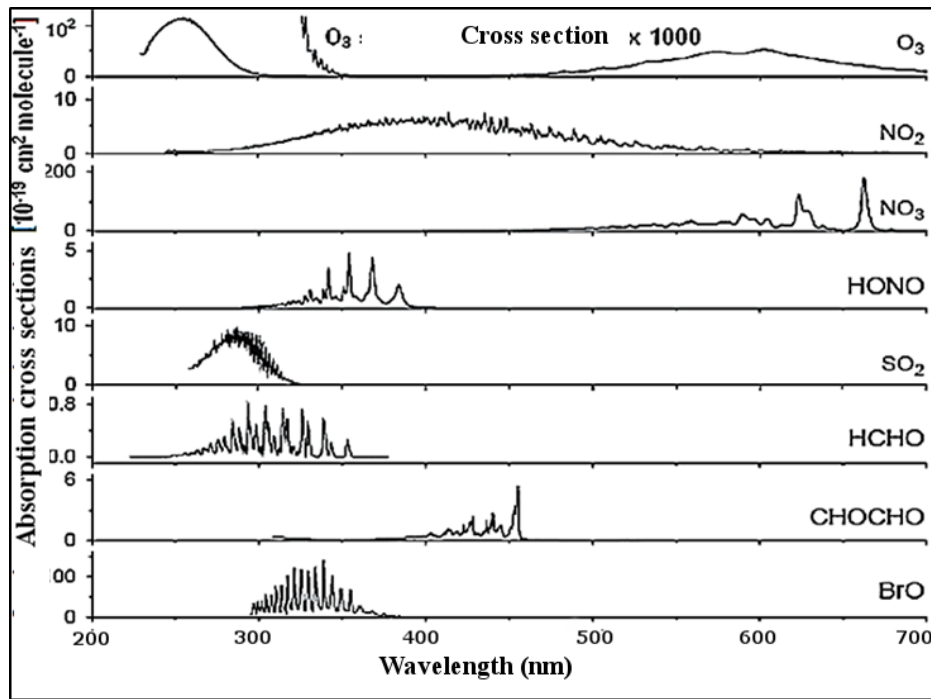


Figure 2.3: The principle of spectroscopic observations in the free atmosphere. Use of scattered radiation in passive DOAS determinations (adaptation after Merlaud, 2013).

Figure 2.4 shows the absorption cross sections of gaseous pollutants found in dense atmospheric layers (troposphere, stratosphere). These spectral structures or absorption cross sections represent "spectral prints" of these atmospheric pollutants.



**Figure 2.4:** Absorption cross section of some chemical compounds from atmospheric layers (adaptation after Platt and Stutz, 2008)

Through the empirical derivation of the Lambert - Beer law, consideration is given to the fact that the intensity of the light decreases by passing through the atmosphere due to some parameters related to the interaction of radiation with the elements in the atmosphere and some factors that reduce the radiation intensity such as: the optical components of the instrument (lenses, deflector, mirrors, optical fiber) and atmospheric turbulence (Platt and Stutz, 2008):

$$I(\lambda) = I_o(\lambda) \cdot \exp \left[ -L \cdot \left( \sum (\sigma_j(\lambda) \cdot c_j) + \varepsilon_R(\lambda) + \varepsilon_M(\lambda) \right) \right] \cdot A(\lambda) \quad (2.2)$$

where the concentration of the absorbant species is  $c_j$  and the absorption cross section of the species  $\sigma_j(\lambda)$ , the Rayleigh extinction and Mie  $\varepsilon_R(\lambda)$  and  $\varepsilon_M(\lambda)$ , instrumental effects and turbulence are quantified by the coefficient  $A(\lambda)$ .

Spectrum differences are recorded and represented on the spectral absorption line of the radiation transmitted as spectral structures in broadband and narrow wavelength band (Platt and Stutz, 2008).

## 2.4 DOAS applications

In DOAS applications in the laboratory the absorbing medium is dense and well defined (size and load with absorbers is known). Based on radiation sources types the DOAS applications can be classified into active (using artificial light sources) and passive (using natural sources).

The active applications of the DOAS technique are carried out in a free atmosphere where the density of absorber molecules is very low requires the use of very powerful external radiation sources. The radiation sources used in such DOAS applications allow observations to be made at distances of tens of kilometers.

Passive DOAS applications involve the use of natural sources of electromagnetic radiation such as the Sun, Moon and stars. This kind of observations can be made at distances up to 1000 km.

A concept called Slant Column Densities (SCD) is defined by the DOAS technique as a quantification of the number of molecules integrated on the path traversed by solar radiation to the detector. This SCD term represents the total density of molecules in the recorded column and its called apparent because it contains the contribution of all the atmospheric layers that are crossed by the solar radiation.

By using radiation transfer models or geometric approximations of the radiation path through the atmosphere, the AMF - Air Mass Factor is calculated. This parameter makes possible the conversion of SCD into vertical columns of density or VCD (Vertical Column Densities):

$$AMF = \frac{SCD}{VCD} \quad (2.3)$$

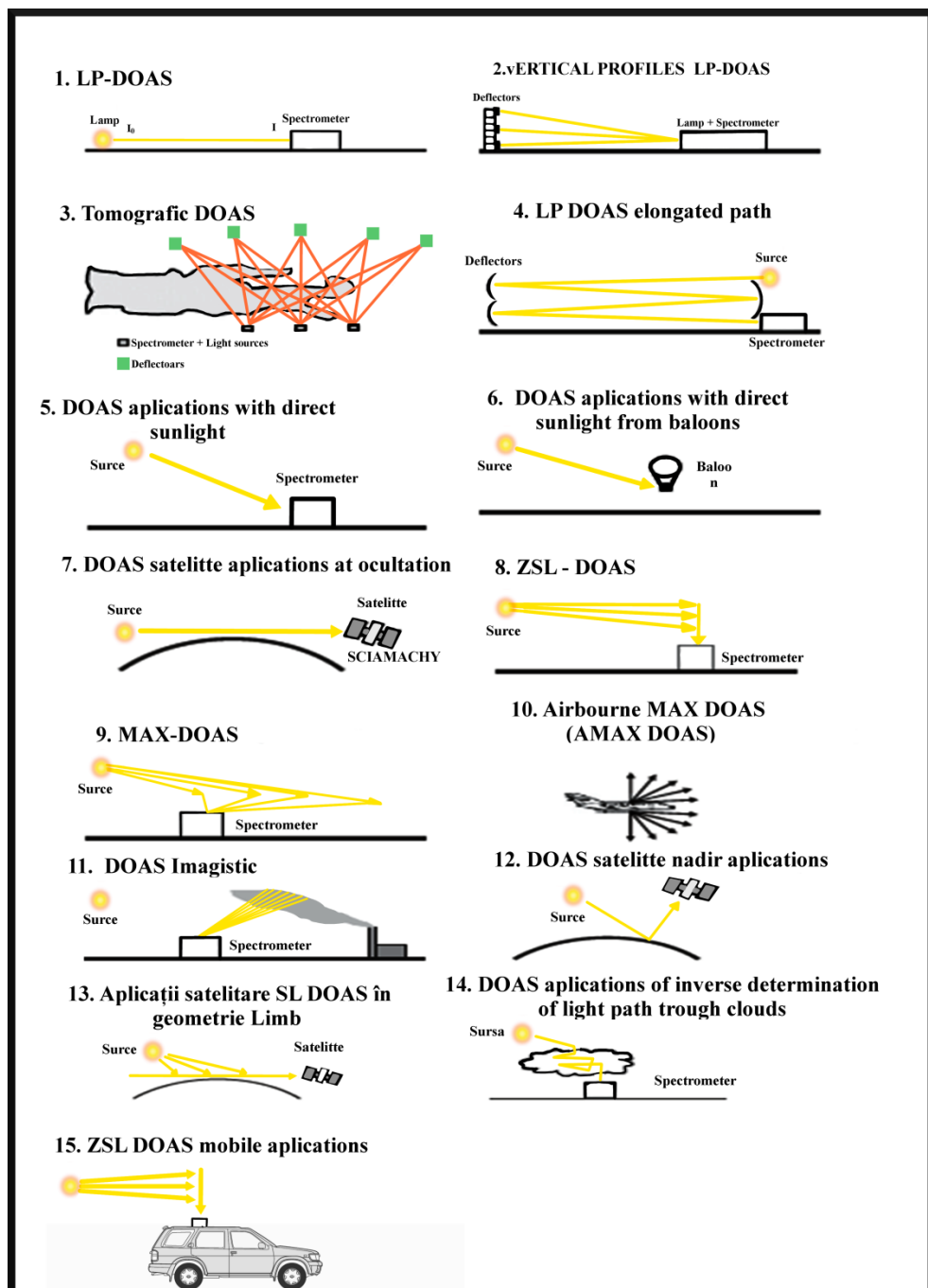


Figure 2.5: Classification of DOAS applications. DOAS applications that use: artificial sources of light (1-4), natural light sources (4-8) or diffused radiation sources (8-15). (adapted from Platz and Stuts, 2008)

Evolution of the DOAS technique shown in Figure 2.5 makes possible today to monitor gaseous pollutants in the lower atmosphere (PBL, troposphere and stratosphere) using different mobile platforms: cars, balloons, Unmanned Airborne Vehicle, airplanes and satellites.

## 2.5 Radiation transfer model used

In the case of passive DOAS applications, the results are difficult to interpret because of the complexity of radiation propagation in the Earth's atmosphere. The use of radiation transfer models (RTM) solves the problem of radiation propagation through the atmosphere by quantifying the effects of the absorption and scattering processes described by the path followed by radiation in any direction.

These quantification models of the atmospheric radiation routes introduce the concept of atmospheric mass factor (AMF). This parameter is crucial in determining the densities of vertical columns (VCD's) of atmospheric absorbers. The model used in this paper is UVSpec/DISORT (Stamnes et al., 2000), which solves the atmospheric radiation trajectory equations. The input parameters of the model must be in line with the real conditions of the DOAS observations. The result of an AMF simulation with this RTM is shown in Figure 2.6.

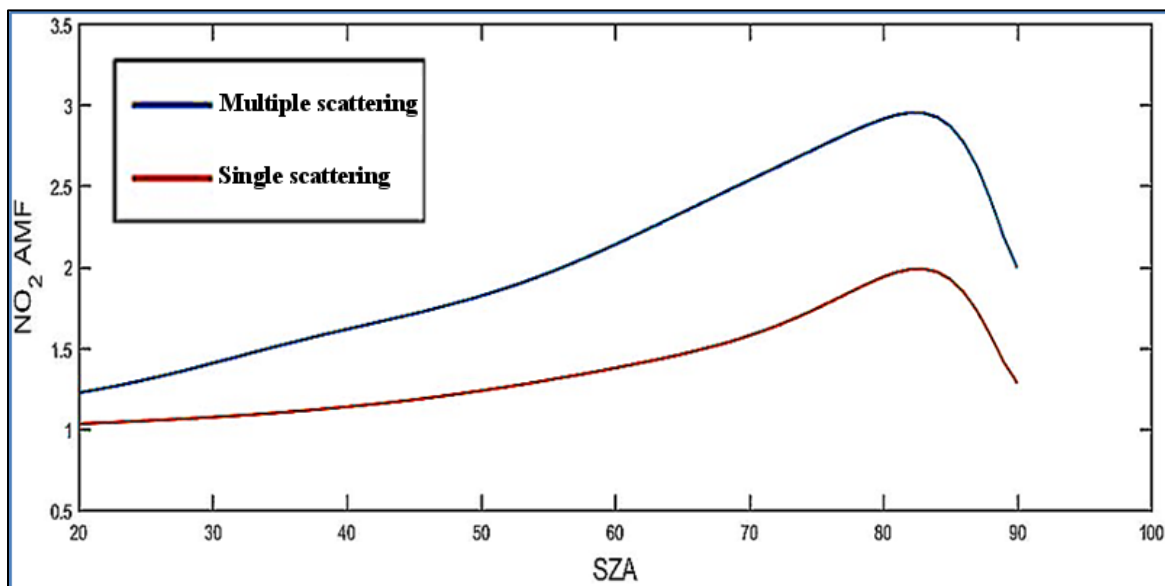


Figure 2.6: AMF variation for multiple and unique diffusion simulated by RTM model UVspec / DISORT

## 2.6 Composition of the spectrophotometer and external optical system used

Componența unui instrument utilizat în aplicațiile DOAS cuprinde: un sistem optic extern de transmitere a radiației și un spectrofotometru.

The composition of a instrument used in DOAS applications includes: an external optical radiation transmission system and a spectrophotometer.

The external optical system transmits the light signal to the instrument. It consists of a deflector, silted lenses (for UV band in UV-Vis applications) and optical fiber (shown in Figure 2.7).



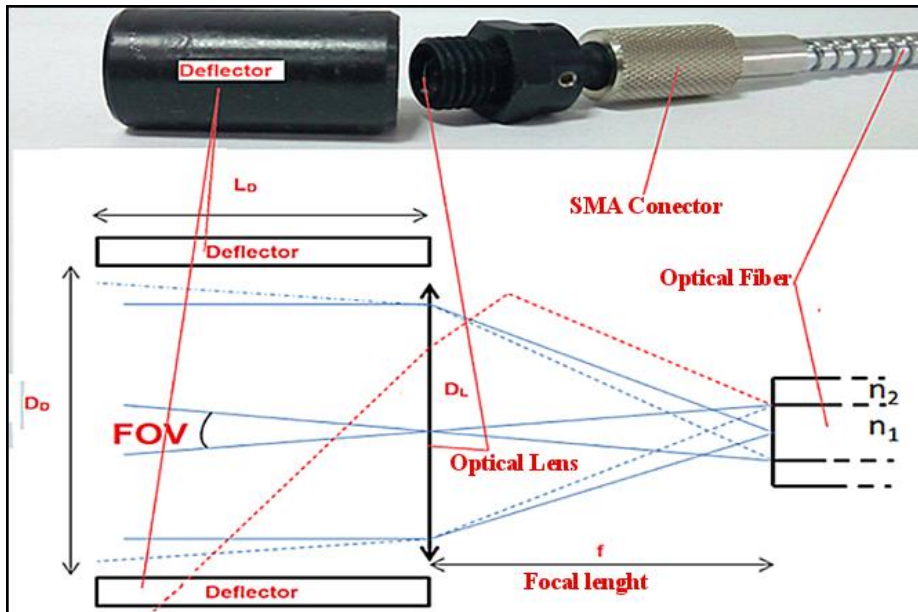


**Figure 2.7:** Scheme of optical radiation capture system. ( $D_D$  and  $L_D$  are the diameter and deflector length,  $D_L$  lens diameter). The optical radiation capture assembly for DOAS applications is presented at the top (adaptation after Merlaud, 2013).

The spectrometer used in the research of this thesis is AvaSpec ULS2048XL Starline (shown in Figure 2.8). The inside of the spectrophotometer includes a series of optical systems that lead the photons to a detector. This spectrophotometer was used in static ZSL - DOAS applications, ZSL - DOAS mobile applications and in MAX - DOAS applications performed in the experiments covered by this thesis. The instrument has an ideal UV / Viz range (295 - 550 nm) for detecting  $\text{NO}_2$  but also other atmospheric pollutants. The advantages of this instrument are: spectral resolution (0.7 nm - FWHM - Full Width at Half Maximum determined experimentally and presented in Figure 2.9), low costs for consumables and maintenance, mobility, study of pollutants detected in the UV / Viz field (295-550 nm), the possibility of using in various DOAS applications, using teledetection.

Disadvantages: dependence on atmospheric nebulosity conditions, dependence on the presence of a constant radiation source, limitation only to diurnal measurements;

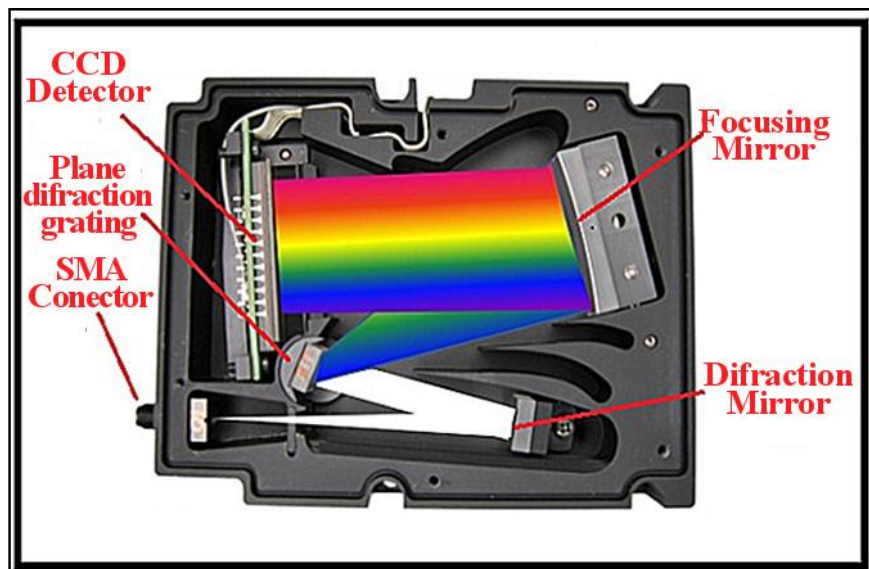


**Figure 2.8:** The internal optical system of a Czerny-Turner AvaSpec ULS2048XL Starline Spectrophotometer (adapted from <https://www.slideshare.net/Themadagen/benno-oderkerk-avantes>).

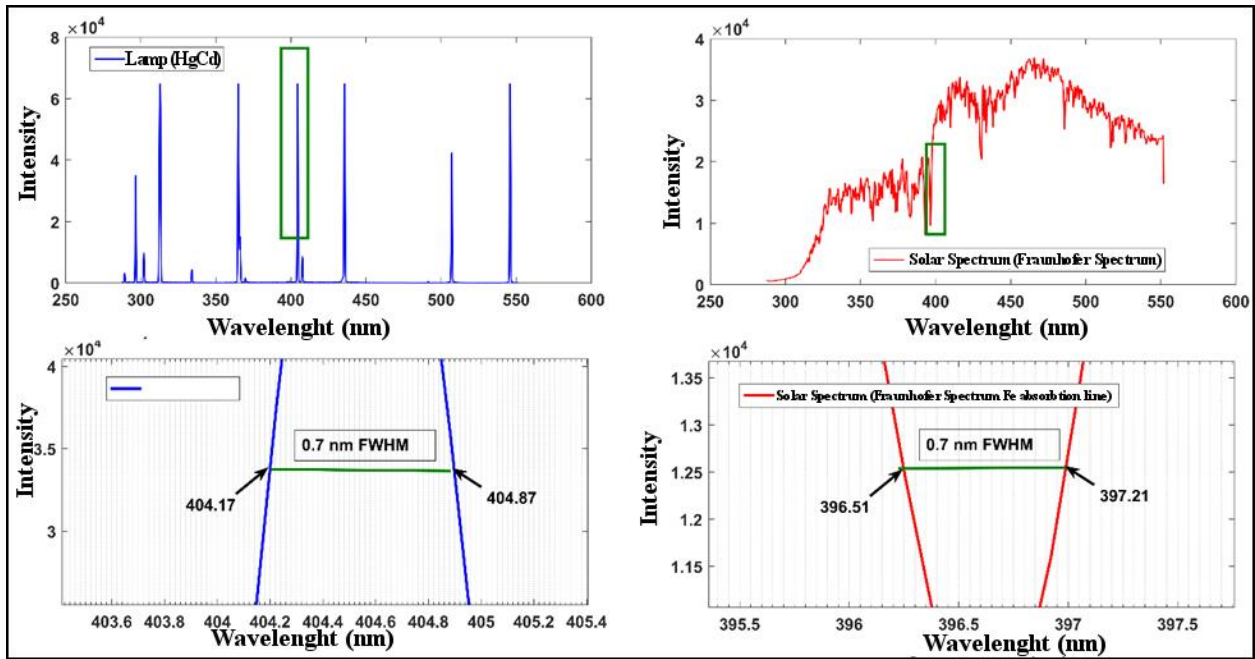


**Figure 2.9:** Experimental determination of spectral resolution (FWHM) with an HgCd lamp (left in blue) and with solar spectrum recorded in zenith geometry (right with red).

## 2.7 The software used in spectral analysis

The spectral analysis of the spectra recorded during the measurement campaigns was carried out using the QDOAS software developed by the Belgian Institute for Space Aeronomy (BIRA-IASN) (Fayt and Van Roozendael, 2001).

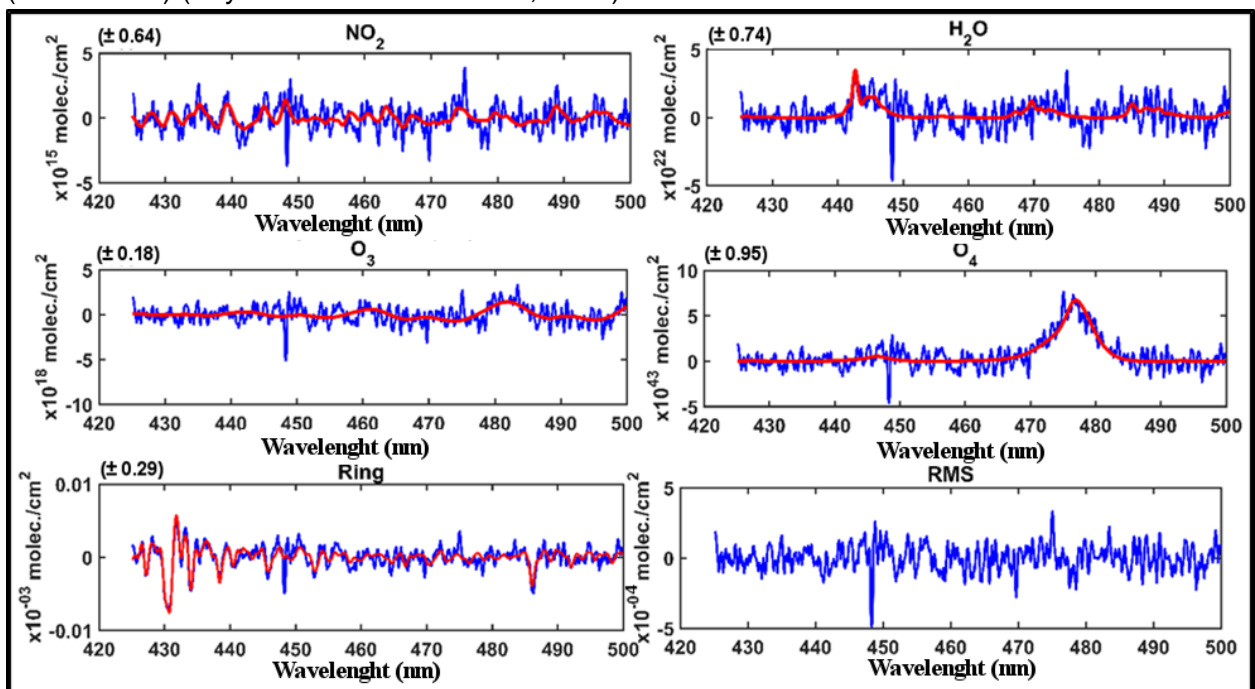


**Figure 2.10:** The results of the first three steps (calibration, preprocessing, fitting) using the QDOAS software to determine the NO<sub>2</sub> DSCD. The red line is the result of the convolution of the cross sections at the resolution of the instrument. The blue line represents the measured spectrum.

The result of the spectral analysis is represented by obtaining the differential slant columns density (DSCD) for the studied pollutant gas. The uncertainties given by the spectral analysis are dependent on the noise signal and are estimated to be between 25 - 30%.

The DSCD values resulting from the spectral analysis show the difference between the reference spectrum and the ones measured by various DOAS applications. In spectral analysis, input parameters (shown in Table 2.1) are used as reference spectrum, spectral absorption prints. The result of a spectral analysis is shown in Figure 2.10. The QDOAS software algorithm is described in four steps: calibration, preprocessing, processing, displaying results in the ASCII file as a DSCD.

**Table 2.1:** Cross sections of the absorbers ( $O_4$ ,  $O_3$ ,  $NO_2$ ,  $SO_2$ ,  $H_2O$ ) used as convolution and fitting parameters in spectral analysis using the QDOAS software

Molecules	Observation temperature	References
$NO_2$	298 K	(Vandaele et. al, 1998)
$O_3$	293K	(Bogumil et. al, 2000)
$O_4$	293 K	(Thalman et. al, 2013)
Ring	N/A	(Chance et. al, 1997)
$SO_2$	294 K	(Vandaele et. al, 1998)
$H_2O$	296K	(Rothman et. al, 2010)
Spectral domain $NO_2$	425-495 nm	
Spectral domain $SO_2$	305-325 nm	
Polinomial fit order	5	



## CHAPTER 3

### Research on the level of NO<sub>2</sub> pollution in Europe

#### 3.1 Research on the evolution of NO<sub>2</sub> concentrations in Europe

##### 3.1.1 Method and data used

For the purpose of these investigations data on NO<sub>2</sub> concentrations at ground level were used from validated database of the European Environment Agency for the period 2000 - 2012. The NO<sub>2</sub> concentrations used in this study are the annual average of hourly observations of air quality monitoring stations in 15 European cities: Amsterdam, Berlin, Bucharest, Budapest, Debrecen, Edinburgh, Galati, Hamburg, London, Milan, Paris, Rome, Rotterdam, Strasbourg and Vienna. The air quality monitoring network at the European level presented in 2012 a total of 8400 monitoring stations of air quality (see Figure 3.1).

For the analysis of the evolution of NO<sub>2</sub> concentrations for the 15 cities, the average annual value recorded at each station was taken into account, taking also into account the type of the station: background and traffic. A classification of the results was carried out according to the NO<sub>2</sub> concentrations observed at each station type and the NO<sub>2</sub> pollution recorded at city level. The values obtained were compared with the EU NO<sub>2</sub> annual concentration limit value proposed by the WHO of 40 µg / m<sup>3</sup>. Also, a statistical analysis was carried out to estimate the percentage of the population affected by the EU threshold exceeded. This threshold has entered into force on 1 January 2010 through Directive 2008/50/EU.

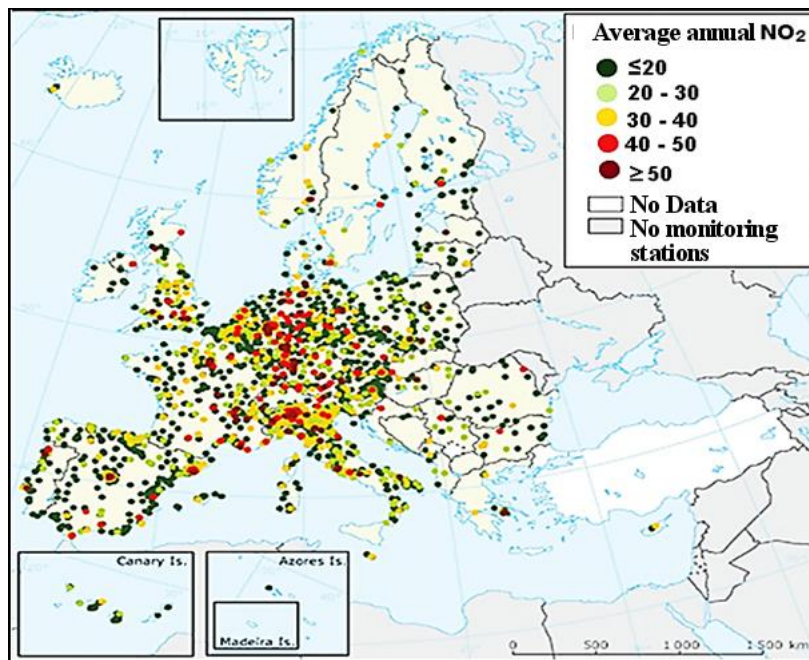


**Figure 3.1:** NO<sub>2</sub> monitoring network at Europe level. The average NO<sub>2</sub> concentrations recorded for 2015 (source [www.eea.europa.eu](http://www.eea.europa.eu))

### 3.1.2 Results and discussions

The presentation of the evolution of the annual NO<sub>2</sub> concentration only at the city level for the period 2000 - 2012 can lead to an erroneous interpretation of the level of pollution to which the population of the 15 European cities is exposed. Data from each station type can accurately tell which areas of the city are more polluted within a year. Another important issue in determining the level of pollution is the recorded number of exceedances of the EU limit value.

Through the Data Quality Objective (DQO), the databases are filtered so that they contain values of the monitored pollutants with uncertainty of determination: 50% for PM<sub>10</sub> and PM<sub>2.5</sub>, 30% for O<sub>3</sub> and 25% for CO, NO<sub>x</sub>, NO<sub>2</sub> and SO<sub>2</sub> (EU, 2008; Castell et al., 2017).

Figure 3.2 presents the result of the statistical analysis of the percentage of inhabitants of each city that is liable to be exposed to NO<sub>2</sub> concentrations exceeding the EU and WHO limit value. In the case of the 15 studied cities, the population most affected by the exceedance of the NO<sub>2</sub> threshold is the population associated with traffic stations.

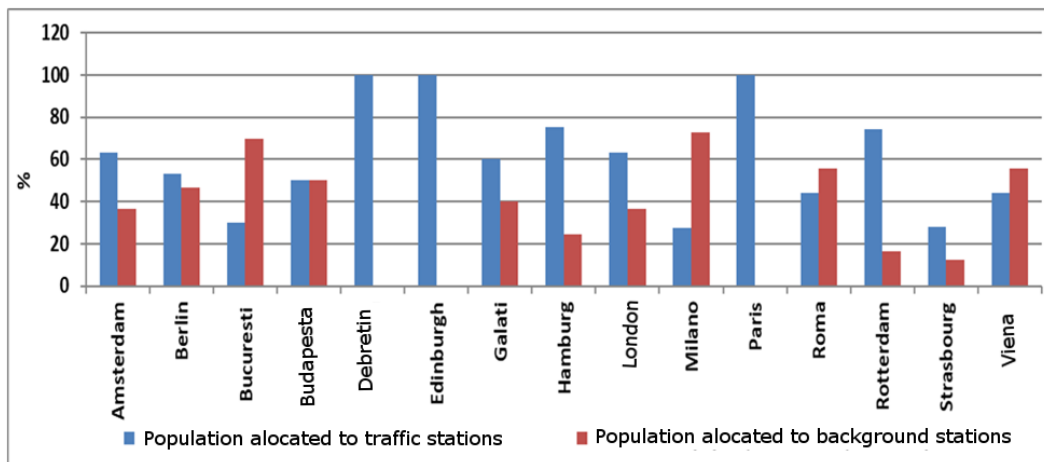


**Figure 3.2:** Percentage of population affected by NO<sub>2</sub> concentrations exceeding the EU / WHO threshold for the 15 cities (B5, Roşu, A. et al., 2016)

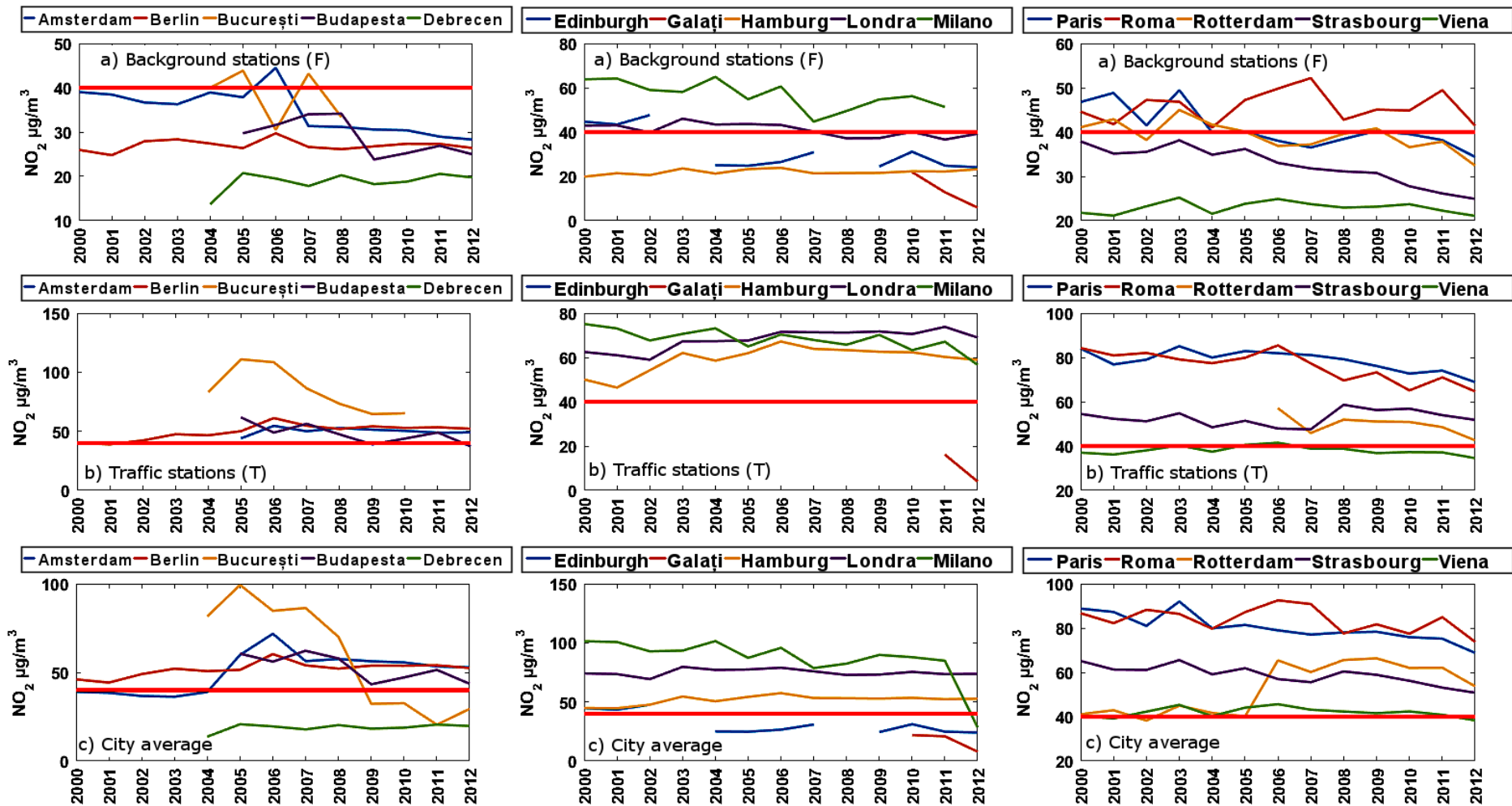


**Figure 3.3:** Annual average NO<sub>2</sub> concentrations for the period 2000 to 2012 at the level of: city (c)background air quality monitoring station (b) traffic air quality monitoring station (a). Comparisons with EU limit value (red line) (B5, Red, A. et al., 2016)

The results of the annual NO<sub>2</sub> analysis presented in Figure 3.3 show the difference between the assessment of the whole city and those observed at the level of each station type. Figure 3.3 shows the difference between NO<sub>2</sub> concentrations observed at the background monitoring stations (lower values) than those of traffic stations (higher values), Traffic stations being generally located in areas where traffic is very intense and there is a high flow of population transit.

The values of the annual average concentrations for NO<sub>2</sub> recorded by the background monitoring stations (Figure 3.3a) show exceedances of the limit values for the cities: Milano, Rome, Paris (2000-2003, 2009), London (2000, 2001, 2010), Rotterdam (2000, 2001, 2003, 2009), Amsterdam (2006), Bucharest (2005, 2007), Edinburgh (2000-2002).

The annual average concentration resulting from the observations of the traffic stations (Figure 3.3b) of the 15 cities exceeds the limit value for almost all cities except: Galati, Budapest (2009), Vienna (2000-2002, 2004, 2009-2012) . These values underline the idea that cars are a very important source of NO<sub>2</sub>.

Annual NO<sub>2</sub> concentrations recorded at city level for the 15 locations selected in this study, shown in Figure 3.3 a decrease in emissions for the period 2000 - 2012.

### **3.1.3 Conclusions**

Conclusions of the study on the evolution of annual NO<sub>2</sub> concentrations at the ground level support the idea that air pollution with nitrogen dioxide for the 15 European cities has decreased. This can be explained by city-level measures to reduce emissions in order to record values in line with the EU's Climate and Energy package proposing 20% reduction by 2020.

The comparison of the annual NO<sub>2</sub> concentrations with the annual limit of 40mg / m<sup>3</sup> entered into force in 2010 highlights the differences that occur in presenting the level of pollution registered by each type of station compared to the one observed at the city level for the period 2000 - 2012. The graphical representations from the study resume the idea that the population is most affected in the regions where NO<sub>2</sub> pollution is high (in the area of traffic air quality monitoring stations) and least affected in the regions with low pollution (background air quality monitoring stations).

The research results presented in this chapter show the level of pollution in Europe based on statistical calculations and measurements that are comprised of validated European databases. The purpose of these studies was to prepare future DOAS measurement campaigns in Europe.

## CHAPTER 4

### Comparison of DOAS measurements at ground level with satellite observations used for NO<sub>2</sub> determination

#### 4.1 State of the art of satellite observations for NO<sub>2</sub> determination

DOAS satellite instruments make observations of atmospheric composition at different spatial resolutions from their displacement on polar heliocynchronous orbits (about 800 km of terrestrial surface). These differences between resolutions are due to the scanning geometry, scanning mode, instrument characteristics (shown in Table 4.1). The satellite instruments capable of detecting NO<sub>2</sub> pollution are shown in Figure 4.1.

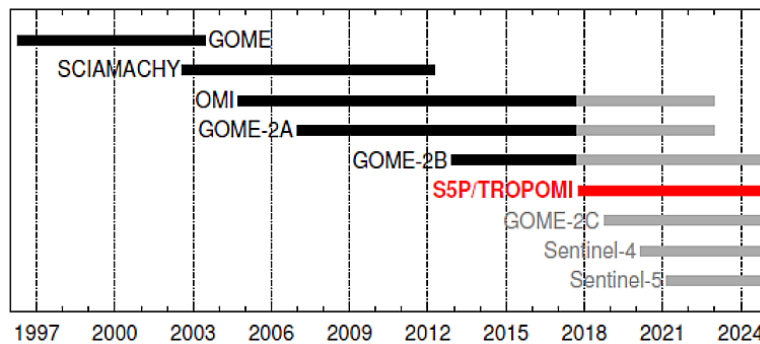


**Figure 4.1:** The expected operating period of the satellite instruments used in the global monitoring of NO<sub>2</sub> in the stratosphere and troposphere (taken from van Geffen et al., 2017)

**Table 4.1:** Characteristics of the satellite instruments dedicated to the monitoring of NO<sub>2</sub> and other minor airborne constituents of troposphere and stratosphere through observations in nadir geometry (adaptation after ESA / NASA)

Satellite platform	DOAS Instrument	Nadir spatial resolution (km <sup>2</sup> )	Global coverage (days)	Spectral resolution FWHM (nm)	Spectral domain (nm)	Ecuator overpass (UTC)	Scanning angle
ERS-2	GOME	40x320	3	0.17 - 0.33	240 - 790	10:30	±32°
ENVISAT	SCHIAMACHY	30x60	6	0.48 - 1.48	240 - 2405	10:00	+32°/-31°
AURA	OMI	24x13	1	0.45 - 1	270 - 500	13:45	±114°
METOP - A	GOME-2A	80x40	1	0.24 - 0.53	240 - 790	9:30	±57°
METOP - B	GOME-2B	80x40	1	0.24 - 0.53	240 - 790	9:30	±57°
S5P	TROPOMI	7x7	1	0.25 - 0.54	270 - 2385	10:00	±114°

The differences between these satellite instruments are usually due to the spatial resolution of a scanned pixel above the overpassed surface (Rotterdam City shown in Figure 4.2).

All spatial DOAS instruments: GOME, SCIAMACHY, GOME-2A, GOME-2B, OMI perform measurements perpendicular to the terrestrial surface (geometry nadir). The SCIAMACHY and TROPOMI instruments are the only satellite instruments that can make observations in limb geometry (tangential to ground) and ocular (shown in Figure 4.3).



**Figure 4.2:** Spatial pixel coverage of DOAS satellite instruments used in NO<sub>2</sub> monitoring. Comparison over Rotterdam, The Netherlands. (adapted from <http://www.tropomi.eu>)

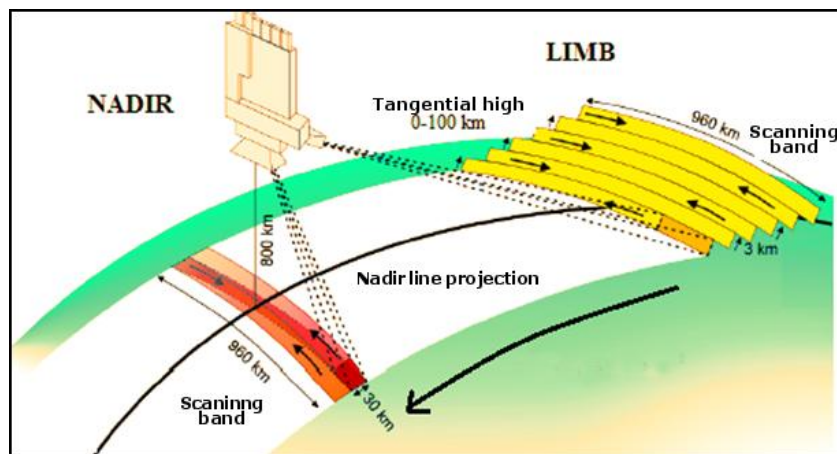


**Figure 4.3:** Schematic of observations made by the SCIAMACHY and TROPOMI space sensors (adaptation by ESA)

## 4.2 Observing the evolution of tropospheric NO<sub>2</sub> content in five major European cities using DOAS satellite instruments

### 4.2.1 Methods and data used

The research aimed at assessing the similarity between the NO<sub>2</sub> concentration levels recorded at ground level with air quality monitoring stations using the chemiluminescence technique and the tropospheric content observed by the DOAS satellite instruments for European cities: Athens, Bucharest, Hamburg, Helsinki, Paris. The data represents the annual averages for the period 2002 - 2015.

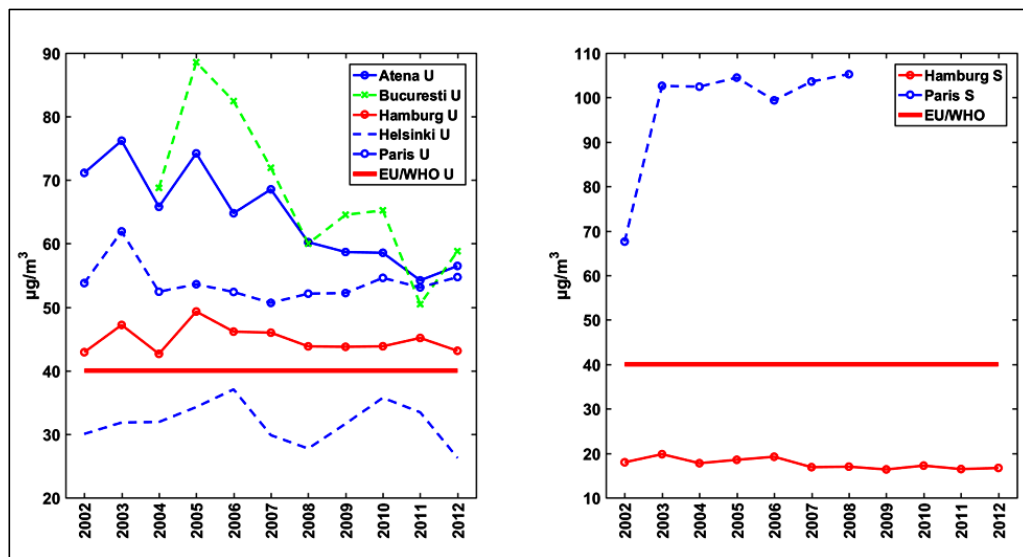
Satellite observations for NO<sub>2</sub> are presented as annual averages of VCD<sub>tropo</sub> (vertical tropospheric column density) extracted from daily determinations of UV-Vis space instruments: OMI, SCHIAMACHY, GOME - 2. For ease of expression, during the course of the thesis the formulation of the tropospheric vertical column of NO<sub>2</sub> (VCD<sub>tropo</sub>) is used, describing the number of NO<sub>2</sub> molecules in a vertical (tropospheric) column from the Earth's surface to the upper limit of the atmosphere (troposphere) having the 1 cm<sup>2</sup> section..



Air quality monitoring stations are classified according to their role and location where they are placed in two categories: suburban (S) and urban (U). Another direction of the study consisted in assessing the annual average concentrations against the limits imposed by Directive 2008/50 / EC, which sets a annual limit value of  $40 \mu\text{g} / \text{m}^3$ .

#### 4.2.2 Results and discussions

By comparing and observing the variation of  $\text{NO}_2$  pollution at ground level (in situ stations - local observations) and in atmospheric layers (satellite instruments - large areas) we can quantify and observe the dispersion of minor constituents. Also, through these comparisons it is possible to check which is the most sensitive satellite instrument in determining the ground air pollution.



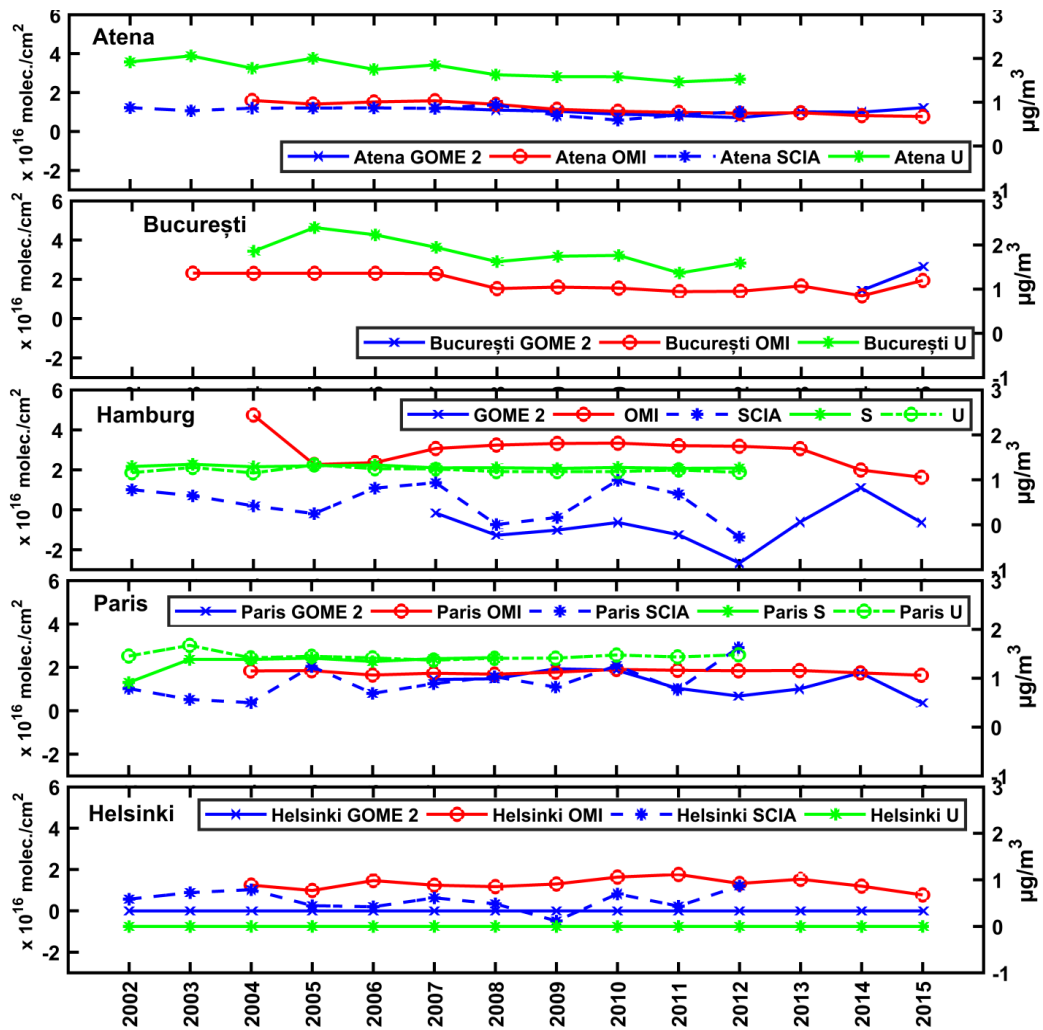
**Figure 4.4:** Annual mean  $\text{NO}_2$  concentrations measured on the ground for the five cities compared to at the EU and WHO limit value (B3 Roşu et al., 2016).

Figure 4.4 shows the  $\text{NO}_2$  concentrations recorded on the ground in the urban and suburban areas of each city where the annual limit value of  $40 \mu\text{g}/\text{m}^3$  established by the WHO and EU has been exceeded in all EU countries, exception: Helsinki U and Hamburg S. The average annual  $\text{NO}_2$  values show a growth trend in the urban area of Hamburg and Paris (U and S).

In this study we presented in parallel the satellite observations with the measurements made by the air quality monitoring stations in order to observe the air pollution trend for the period 2002 - 2015 in the 5 European cities, but also to observe whether the two methods for the quantification of  $\text{NO}_2$  shows correlations for this period.

The uncertainties associated with determining the density of the tropospheric  $\text{NO}_2$  molecules from satellite measurements are: for OMI-  $0.75 \times 10^{15}$  molecules /  $\text{cm}^2$  (Boersma et al., 2007, 2011) for SCHIAMACHY 15% (Richter et al., 2005) 40 - 80% (Valks et al., 2011). The negative values of the tropospheric  $\text{NO}_2$  columns are explained by using the same reference spectrum to extract all  $\text{VCD}_{\text{tropo}} \text{NO}_2$ . These negative values do not show the lack of  $\text{NO}_2$  but indicate that the density of the molecules is lower than the reference spectrum used by the DOMINO v2.0 algorithm (Boersma, 2007, 2011).

UTILIZATION OF THE DIFFERENTIAL OPTICAL ABSORPTION SPECTROSCOPY IN QUANTIFICATION OF ATMOSPHERIC POLLUTION WITH NITROGEN DIOXIDE



**Figure 4.5:** Annual averages of  $VCD_{tropo}$  for  $NO_2$  observed by satellite instruments compared to the annual average  $NO_2$  concentrations recorded by the two categories of air quality monitoring stations: U (urban) and S (rural) for the five cities between 2002 and 2015 (B3 Roşu et al., 2016).

In Figure 4.5 It can be noted that the evolution of the vertical column of  $NO_2$  observed by the satellite sensors (OMI, SCIAMACHY and GOME 2) is somewhat similar to what concentration of the  $NO_2$  was recorded by air quality monitoring stations (U) (both show a slight downward trend). The values of the R correlation factor between the measurements of the monitoring stations and those of the satellite instruments are shown in Table 4.2. This shows that the satellite OMI instrument with the best spatial resolution (details in Table 4.1) can be used to accurately determine the pollution by  $NO_2$  at the ground level above large cities.

**Table 4.2:** Valoarea factorului R2 de corelare între observațiile DOAS satelit și stațiile de monitorizare a calității aerului pentru cele 5 orașe europene cifrele îngroșate corespund unor valori semnificative ale coeficientului de corelație ( $p < 0,05$ ) (B3 Roşu et al., 2016);

City/ DOAS Instrument	OMI	SCIAMACHY	GOME_2
<b>HAMBURG_U</b>	<b>0.78</b>	0.18	0.49
<b>HELSINKI_U</b>	0.38	0.31	0.23
<b>PARIS_U</b>	<b>0.69</b>	0.09	0.29
<b>ATHENA_U</b>	<b>0.78</b>	0.50	0.45
<b>BUCURESTI_U</b>	<b>0.74</b>	N/A	N/A
<b>HAMBURG_S</b>	0.38	0.30	0.29
<b>PARIS_S</b>	0.38	0.13	0.48



### **4.2.3 Conclusions**

This subchapter presents the study of the anthropogenic NO<sub>2</sub> variation from five European cities observed by DOAS satellite instruments between 2002 and 2015. In order to have a clear picture of the spatial and temporal distribution of NO<sub>2</sub> pollution in the five cities, we analyzed complementary the amounts of NO<sub>2</sub> recorded by the satellite observations and the ones measured by the air quality monitoring stations.

The results of the study show that there was a decrease in the evolution of NO<sub>2</sub> content in the five cities in Europe: Athens, Bucharest, Hamburg, Helsinki, Paris. The study shows that the satellite UV-Vis instruments provide information on the annual variation of NO<sub>2</sub> pollution from urban agglomerations. It has been shown that the most important satellite instrument in accurately recording the NO<sub>2</sub> content of urban agglomerations is the OMI, which is supported by the high number of correlations with ground determinations ( $R > 0.5$ ).

The values recorded by the air quality monitoring stations in the 5 cities present the state of the ground pollution inside cities through urban stations and in peripheral areas through the suburban stations. In the case of concentrations registered in the cities area, they exceeded the EU-regulated annual limits in 4 cities except in Helsinki and Bucharest in 2011.

## **4.3 Observations of NO<sub>2</sub> in the South Eastern Region of Romania using the DOAS mobile technique in zenith geometry**

### **4.3.1 Method and data used**

In this study, we used DOAS technique onboard of a vehicle to determine the tropospheric NO<sub>2</sub> columns inside and outside of Galați city. The results obtained are complementary to the values recorded by the air quality monitoring stations in the city. Another objective of the study was to produce dispersion maps using interpolation models based on DOAS observations made in Galati.

DOAS mobile observations were made in Galati (located 45 ° 26'22 "N, 28 ° 2'4" E) during 2 - 4 February 2017. No satellite observations were available for the campaign period. This has led to the comparison of the NO<sub>2</sub> content detected by the ZSL-DOAS UGAL system with other methods that quantify the NO<sub>2</sub> content (local air quality monitoring stations).

Figure 4.6 shows the track followed by the DOAS mobile system for determining the NO<sub>2</sub> content. The weather conditions, wind direction and velocity used in this study were extracted from the database [www.wunderground.com](http://www.wunderground.com).

One of the objectives of the DOAS mobile observations was the intersection with air quality monitoring stations (GL) locations in order to achieve a qualitative comparison with the NO<sub>2</sub> concentration values recorded by them (see Table 4.3).

UTILIZATION OF THE DIFFERENTIAL OPTICAL ABSORPTION SPECTROSCOPY IN QUANTIFICATION OF ATMOSPHERIC POLLUTION WITH NITROGEN DIOXIDE

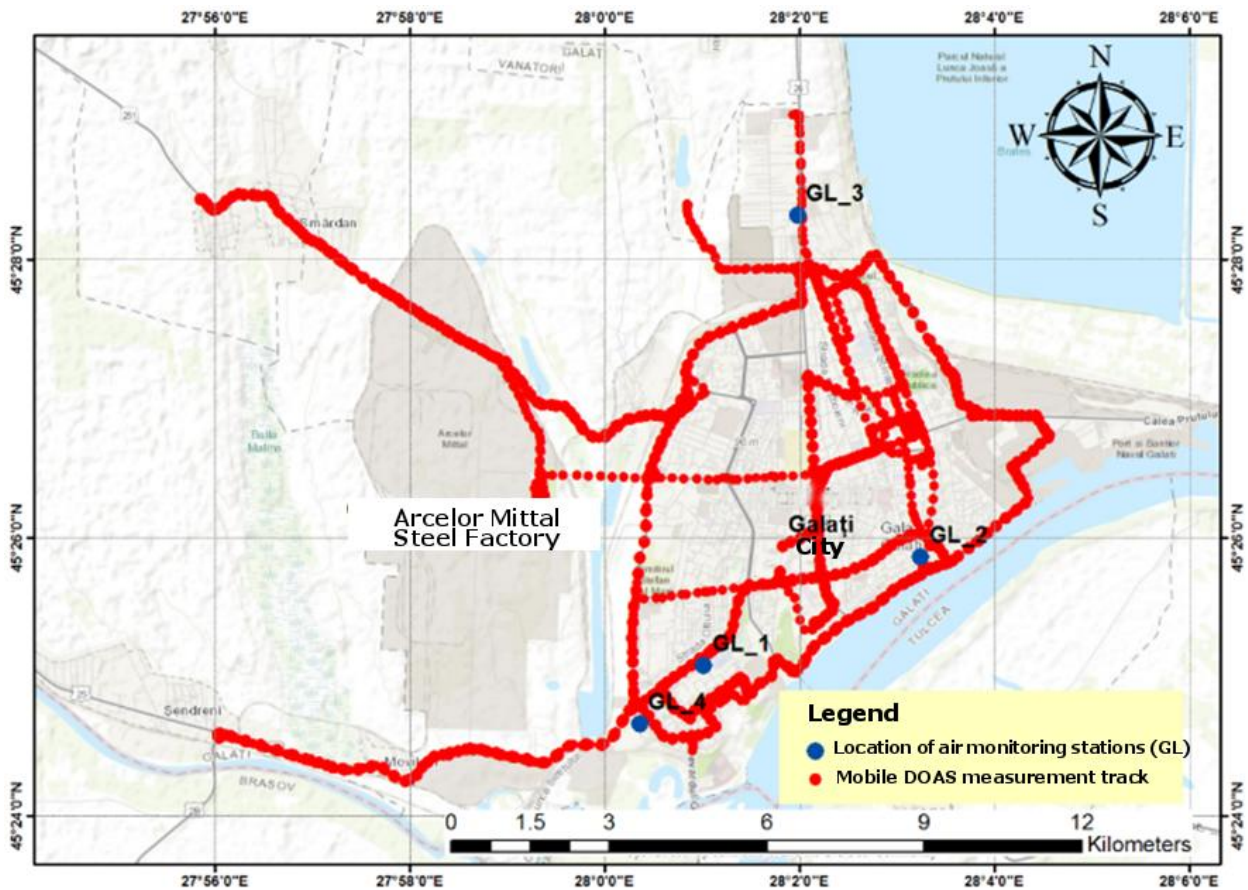


**Figure 4.6:** The route followed by the DOAS mobile system to make observations in Galati in the period February 2 - 4, 2017 (dotted with red). Air quality monitoring stations (blue points) (B1 Rosu et al. 2016).

**Table 4.3:** Type and locations of air quality monitoring stations in Galati city (source ANMP Galați, 2017)

Station code	Longitude (E)	Latitude (N)	Station type
GL_1	28°1'4.26"	45°25'77"	Industry
GL_2	28°3'17"	45°25'53"	Suburban
GL_3	28°2'2.18"	45°28'22"	Urban
GL_4	28°0'23"	45°24'40"	Traffic

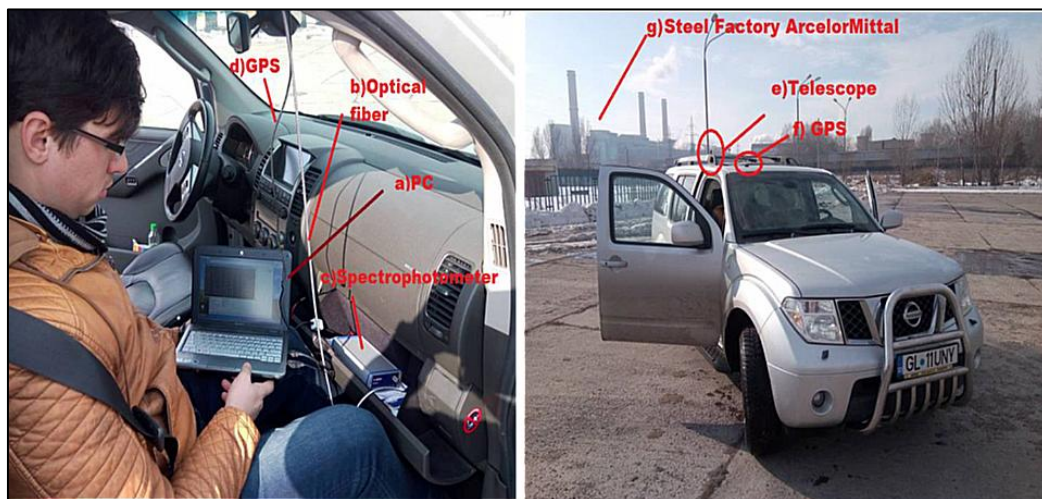


**Figure 4.7:** ZSL - DOAS UGAL mobile system configuration (left). Mobile platform or vehicle (right) (B1 Rosu et al 2016)

Sistemul mobil ZSL - DOAS UGAL a fost utilizat în determinarea conținutului troposferic de NO<sub>2</sub>. Acesta cuprinde: platforma mobilă sau laborator mobil – autolaboratorul din dotarea Facultății de Științe și Mediu din Galați, instrumentul de determinare a densităților de molecule de NO<sub>2</sub> - spectrofotometru AvaSpec ULS2048XL (Figura 4.7). Spectrofotometrul este alimentat și transmite spectrele înregistrate către un laptop (PC) printr-o interfață USB 2. Poziția geografică a sistemului DOAS este înregistrată simultan cu fiecare determinare DOAS prin intermediul unui GPS tip mouse model BR-355S4. Ansamblul complet al sistemului mobil DOAS se poate observa în Figura 4.7

The ZSL-DOAS UGAL mobile system was used to determine the tropospheric NO<sub>2</sub> content. This includes: mobile platform or mobile laboratory – test car from the Faculty of Sciences and Environment of Galati, the instrument for determining the densities of NO<sub>2</sub> molecules - AvaSpec ULS2048XL spectrophotometer (Figure 4.7). The spectrophotometer is powered and transmits the spectra to a laptop (PC) through a USB interface 2. The geographic position of the DOAS system is recorded simultaneously with each DOAS determination via a GPS BR-355S4 mouse model. The complete DOAS mobile assembly can be seen in Figure 4.7

ZSL - DOAS mobile observations consist of placing the telescope on the roof of the vehicle, being positioned in zenith geometry or 90 ° from the horizontal (Figure 4.7).

The analysis of recorded spectra was performed using the QDOAS software developed by the BIRA Institute (Fayt and Van Roozendaal, 2001; Van Roozendaal et al., 2002). The spectral window in which the NO<sub>2</sub> analysis is performed includes the spectral range between 425 - 500 nm. The result of the spectral analysis represents the Differential Slant Column Density (DSCD) which represents the difference between the measured spectrum and a reference spectrum (SCD<sub>ref</sub>):

$$SCD = DSCD + SCD_{ref} \quad (4.1)$$

The reference spectrum was recorded in a rural area near the city of Galati with a value of  $2.8 \times 10^{15}$  molecules / cm<sup>2</sup> and the measurement uncertainty calculated by the QDOAS software is  $\pm 0.42 \times 10^{15}$  molecules / cm<sup>2</sup>. The mean uncertainty of NO<sub>2</sub> DSCD recorded in the 3 days is below 30%.

The results of the DOAS determinations made in Galati Municipality were subsequently mediated and used in the generation of dispersion prediction maps. Predictive maps were developed using GIS software to apply the interpolation methods: Kriging and IDW (Inverse Distance Weighted). For the Kriging interpolation method we used two types KOPs (Kriging Ordinary Prediction) and KUC (Kriging Universal Constant) (Wong et al., 2004).

In this research, a new approach was used to approximate DSCD as being equal to VCD by considering that DOAS mobile observations were made around noon and SCD<sub>ref</sub> was recorded in a rural area where NO<sub>2</sub> loading in the atmosphere is very low.

The atmospheric mass factor used in the conversion of the slant column in VCD was geometrically estimated by the relation:

$$AMF(geo) = 1/\sin(\alpha) \quad (4.2)$$

where  $\alpha$  represents the solar zenith angle of each DOAS determinations  
AMF (geo) can be calculated using the geographic position and time at which the DOAS measurements are performed using the relation 4.4

### 4.3.2 Results and discussions

The results of spectral analysis are shown in Figure 4.8 (right) as NO<sub>2</sub> DSCD from which NO<sub>2</sub> VCD values were extracted by applying an atmospheric mass factor calculated by the relationship 4.4. This estimation method can be applied only for determinations made when the sun is positioned at low zenith angles (at noon) under clear sky conditions. Figure 4.8 (right) shows two high values of NO<sub>2</sub> VCD within the time range of 11-12 UTC for all three days. These values are mainly due to the passage under the emission plume of the ArcelorMittal Steel Factory. Other high NO<sub>2</sub> VCD values are due to the intersection of emissions of local road traffic or other sources within the city.

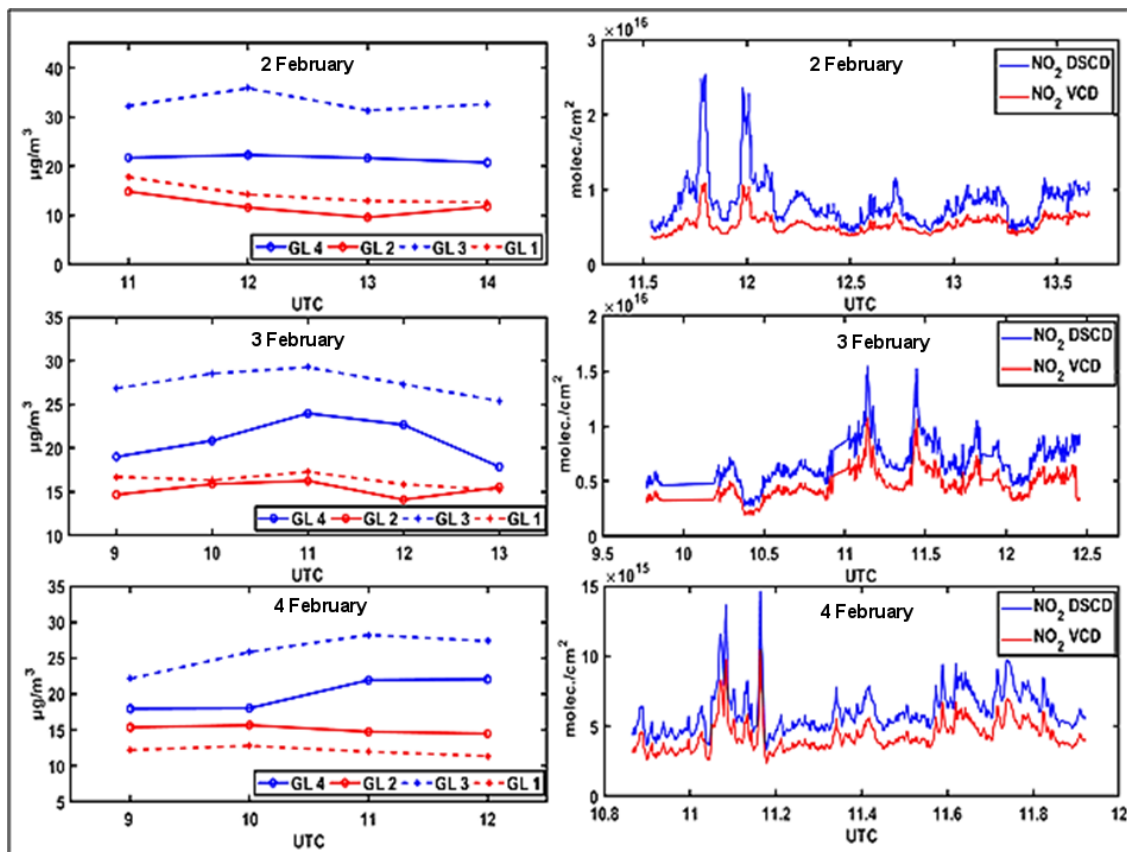


**Figure 4.8:** Variation of NO<sub>2</sub> DSCD and VCD extracted from DOAS observations (right) and NO<sub>2</sub> concentrations (left) recorded between 9-14 UTC in Galati (B1 Rosu et al. 2016).

Figure 4.8 shows the comparison between the NO<sub>2</sub> concentration values recorded by the GL stations and the values of the tropospheric vertical column densities extracted from the ZSL - DOAS mobile observations. It is noted that both DOAS observations and those of GL stations record high NO<sub>2</sub> values in the northern zone of the city (GL 3 station).

Using a GIS software a graphical representation was made (presented in Figure 4.9). High NO<sub>2</sub> VCD values can be noticed on the main roads of Galati. On the Galați ring road during the first 2 days. NO<sub>2</sub> VCD values were recorded between 10.7 - 5.3 x 10<sup>15</sup> molecules/cm<sup>2</sup>. The interval in which these values were observed coincides with the times when traffic is intense. On February 4th, a weekend day, there was a sharp drop in the NO<sub>2</sub> quantities measured on the same route within the same timeframe. The only area that remained high polluted was the area located near the ArcelorMittal Iron Factory that was detected in all three days by the DOAS mobile system. It can also be seen on using the color code that the GL\_3 station in the north of the city recorded the highest values of the NO<sub>2</sub> concentration in the time interval in which the DOAS mobile determinations were made.



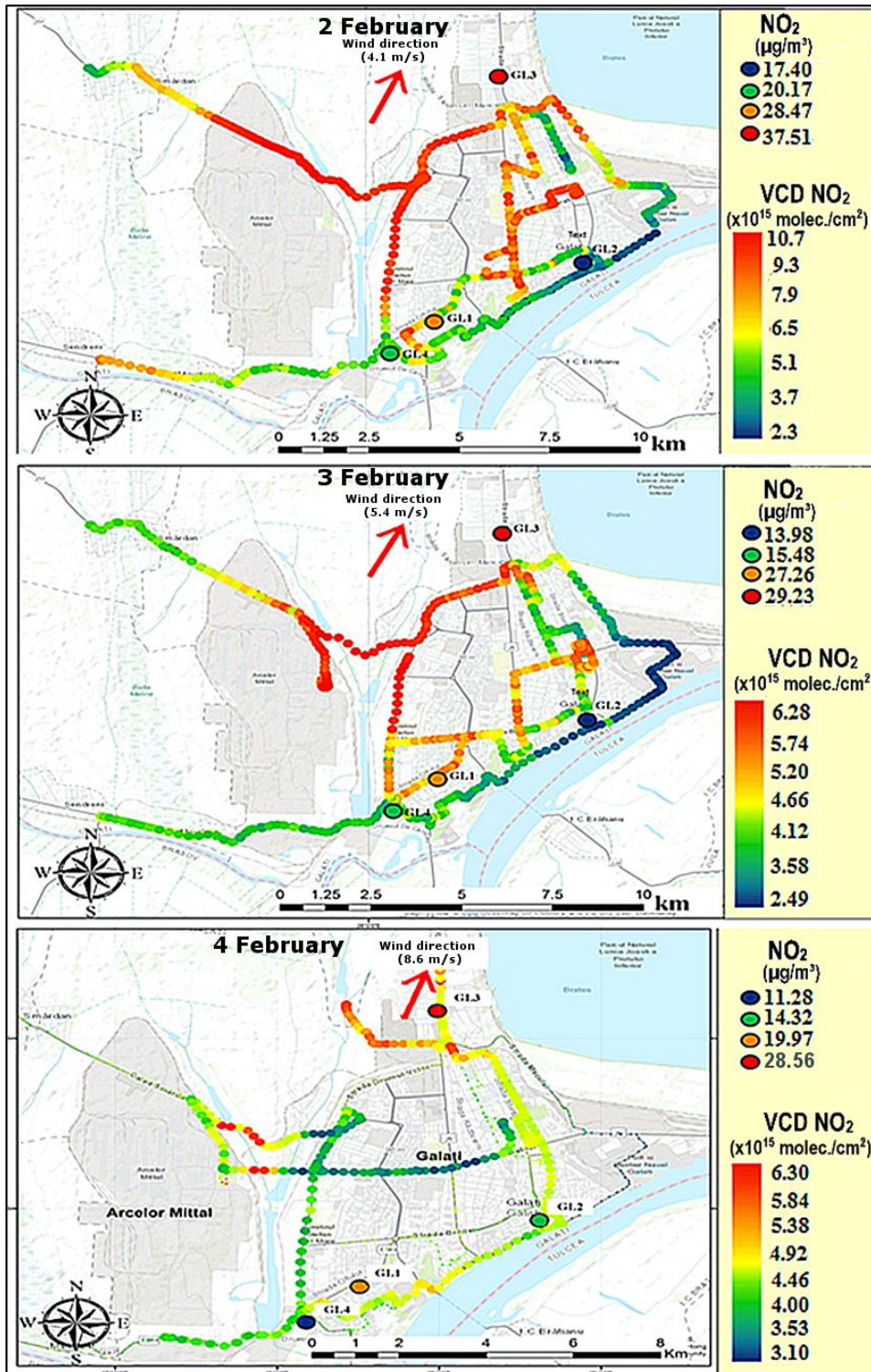


**Figure 4.9:** NO<sub>2</sub> VCD maps obtained from DOAS mobile observations in zenith geometry conducted between February 2 and 4, 2017. The average NO<sub>2</sub> concentration values recorded by air quality monitoring stations in Galati during the DOAS observations (**B1 Roşu et al 2016**).

The NO<sub>2</sub> VCD average resulting from the same time interval for the three DOAS observation days was used to generate three prediction models for the dispersion of tropospheric NO<sub>2</sub> content. These dispersion prediction maps were made using IDW and Kriging interpolation methods (KOP and KUC) as illustrated in Figure 4.10. The total area on which the distribution prediction was made comprises a square with a surface area of 225 km<sup>2</sup>. The dispersion models used integrate and mediate DOAS values in rasterized surfaces where the distribution of the troposphere vertical is uniform for the size of a pixel of the generated maps.



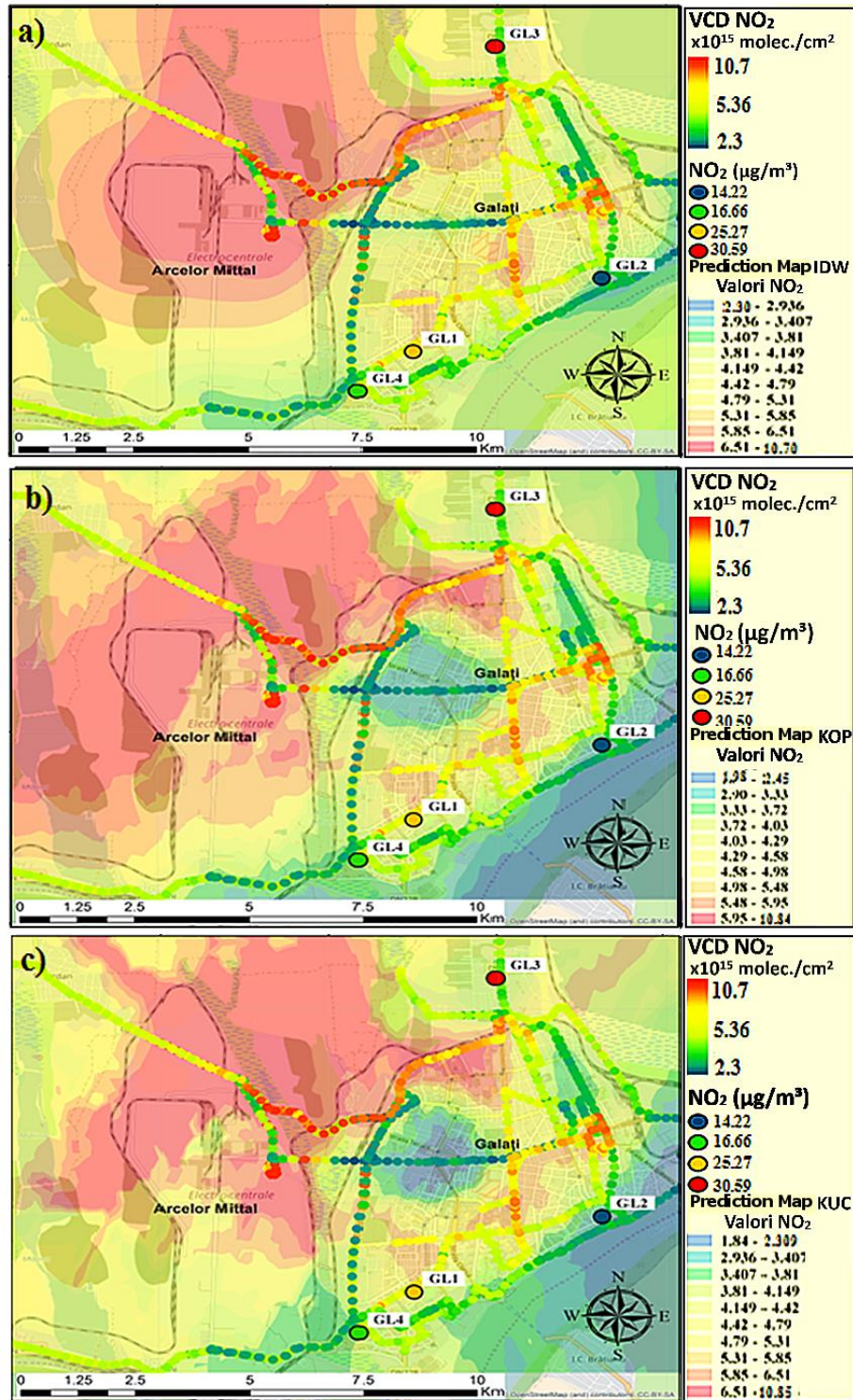


**Figure 4.10:** NO<sub>2</sub> dispersion prediction maps generated based on DOAS mobile observations (NO<sub>2</sub> VCD) made by interpolation methods: a) IDW, b) KOP c) KUC (B1 Red et al 2016).

In Figure 4.10 it is noted that in all prediction maps the major source of NO<sub>2</sub> emissions in Galati is represented by the ArcelorMittal Steel Factory. Values emission made by local traffic have "flattened" values due to the DOAS observations mediation but also due to the effects of rasterization of the tropospheric layer interpolated by different methods. This flattening is displayed differently for each raster. In the southern part of Galati municipality, in all three prediction models, low values of the NO<sub>2</sub> troposphere, values that are also observed in the VCD measured directly by the DOAS system.

The statistical analysis of the measured and predicted VCD of the three interpolation methods show that IDW is the most appropriate prediction model of the distribution of tropospheric NO<sub>2</sub> columns of the analyzed area, followed by KUC and KUP model. The values recorded for correlation factors between predicted and measured values are presented in Table 4.4.

**Table 4.4:** Correlation coefficients between mobile DOAS observations and dispersion prediction maps

Metodă de interpolare	Rădăcina pătratică (R <sup>2</sup> )	Factor de corelare Pearson (ρ)
DOAS vs IDW	0.717	0.847
DOAS vs KOP	0.604	0.777
DOAS vs KUC	0.699	0.836

### 4.3.3 Conclusions

In this study we presented a series of DOAS mobile observations made in same time interval in Galati between 2 and 4 February 2017. These determinations are complemented by comparison with NO<sub>2</sub> concentrations values recorded by the local air quality monitoring stations and presented in relation to the wind direction. Using GPS coordinates and a geographic information system we obtained maps of the spatial distribution of NO<sub>2</sub> by interpolation of DOAS observations results.

The GIS spatial representation according to the GPS coordinates of the values obtained for NO<sub>2</sub> VCD from the mobile DOAS observations and those measured by the GL stations presents the ArcelorMittal Steel Factory as the main source of NO<sub>2</sub> emissions in Galati. Other major sources are the mobile sources generated by road traffic on the main roads. By mediating the demined NO<sub>2</sub> VCD values for the 2 - 4 February period, three local NO<sub>2</sub> dispersion prediction maps were obtained based on two interpolation methods: IDW and Kriging. All maps have indicated that the main source of NO<sub>2</sub> emissions in Galati is the steel factory. Only a few traffic sources have been identified within the city. The evolution of NO<sub>2</sub> emissions determined in this campaign shows that urban population activity has a significant impact on how air pollution is detected with NO<sub>2</sub>. This is evidenced by the effect of "end of the week" phenomenon. By statistical analysis of the results obtained from interpolation of DOAS observations, it has been established that the dispersion prediction map described by the IDW method is most appropriate in presenting NO<sub>2</sub> emission prediction distributions.

## 4.4 Determination of the tropospheric NO<sub>2</sub> densities using DOAS tehnique on board of a vehicle in Eastern Europe

### 4.4.1 Methodology

In this section are presented results of ZSL - DOAS mobile measurements carried out in Eastern Europe using the ZSL - DOAS UGAL system. DOAS mobile observations were made between 2015 and 2016 in Romania, Bulgaria, Moldova and Greece. The total route of ZSL - DOAS determinations equals 1400 km and is shown in Figure 4.11 and Table 4.5. For the observations made in Eastern Europe was used a ZSL-DOAS system identical to that used for observations made in Galati.

The recorded spectra were analised using version 3.2 of the QDOAS software (Danckaert et al., 2017).

**Table 4.5:** The detailing of the ZSL-DOAS UGAL mobile track 2015-2016 (L2 Constantin et al., 2017)

Country	Date	DOAS observations tracks	Mileage
Bulgaria	19 May 2016	Graichar - Varna	100 km
Grece	22 March 2016	Agia triada - Alexandropolis	330 km
Romania	24 June 2015	Craiova - Rovinari	90 km
	1 May 2016	Sebeş - Slobozia	470 km
	19 May 2016	Galați – Vama Veche	300 km
Moldavia	5 September 2015	Sărata galbenă - Cricova	70 km



**Figure 4.11:** The route of DOAS observations conducted onboard a motor vehicle in South East Europe (L2 Constantin et al., 2017)

To extract the NO<sub>2</sub> tropospheric content a complex algorithm was used that can be represented by the following relation:

$$VCD_{tropo} = \frac{(DSCD + SCD_{ref})}{AMF_{tropo}} - VCD_{stratoOMI} \quad (4.3)$$

where VCD<sub>tropo</sub> - the NO<sub>2</sub> tropospheric content extracted from the observations of the ZSL DOAS UGAL system, DSCD - the NO<sub>2</sub> content resulting from spectral analysis of spectra recorded by the ZSL - DOAS UGAL system, SCD<sub>ref</sub> - the reference spectrum whose NO<sub>2</sub> content is accurately determined by complementary observations ZSL - DOAS made at dawn and applying Langley-plot for different SZA intervals, AMF<sub>tropo</sub> - air mass factor resulting from successful simulations using UvSpecDisort RTM, VCD<sub>strato</sub> - stratospheric content extracted from the observations of satellite observation of OMI instrument.

The algorithm for the estimation of the tropospheric NO<sub>2</sub> column in the ZSL-DOAS observations is highly complex due to the multiple steps required to determine each of the parameters used. Each step of determining the parameters is susceptible to introducing an error budget in the final determination of the vertical tropospheric columns of NO<sub>2</sub>.

$$\sigma VCD_{tropo} = \sqrt{\left(\frac{\sigma_{DSCD}}{AMF_{tropo}}\right)^2 + \left(\frac{\sigma_{SCD_{ref}}}{AMF_{tropo}}\right)^2 + \left(\frac{\sigma_{SCD_{strato}}}{AMF_{tropo}}\right)^2 + \left(\frac{\sigma_{SCD_{tropo}}}{AMF_{tropo}^2} * \sigma_{AMF_{tropo}}\right)^2} \quad (4.4)$$

The uncertainty of determination of VCD<sub>tropo</sub> NO<sub>2</sub> introduced by relation 4.4 is between 20-25%.



#### 4.4.2 Comparison of ZSL - DOAS mobile observations with satellite observations of the sensor OMI in Eastern Europe

Eroneous values due to field obstruction (FOV) of the ZSL- DOAS UGAL system were eliminated using spectral analysis results for RMS and  $O_4$ . These spectral analysis results for DSCD  $O_4$  and RMS are used to filter the anomalies of DSCD  $NO_2$  spectra (very low or extremely high values). Since the diurnal variation of DSCD  $O_4$  and RMS density columns is very low, a verification of recorded  $NO_2$  values can be made by identifying spectral anomalies. Thus, the erroneous values of FOV obstruction densities of  $NO_2$  molecules can easily be filtered out.

In Figure 4.12 we can observe the variations of  $NO_2$  extracted from the spectra recorded in June 2015 near the power plant in Craiova, Isalnita, Turceni and Rovinari. For the route performed on the territory of Romania, the highest value of the tropospheric VOC  $NO_2$  column of  $1 \times 10^{17}$  molecules/cm<sup>2</sup> was recorded by the ZSL - DOAS UGAL mobile system near the Plant from Turceni, which is 10 times higher than the average DOAS observations made on the same day and are comparable to highly polluted areas such as Beijing, China (Hendrick et al., 2014).

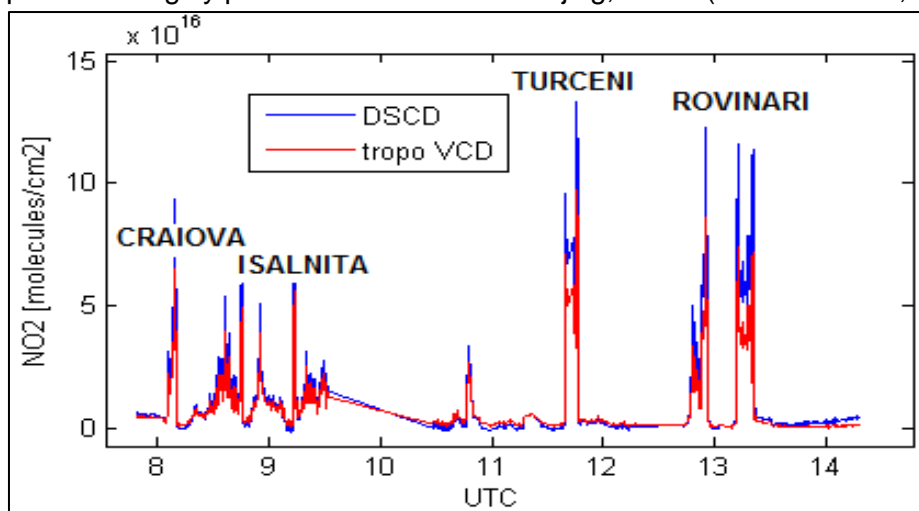


**Figure 4.12:** The diurnal variation of DSCD and  $VCD_{\text{tropo}} NO_2$  determined by ZSL - DOAS mobile observations in Jiu Valley, Romania on June 24, 2015 (L2 Constantin et al., 2017).

In Romania the satellite observations of the OMI instrument recorded values of  $NO_2$   $VCD_{\text{tropo}}$  between  $2.65 - 3.01 \times 10^{15}$  molecules/cm<sup>2</sup>, the uncertainty being estimated between  $0.95 - 1.24 \times 10^{15}$  molecules/cm<sup>2</sup> using DOMINO v2.0.

Figure 4.13 shows the comparison in color codes between satellite observations and determinations with the ZSL - DOAS UGAL system performed on routes made in Romania, Bulgaria, Greece and Moldova intersecting important cities from Eastern Europe. The most interesting results were obtained by ZSL - DOAS observations performed on 1 May 2016 in the border zone of Bucharest on the DNCB / Șoseau Odăii National Road, where a maximum value of the vertical tropospheric column of  $8(\pm 1.05) \times 10^{15}$  molecules/cm<sup>2</sup>. Values and errors of  $NO_2$  VCD determination observed by the OMI satellite instrument on this day were extracted from pixels covering the entire area of Bucharest and show a value of  $5.9 (\pm 2.87) \times 10^{15}$  molecules / cm<sup>2</sup>.

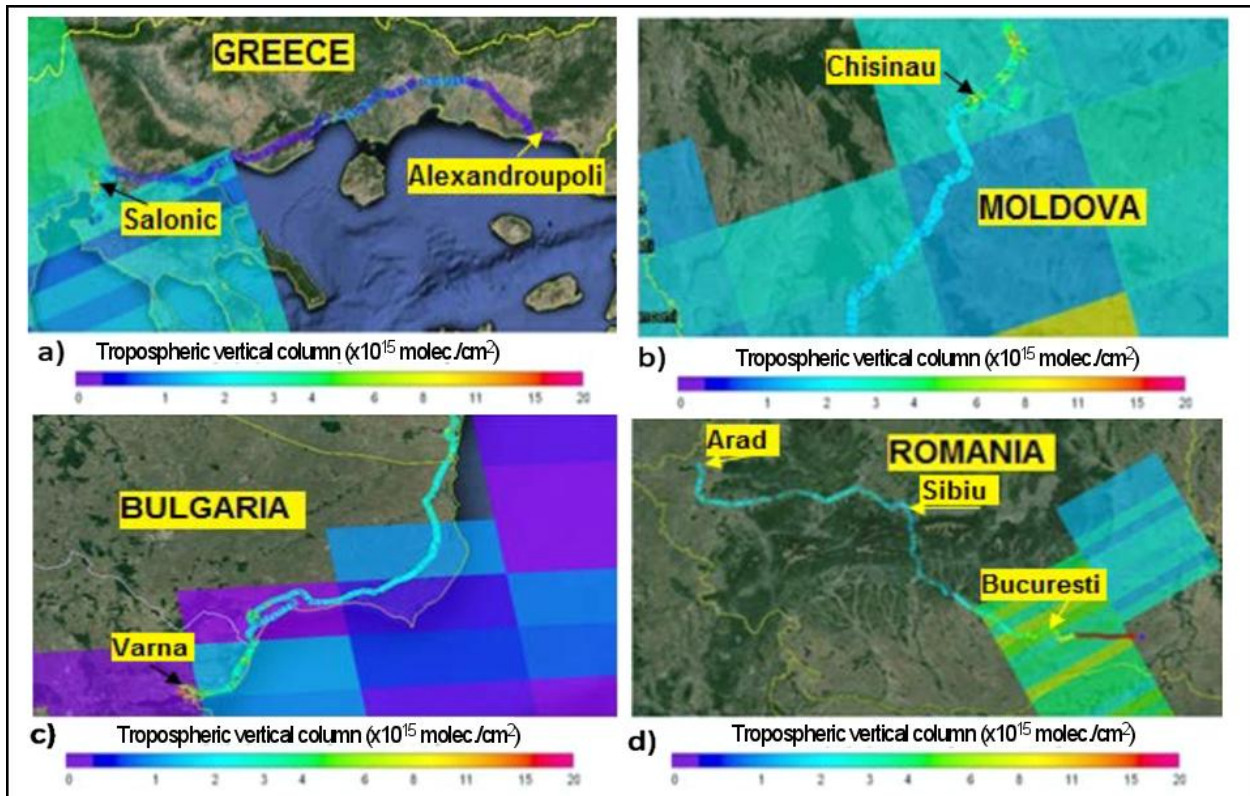


**Figure 4.13:** Comparison of the NO<sub>2</sub> VCD observed in Eastern Europe by the ZSL - DOAS mobile system compared to the observed by the OMI satellite sensor above the routes made in: a) Greece b) Moldova c) Bulgaria d) Romania (**L2 Constantin et al., 2017**)

Figure 4.13 illustrates the spatial distribution of the tropospheric density columns for NO<sub>2</sub> extracted from the observations of the DOAS mobile system and those of the OMI satellite sensor. The tropospheric NO<sub>2</sub> content detected near the main cities encountered on the observation track by both the ZSL - DOAS UGAL system and the OMI instrument are shown in Table 4.6.

Mobile DOAS observations recorded inside the spatial mapping pixels observed by the OMI satellite sensor were mediated according to the pixels corners coordinates. For major urban agglomerations, e.g. Bucharest and Thessaloniki there is a good concordance between the observations made by the OMI from space and the ZSL - DOAS observations from the ground. High NO<sub>2</sub> VCD<sub>tropo</sub> values can be observed in near-urban areas indicating that urban agglomerations have a major impact on the tropospheric NO<sub>2</sub> emission budget. The mean NO<sub>2</sub> VCD<sub>tropo</sub> observations on the ground indicate that the OMI sensor underestimates NO<sub>2</sub> from the tropospheric columns. A first explanation is given by the fact that the spatial resolution of the OMI satellite instrument is large (13x24 km<sup>2</sup>) compared to the mobile system (116 m<sup>2</sup>) so that a pixel of the satellite instrument represents a mean between the high values close to the source of NO<sub>2</sub> and the smaller ones in its neighborhood

**Table 4.6:** NO<sub>2</sub> content extracted from mobile ZSL-DOAS observations and observations of the OMI satellite instrument (L2 Constantin et al., 2017) **(L2 Constantin et al., 2017)**

Town	Date	Averaged NO <sub>2</sub> VCD <sub>tro</sub> (x10 <sup>15</sup> molec./ cm <sup>2</sup> )	Time interval of ZSL - DOAS UGAL (UTC)	OMI NO <sub>2</sub> pixel value (x10 <sup>15</sup> molec./cm <sup>2</sup> )	OMI Overpass (UTC)
Arad (RO)*	01.05.2016	2.12(±0.42)	8.30-8.58	n/a	n/a
Braila (RO)	19.05.2016	12.6(±0.26)	7.60-8.05	1.62(±0.95)	11.61
Bucuresti (RO)	01.05.2016	4.11(±0.61)	15.81-16.53	5.94(±2.87)	10.26
Constanta (RO)	19.05.2016	6.02(±1.21)	10.28-10.41	1.21(±0.88)	11.61
Craiova (RO)	24.06.2015	23.4(±4.4)	7.91-8.23	2.95(±0.95)	11.01
Galati (RO)	19.05.2016	10.3(±2.74)	6.88-7.51	0.86(±0.75)	
Isalnita (RO)	24.06.2015	10.9(±3.45)	8.39-9.51	2.95(±0.95)	11.01
Pitesti (RO) *	01.05.2016	2.09(±0.49)	14.8-14.97	n/a	n/a
Rovinari (RO)	24.06.2015	15.4(±3.56)	12.72-13.55	3.0(±1.24)	11.01
Sebes (RO) *	01.05.2016	3.11(±0.77)	11.41-11.81	n/a	n/a
Sibiu (RO) *	01.05.2016	1.69(±0.34)	12.37-12.48	n/a	n/a
Turceni (RO)	24.06.2015	15.4(±2.77)	10.50-12.01	2.65(±0.95)	11.05
Chisinau (MD)	05.09.2015	3.43(±0.68)	13.84-14.06	1.56(±0.64)	10.99
Albena (BG)	19.05.2016	3.30(±0.59)	13.84-13.91	0.05(±0.95)	11.61
Varna (BG)	19.05.2016	5.82(±0.47)	15.81-16.53	2.14(±1.58)	11.61
Alexandroupoli (GR)*	22.03.2016	0.92(±0.24)	16.29-16.42	n/a	11.01
Kavala (GR) *	22.03.2016	0.78(±0.13)	14.67-14.81	n/a	11.01
Komotini (GR) *	22.03.2016	1.23(±0.19)	15.55-15.79	n/a	11.01
Thessaloniki (GR)	22.03.2016	5.44(±0.84)	13.21-13.45	5.66(±1.56)	11.01

#### 4.4.3 Conclusions

This subchapter presents an extensive study of the spatial and temporal distribution of the NO<sub>2</sub> content of the troposphere observed with a DOAS system aboard a car in Eastern Europe. Determination of the tropospheric NO<sub>2</sub> content requires complementary observations ZSL - DOAS stationary at sunrise and multiple simulations of AMF mass factor. The analysis was statistically determined the importance of these parameters used in the calculation of the tropospheric VCD NO<sub>2</sub> determination errors. The statistical calculation demonstrated that the errors of determination are between 20 - 25% and are largely due to spectral analysis, which is determined by the QDOAS software.

The NO<sub>2</sub> content of the tropospheric columns was determined from ground observations using the ZSL - DOAS UGAL system and compared with the satellite observations of the OMI UV - Vis satellite instrument. It has been found a good correlation between the DOAS observations made from space and those performed on the ground especially for large urban agglomerations (Bucharest and Thessaloniki). We showed that for point sources, under atmospheric stability, the OMI satellite instrument sub-estimates the tropospheric amount of NO<sub>2</sub> on the other hand for spatial extended sources (cities) the determined quantity is close to what was recorded from the ground (ZSL - DOAS observations)

We can conclude that both ZSL - DOAS UGAL system and the OMI sensor are sensible tools for determining the NO<sub>2</sub> tropospheric load in areas where anthropogenic sources (industrial platforms and large cities) are present.

#### 4.5 ZSL - DOAS observations made on board a vehicle for the determination of NO<sub>2</sub> tropospheric VCD in Europe

In this subchapter will be presented the results of the longest DOAS mobile observation tracks conducted in Europe for the determination of the tropospheric nitrogen dioxide (article in

preparation). The measurements took place between 13 September - 2 October 2016 in: Romania, Hungary, Austria, Germany, Netherlands, Belgium, Luxembourg, France, Spain, Portugal, Italy, Slovenia. These measurements were carried out during the DEDICAT campaign, being the result of main objective of the **PN1** project. The total route covered approximately 11,000 km, of which 5600 km are ZSL - DOAS observations. Details of the ZSL - DOAS routes and the period during which they were performed can be found in Table 4.7. All observations were made in clear sky or with a cloud coverage of 10 – 20%.

**Table 4.6:** Routes traveled by ZSL - DOAS UGAL in Eastern Europe

Country	Date	Track	Measured distance (km)
Hungary- Austria	13.09.2016	Zseged – Budapesta – Bratislava - Viena	580
Germany - Netherlands	14.06.2016	Mainz - Koln - Ninjmegeen – Utrech-Lopik	500
Netherlands -Belgium- Luxembourg	25.09.2016	Utrech-Amsterdam – Antwerp – Bruxeles - Luxembourg	620
France	26.09.2016	Dijon-Paris – Orleans - Limoges	680
France- Spain	27.09.2016	Toulouse - Zaragoza	480
Spain	28.09.2017	Madrid - Salamanca	500
Spain -Portugal	29.09.2017	Vitoria - Gasteiz – Valadolid - Porto	650
France	30.09.2018	Toulouse - Marseille - Monaco	580
Italy-Slovenia	01.10.2016	Milano – Venice – Trieste - Zagreb	550
Romania	02.10.2016	Arad - Sebeş – Deva - Piteşti	470

All the spectra were recorded with a ZSL - DOAS system similar to that used in observations made in Galati and Eastern Europe. During the measurement campaign, the ZSL-DOAS UGAL system recorded a number of 18,000 spectra that were analyzed using the QDOAS software.

The recorded spectra were analyzed using the QDOAS software results being expressed as DSCD NO<sub>2</sub> and represented using a GIS sotware in Figure 4.16 in the form of ZSL - DOAS UGAL observations map.

Figure 4.14 illustrates high values of NO<sub>2</sub> DSCD recorded in areas near large urban agglomerations. The highest NO<sub>2</sub> values in the apparent columns were recorded on the Paris ring on September 26, 2016, values ranging from 8.36 to 6.8 x 10<sup>16</sup> molecules/cm<sup>2</sup>. The lowest values range from 3.5 to 0.13 x 10<sup>16</sup> molecules/cm<sup>2</sup> were recorded near the border between France and Luxembourg, at the border between Spain and France (mountain area), eastern Portugal, western Spain and western Romania. Low values of DSCD NO<sub>2</sub> have been detected by the ZSL - DOAS UGAL system in mountain areas or areas near ocean where maritime breezes act (Iberian Peninsula, coasts of the Tyrrhenian and Adriatic seas). Urban areas were generally characterized by high NO<sub>2</sub> DSCD values ranging from 4.93 to 8.36 x 10<sup>16</sup> molecules/cm<sup>2</sup>.

The recorded values of DSCD NO<sub>2</sub> for the entire ZSL - DOAS observation campaign were converted to VCD<sub>tropo</sub> using the algorithm utilized for observations made in Eastern Europe.



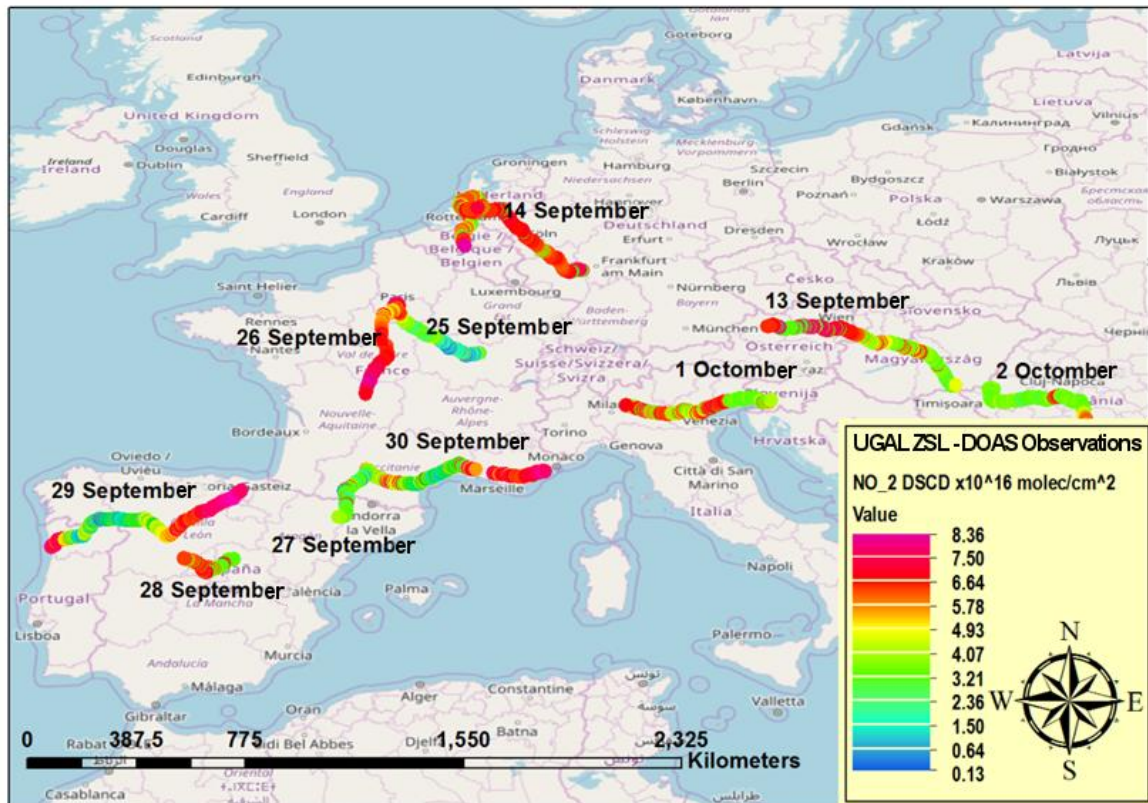


Figure 4.14: The DSCD distribution map NO<sub>2</sub> observed by the ZSL - DOAS UGAL system during the DEDICAT campaign

#### 4.5.1 Comparison with observations of the OMI satellite instrument

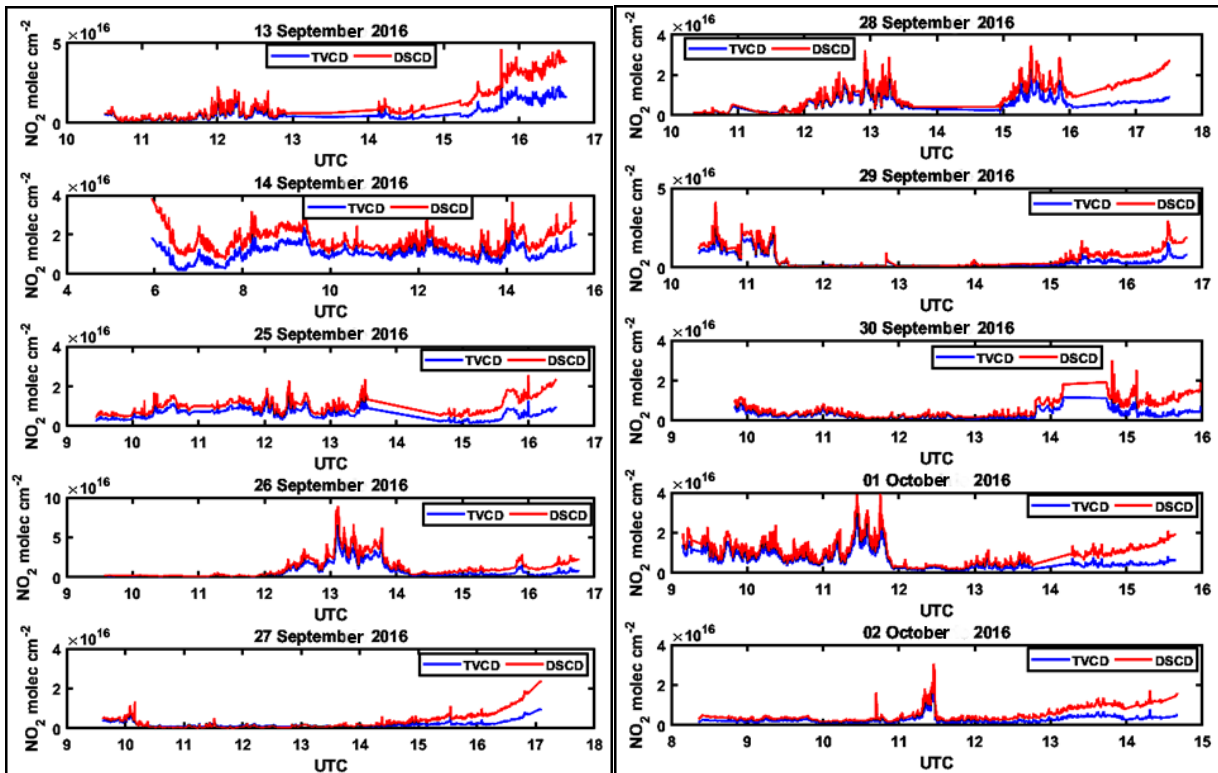
Results expressed as NO<sub>2</sub> VCD<sub>tropo</sub> derived from ZSL - DOAS mobile observations were compared with determinations of the most advanced satellite instrument, OMI. Satellite determinations were downloaded from the OpenDap / NASA portal as georeferenced global raster (netcdf or .n4 files). The tropospheric amount of NO<sub>2</sub> extracted from OMI observations was converted by recombining the pixels to a resolution of 25 x 25 km<sup>2</sup>. DOAS satellite observations in nadir geometry for a given geographic coordinate set are done once a day at about the same time. On the other hand, ZSL - DOAS UGAL system observations were made continuously.

Figure 4.15 illustrates the diurnal variations in the density of NO<sub>2</sub> molecules from the troposphere vertical columns extracted from the 10 days of ZSL - DOAS observations. High values of NO<sub>2</sub> VCDs were recorded between 10:30 and 15:30 UTC when the mobile system was passing by fixed sources generally represented by large urban agglomerations.

High NO<sub>2</sub> DSCD and VCD<sub>tropo</sub> values, recorded at sunset (15-18 UTC) due to the integration of a larger number of NO<sub>2</sub> molecules at the passing of solar radiation through all the layers of the atmosphere. During this timeframe, the trajectory of solar radiation increases with the sun's descent on the celestial vault (SZA).

Between 12 and 13 UTC, overlapping of the NO<sub>2</sub> values recorded by DSCD and VCD was identified. This demonstrates that the AMF factor used in the determination of NO<sub>2</sub> VCD shows values close to real ones, where the ratio of the SCD to the vertical (VCD) at SZA 0° is equal to 1.

UTILIZATION OF THE DIFFERENTIAL OPTICAL ABSORPTION SPECTROSCOPY IN QUANTIFICATION OF ATMOSPHERIC POLLUTION WITH NITROGEN DIOXIDE



**Figure 4.15:** Variations of  $\text{NO}_2$  DSCD and  $\text{VCD}_{\text{tropo}}$  extracted from ZSL - DOAS observations made in Europe for September 13 to 2 October..

High  $\text{NO}_2$  VCD values are found close to fixed sources or sources located within cities. Detection of high  $\text{NO}_2$  values by the ZSL - DOAS UGAL system near or at a considerable distance from cities is mainly due to wind dispersion. Also, these values may also be the results of the high road traffic on the routes where the ZSL - DOAS mobile determinations were made. The highest  $\text{NO}_2$  value of  $6.23 (\pm 0.05) \times 10^{16} \text{ molec./cm}^2$  was recorded on the 26th September at 13:06 UTC in the northeast area of Paris. Relatively high  $\text{NO}_2$  values were recorded on the route traveled in Western Europe on the Mainz - Utrecht section on September 14, averaging  $1.87 (\pm 0.04) \times 10^{16} \text{ molec / cm}^2$ . It was noted that the average tropospheric  $\text{NO}_2$  VCD values observed in mountain areas (Toulouse - Zaragoza -  $2.53 \pm 0.04 \times 10^{15} \text{ molec./cm}^2 \text{ NO}_2$ ) and in East of Europe (Arad - Pitesti route -  $2.84 \pm 0.02 \times 10^{15} \text{ molec./cm}^2 \text{ NO}_2$ ), shows values 6 times lower than those recorded in the West of Europe.

To compare the amount of tropospheric  $\text{NO}_2$  recorded by the ZSL - DOAS UGAL system to those recorded by the OMI space sensor was selected only the pixels with their center located at a distance of 10-15 km from the DOAS mobile ground observation route. In order to reduce the differences between the  $\text{NO}_2$  tropospheric  $\text{NO}_2$  content recorded by the OMI sensor and the one detected by the ZSL - DOAS observations, we averaged the  $\text{VCD}_{\text{tropo}}$  values from ZSL - DOAS observations for each satellite pixel that was overlapping. The maximum, minimum and average values recorded by the OMI satellite instrument and the ZSL - DOAS system are shown in Table 4.8.

The routes made on September 13 and September 14 do not overlap with the scans performed by the OMI satellite instrument.

**Table 4.8:** Comparison of the tropospheric NO<sub>2</sub> content detected by the OMI satellite instrument and the ZSL - DOAS UGAL system during the DEDICAT campaign

Instrument/VCD (x10 <sup>16</sup> molec./cm <sup>2</sup> )	NO <sub>2</sub> VCD <sub>min</sub>	NO <sub>2</sub> VCD <sub>max</sub>	NO <sub>2</sub> VCD <sub>mean</sub>	Date	Compared distance (km)
ZSL – DOAS UGAL Sistem	0.05 (±0.01)	3.7 (±0.52)	0.86 (±0.08)	26.09.2016	152
Satellite Instrument OMI	1.87 (±0.85)	3.5 (±1.28)	1.92 (±0.95)	26.09.2017	152
ZSL – DOAS UGAL Sistem	2.31 (±0.29)	2.55 (±0.42)	2.48 (±0.47)	29.09.2017	57
Satellite Instrument OMI	2.55 (±1.03)	2.89 (±0.89)	2.62 (±1.08)	29.09.2018	57
ZSL – DOAS UGAL Sistem	0.07 (±0.02)	4.82 (±0.78)	3.26 (±0.48)	28.09.2016	500
Satellite Instrument OMI	1.52 (±0.89)	4.27 (±1.52)	2.96 (±1.31)	28.09.2017	500
ZSL – DOAS UGAL Sistem	0.02 (±0.008)	4.62 (±0.59)	3.68 (±0.18)	01.10.2016	550
Satellite Instrument OMI	0.93 (±0.44)	3.1 (±1.27)	2.57 (±1.30)	01.10.2016	550
ZSL – DOAS UGAL Sistem	0.07 (±0.01)	4.82 (±0.75)	1.78 (±0.44)	25.09.2016	620
Satellite Instrument OMI	1.47 (±0.58)	3.14 (±1.14)	2.6 (±1.04)	25.09.2016	620
ZSL – DOAS UGAL Sistem	0.08 (±0.02)	3.16 (±0.58)	0.92 (±0.35)	30.09.2016	210
Satellite Instrument OMI	1.57 (±0.88)	2.25 (±1.35)	1.36 (±0.55)	30.09.2016	210
ZSL – DOAS UGAL Sistem	0.08 (±0.03)	3.98 (±0.42)	0.85 (±0.63)	27.09.2016	480
Satellite Instrument OMI	0.37 (±0.18)	1.57 (±0.87)	0.56 (±1.20)	27.09.2016	480
ZSL – DOAS UGAL Sistem	0.01 (±0.008)	4.22 (±0.97)	1.37 (±0.47)	02.10.2016	470
Satellite Instrument OMI	1.06 (±0.68)	2.34 (±1.25)	1.18 (±0.85)	02.10.2016	470

In the case of the ZSL - DOAS observations made on 26 September, Figure 4.16 shows similarities with the OMI determinations. The DOAS UGAL system recorded a mean value of VCD<sub>tropo</sub> NO<sub>2</sub> of 8.64(± 0.43)x10<sup>15</sup> molecule/cm<sup>2</sup>, the mean value of the pixels recorded by the OMI instrument being 1.92(± 0.95)x10<sup>16</sup> molecules/cm<sup>2</sup>. The comparison values only correspond to the temporal overlap of the observations of the 2 instruments performed around 11 UTC.

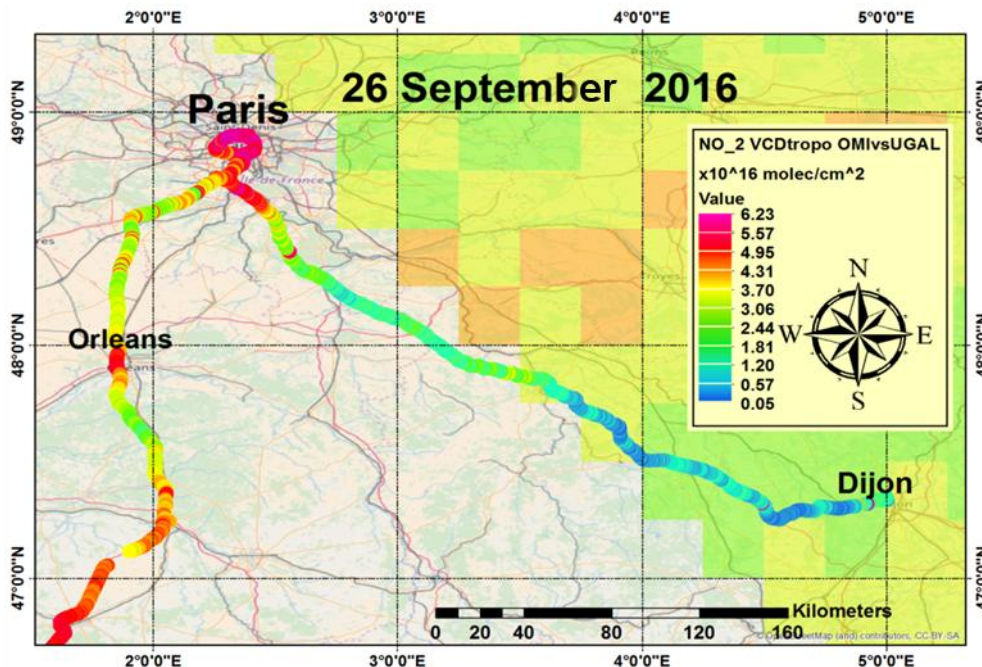


**Figure 4.16:** Comparisons between VCD<sub>tropo</sub> NO<sub>2</sub> observed by the ZSL-DOAS system and the OMI sensor on September 26, 2016

The NO<sub>2</sub> VCD<sub>tropo</sub> values extracted from observations of the ZSL-DOAS system above Porto (29 September) (Figure 4.17) show an average of 2.48(± 0.47)x10<sup>16</sup> molecules/cm<sup>2</sup>. The average nitrogen dioxide of 2.62(± 1.08)x10<sup>16</sup> molecules/cm<sup>2</sup> was determined from the pixels of the OMI instrument recorded along the track of the ground DOAS observations. High levels of nitrogen dioxide pollution have been recorded by the ZSL - DOAS system near major urban



UTILIZATION OF THE DIFFERENTIAL OPTICAL ABSORPTION SPECTROSCOPY IN QUANTIFICATION OF ATMOSPHERIC POLLUTION WITH NITROGEN DIOXIDE

agglomerations such as Porto and Valladolid. The overlay of satellite and ground observations are recorded only in region near the city of Porto.

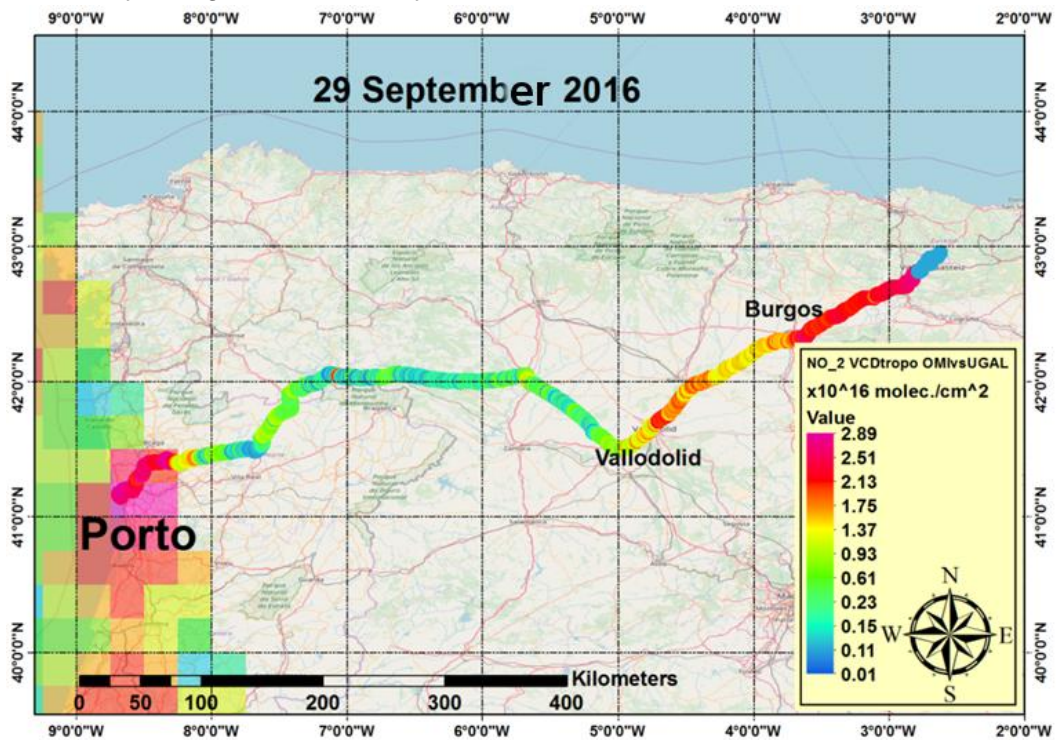


Figure 4.17: Comparisons between  $VCD_{\text{tropo}} \text{NO}_2$  observed by the ZSL-DOAS system and the OMI sensor on September 29, 2016

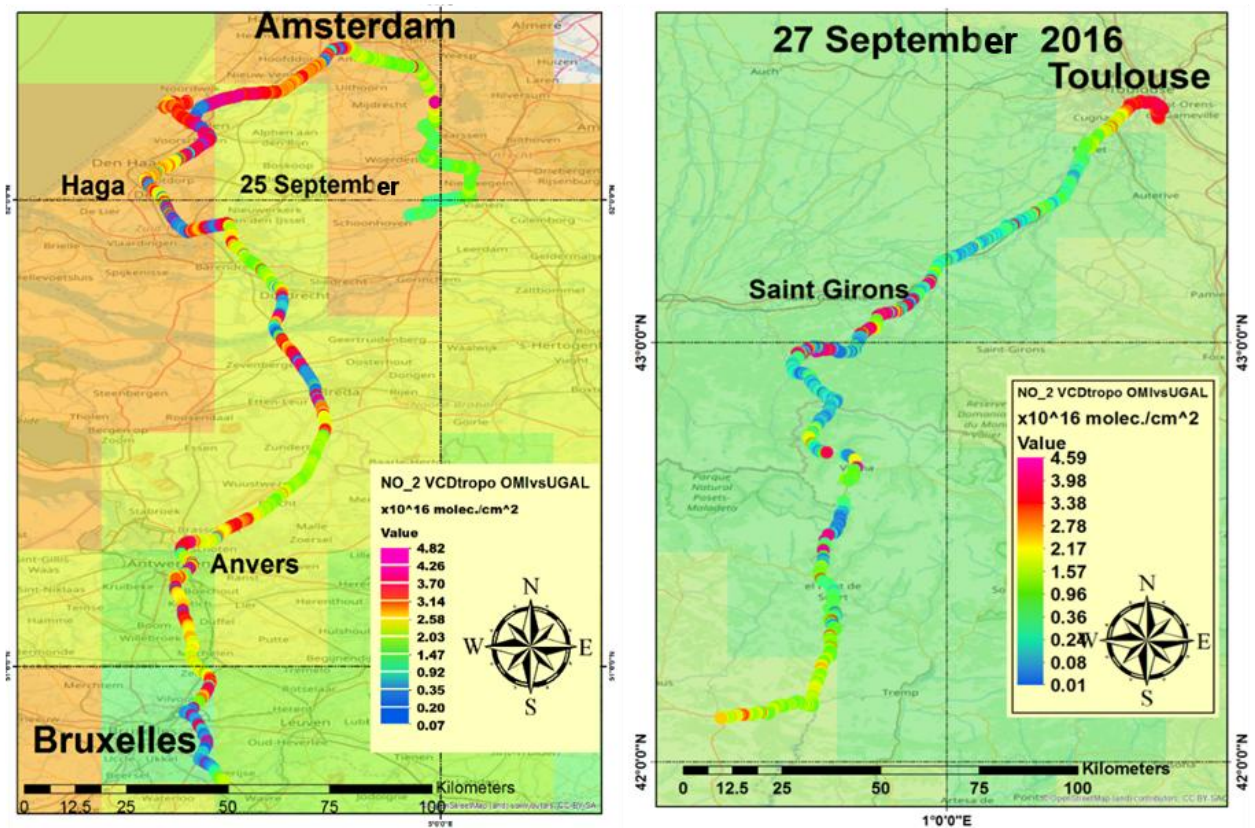
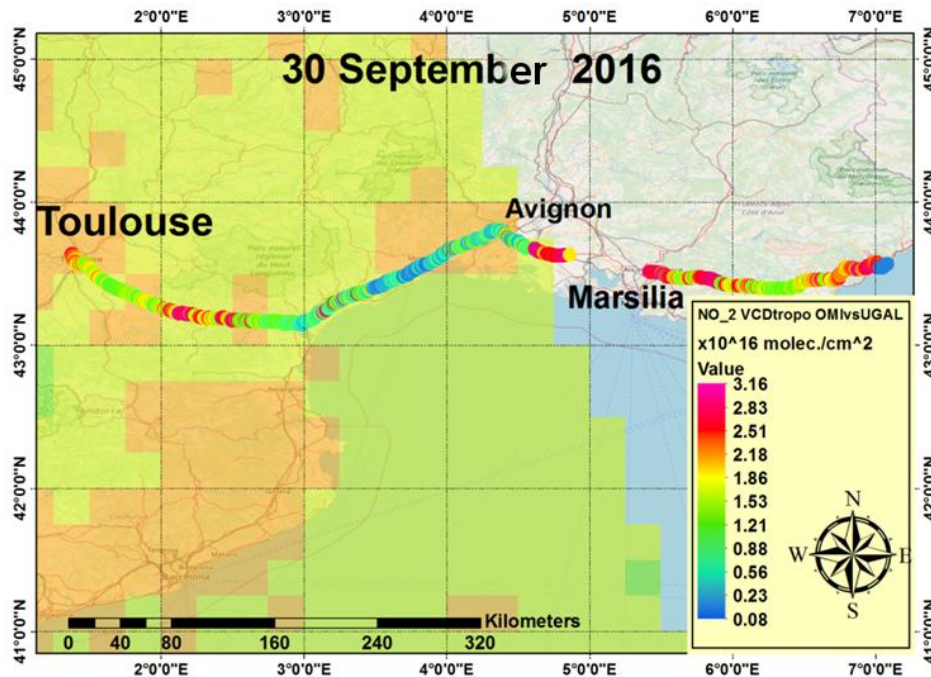


Figure 4.18: Comparisons between  $VCD_{\text{tropo}} \text{NO}_2$  observed by the ZSL-DOAS system and the OMI sensor on September 25 and 27, 2016.



The tropospheric NO<sub>2</sub> content detected by the UGAL mobile system on September 25 (Figure 4.18 left) is not similar to the OMI instrument in the first portion of the route. These observations were made around 9 UTC. The time at which satellite observations were made in this region coincides with the 11-12 UTC interval. The average VCD<sub>tropo</sub> NO<sub>2</sub> recorded by the OMI compared to those recorded by the DOAS measurements shows similar values. On this route, the average VCD<sub>tropo</sub> NO<sub>2</sub> value detected by OMI instrument pixels is  $2.6(\pm 1.04) \times 10^{16}$  molecules/cm<sup>2</sup>. The tropospheric nitrogen content detected by the ZSL - DOAS system shows an average value of  $1.78 (\pm 0.18) \times 10^{16}$  molecules / cm<sup>2</sup>. The large VCD<sub>tropo</sub> NO<sub>2</sub> values recorded by both DOAS systems are found in the area southwest of Amsterdam.

Low VCD<sub>tropo</sub> NO<sub>2</sub> values were detected on the route on September 27 (Figure 4.18 right). The average of ZSL-DOAS observations being equal to  $8.53(\pm 0.63) \times 10^{15}$  molecules / cm<sup>2</sup> of NO<sub>2</sub>. The values determined from the OMI sensor pixels for the same route show an average of  $5.59(\pm 1.20) \times 10^{15}$  molecules/cm<sup>2</sup>. Low values were recorded by both DOAS systems near a mountain natural reservation located on the border between France and Spain. In the case of ZSL - DOAS observations, high values can be observed near the city of Toulouse and sporadically along the route, being caused by local small - scale sources (agglomerations of road traffic).



**Figure 4.19:** Comparisons between VCD<sub>tropo</sub> NO<sub>2</sub> observed by the ZSL-DOAS system and the OMI sensor on September 30, 2016

Figure 4.19 shows high values of VCD<sub>tropo</sub> NO<sub>2</sub> for both DOAS systems near Toulouse, 100 km from it and near Avignon. The average wind direction during this period was predominant in the Southwest. Note that space observations record a displacement of high NO<sub>2</sub> plume to this direction, NO<sub>2</sub> pollution being recorded by the UGAL DOAS system in the same area. The mean NO<sub>2</sub> VCD<sub>tropo</sub> detected by the OMI sensor on the Toulouse - Monaco route is  $1.36(\pm 0.55) \times 10^{16}$  molecules/cm<sup>2</sup>. Observations of ZSL - DOAS overlaps with OMI satellite instrument observations are estimated at an average value of  $0.92(\pm 0.35) \times 10^{16}$  molecules/cm<sup>2</sup> NO<sub>2</sub>.

For the route made on September 28 (Figure 4.20) on the territory of Spain, the ZSL - DOAS UGAL system recorded an average value of tropospheric nitrogen dioxide of  $3.26(\pm 0.39) \times 10^{16}$  molecules/cm<sup>2</sup>. High values ranging from  $4.82$  to  $3.60 \times 10^{16}$  molecules/cm<sup>2</sup> were recorded between 11 - 13 UTC at the border of Madrid city. Inside the metropolis was found a good

correlation between the observations of the OMI instrument with the DOAS mobile system. The average amount of  $\text{NO}_2$  extracted from the spatial observations pixels on the route to Spain is  $2.96 (\pm 1.31) \times 10^{16}$  molecules/cm<sup>2</sup>.

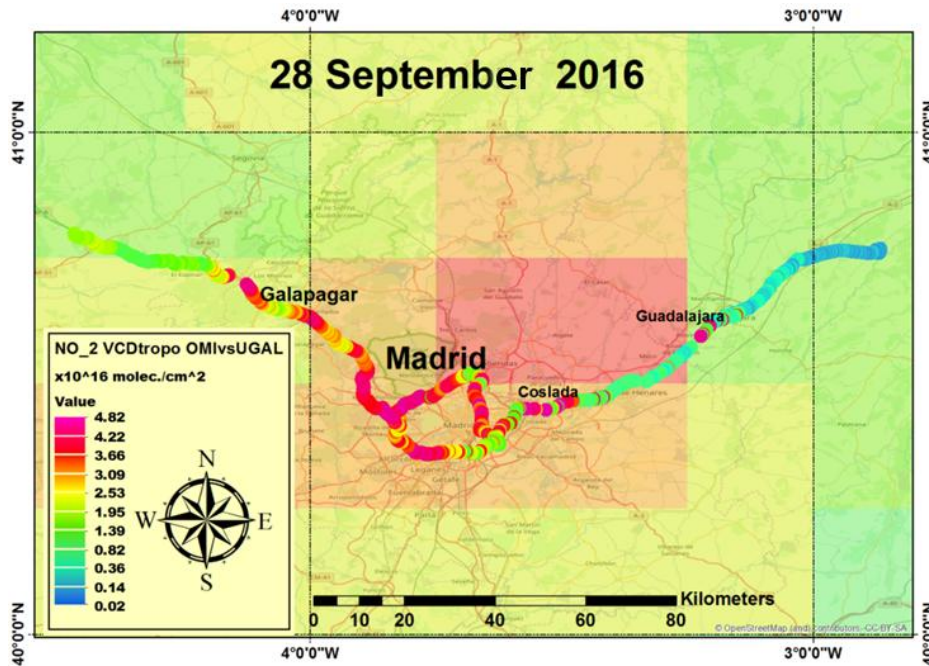


**Figure 4.20:** Comparisons between  $\text{VCD}_{\text{tropo}} \text{NO}_2$  observed by the ZSL-DOAS system and the OMI sensor on September 28, 2016

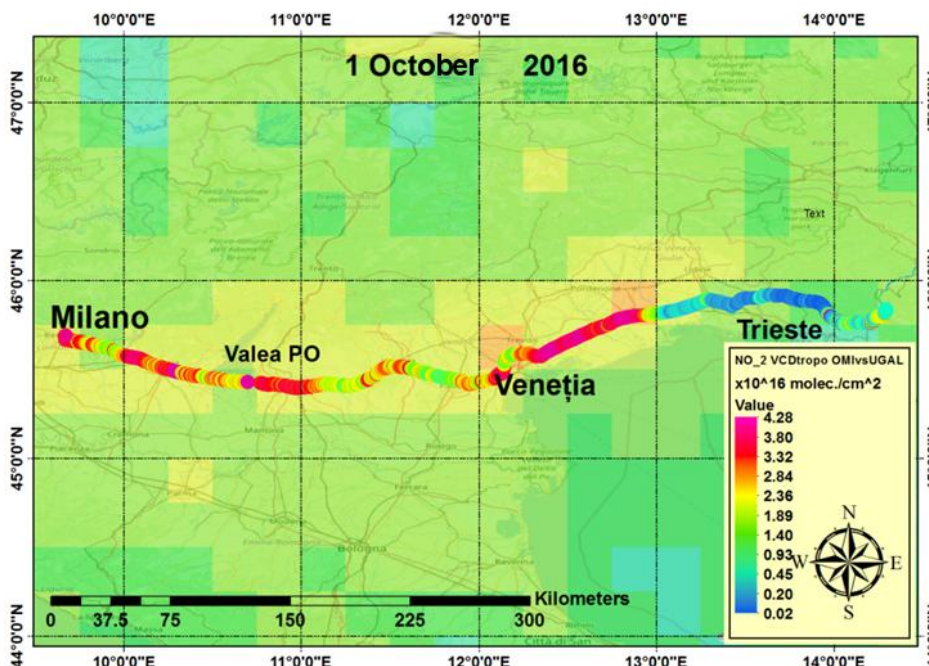


**Figure 4.21:** Comparisons between  $\text{VCD}_{\text{tropo}} \text{NO}_2$  observed by the ZSL-DOAS system and the OMI sensor on October 1, 2016

The measurements made on October 1 (Figure 4.21) aimed at assessing the tropospheric content in the PO valey in Italy, a region recognized for high concentrations of  $\text{NO}_2$  (Boersma et al., 2011). This route includes a series of ZSL - DOAS observations on the Milano - Trieste section where there was found a good correlation with observations of the OMI satellite instrument in the 11 - 13 UTC timeframe. In the PO Valley region, the DOAS mobile system recorded high amounts of  $\text{NO}_2$  average value being approximated to  $3.68(\pm 0.37) \times 10^{16}$



molecules/cm<sup>2</sup>. For the same route, the mean NO<sub>2</sub> loading of the troposphere derived from the OMI sensor pixels showed a value of  $2.57(\pm 1.3) \times 10^{16}$  molecules/cm<sup>2</sup>.

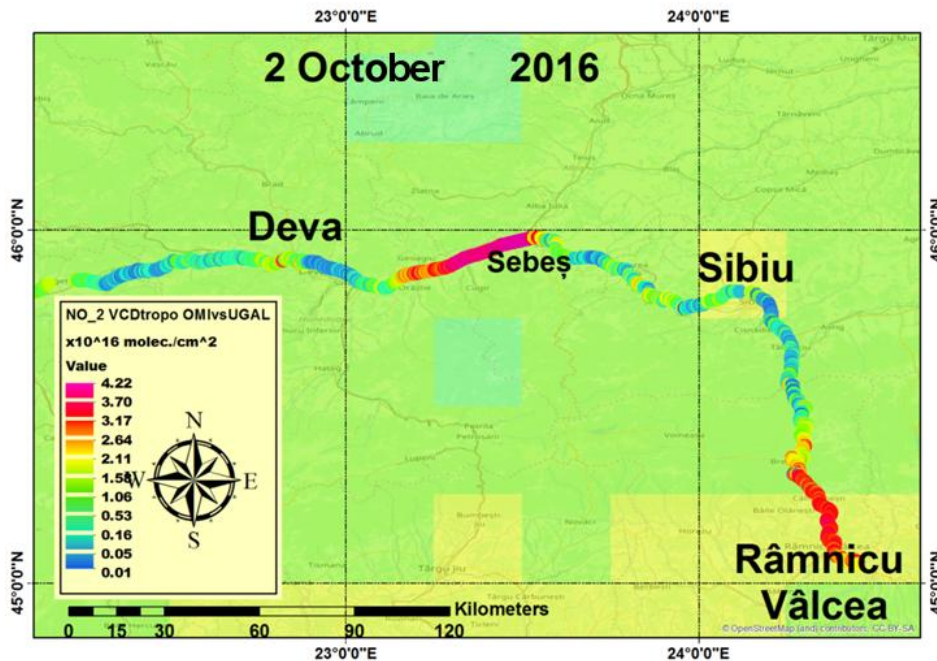


**Figure 4.22:** Comparisons between VCD<sub>tropo</sub> NO<sub>2</sub> observed by the ZSL-DOAS system and the OMI sensor on October 2, 2016

The average tropospheric NO<sub>2</sub> recorded by the OMI satellite instrument for the route performed on October 2 (Figure 4.22) is  $1.18(\pm 0.85) \times 10^{16}$  molecules/cm<sup>2</sup>. This tropospheric amount of NO<sub>2</sub> was determined for the 11-13 UTC time interval. The ZSL-DOAS observations performed in the same time interval detected an average of  $1.37(\pm 0.47) \times 10^{16}$  molecule/cm<sup>2</sup>. Differences between mobile DOAS observations and spatial determinations can be observed between Deva and Sebeș. The high values recorded by the ZSL - DOAS UGAL system between  $4.22 - 2.54 \times 10^{16}$  molecules/cm<sup>2</sup> on this section are probably caused by the industrial objectives belonging to Sebeș Municipality. Due to the wind these emissions were dispersed on a small area along the A1 road. And thus the OMI satellite instrument did not detect similar values to those detected by the DOAS mobile system.

#### 4.5.2 Conclusions

This subchapter presents the longest time series observations made in Europe using a DOAS system in zenith geometry, mounted on board a motor vehicle. Mobile DOAS determinations represent the DEDICAT campaign main objective and were conducted between September 13 and October 2 with a ZSL-DOAS system with the same characteristics as those used for observations in Eastern Europe.

The DSCD NO<sub>2</sub> distribution map for all routes shows high values of the total NO<sub>2</sub> apparent columns near major cities, pollution with NO<sub>2</sub> being more intense in Western Europe than in the East. Low NO<sub>2</sub> values from Europe were recorded in mountain areas or on routes near which there was no major surface NO<sub>2</sub> pollution sources (cities or industrial platforms).

By comparing the NO<sub>2</sub> VCD<sub>tropo</sub> of the two instruments, good correlations were observed for observations made near cities of size comparable to those of an OMI pixel. The degree of correlation between the values observed by the ZSL - DOAS UGAL system and the OMI sensor differs according to the time at which the determinations are made. Similar levels of NO<sub>2</sub> pollution was detected by both DOAS systems near cities: Porto, Madrid, Milan, Venice,

Toulouse, Amsterdam, The Hague, etc. Low  $\text{NO}_2$   $\text{VCD}_{\text{tropo}}$  were recorded on September 27 in a rezevation from the Pyrenees and on October 2 in west of Romania.

Through the comparisons made it can be concluded that the OMI instrument is suestimating the tropospheric  $\text{NO}_2$  content in the areas above the urban agglomerations. OMI satellite instrument has the advantage of studying  $\text{NO}_2$  variations in the troposphere at regional level (due to spatial resolution of  $13 \times 24$  km), while ZSL - DOAS determinations are specialized in the analysis of narrower areas (of a hundred square meters).

The research results obtained from the measurements made by sattelite instrument OMI and ZSL-DOAS UAGAL system in Europe showed that the observations performed by both instruments are complementary into understanding the complexity of spatial-temporal variation of  $\text{NO}_2$  in the troposphere.

## 4.6 DOAS international measurement campaigns

### 4.6.1 AROMAT - 2 measurement campaign

Campania de măsurători AROMAT (The Airborne ROmanian Measurements of Aerosols and Trace gases) (<http://uv-vis.aeronomie.be/aromat/>)\_s-a desfășurat în doua etape. Prima etapă a avut loc în Septembrie 2014 (AROMAT-1), iar cea de-a doua etapă în luna August 2015 (AROMAT-2). Campaniile AROMAT au fost finanțate de ESA( Agenția Spațială Europeană). La această campanie de măsurători au participat 9 echipe de cercetare din 5 țări: România - UGAL, INOE, INCAS; Germania – U. Bremen, U. Berlin, MPIC; Belgia – BIRA; Olanda – KNMI; Norvegia – NILU.

AROMAT Measurement Campaign (<http://uv-vis.aeronomie.be/aromat/>) was conducted in two stages. The first stage took place in September 2014 (AROMAT-1) and the second stage in August 2015 (AROMAT-2). The AROMAT Campaigns were funded by ESA (European Space Agency). At the campaign 9 research teams from 5 countries participated: Romania - UGAL, INOE, INCAS; Germany - U. Bremen, U. Berlin, MPIC; Belgium - BIRA; Netherlands - KNMI; Norway - NILU.

DOAS measurements were conducted during the AROMAT-2 campaign in the summer of 2015 in Bucharest, Craiova, Turceni and Rovinari. These locations were chosen due to the high level of  $\text{NO}_2$  pollution, which can be observed through satellite determinations (Constantin et al., 2016).



Figure 4.23: DOAS mobile systems used in the AROMAT-2 campaign



The three mobile systems was used for the determination of tropospheric NO<sub>2</sub> the systems are presented in Figure 4.23. A comparison on observations of each system was performed based on the color code using a GIS software.

The primary objective of this campaign was to study the amount of pollutants in the troposphere through DOAS airborne instruments dedicated to validating satellite observations.

In this section we present the comparison of DOAS mobile observations made on 28 (Turceni - Rovinari) and 31 August (Bucharest) respectively by the DOAS UGAL, BIRA, MPIC mobile systems.

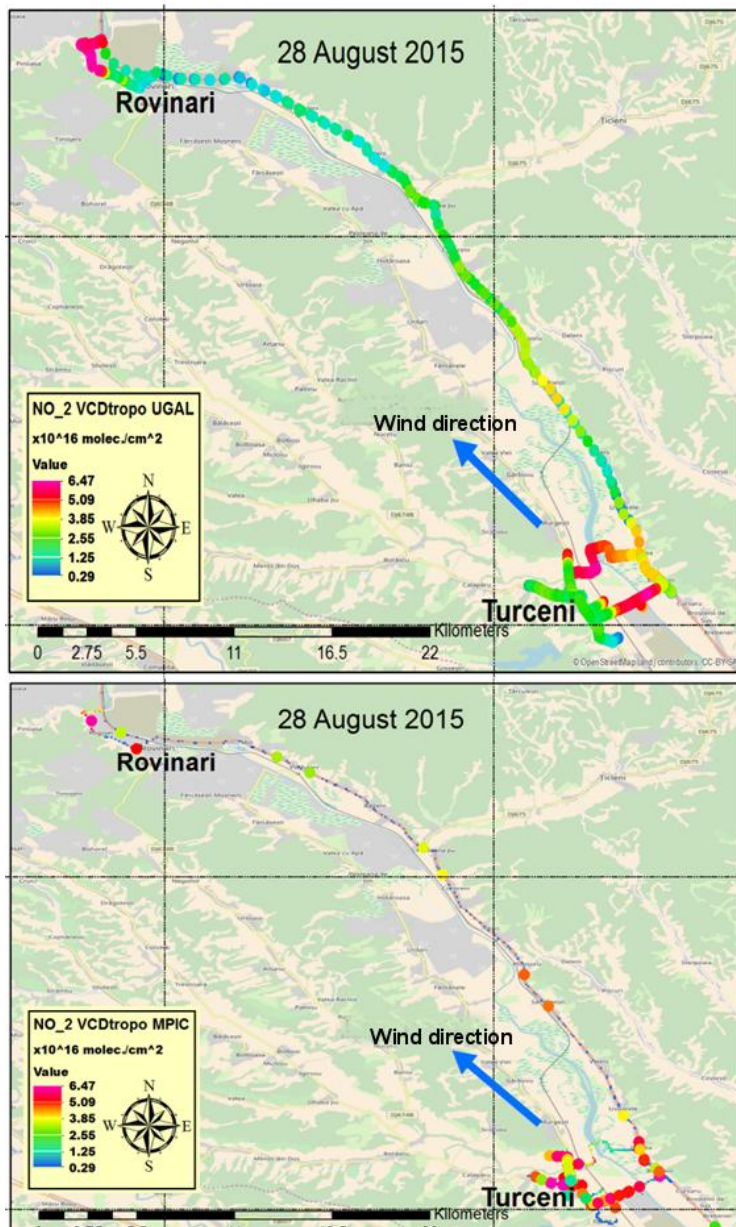


**Figure 4.24:** The comparison between VCD<sub>tropo</sub> NO<sub>2</sub> obtained by the MAX - DOAS MPIC system (bottom image) and the ZSL - DOAS UGAL system (top image) on 28.08.2015 09:00 10:00 UTC

Values are detected within the same time range. The SWING instrument (BIRA) detected in Turceni a maximum NO<sub>2</sub> VCD of  $6.5 \times 10^{16}$  molecules /cm<sup>2</sup>. The values of the ULM DOAS instrument have detected a similar maximum NO<sub>2</sub> VCD of  $4.5 \times 10^{16}$  molecules/cm<sup>2</sup>.

Figure 4.24 compares the NO<sub>2</sub> VCD results extracted from the observations of the UGAL and MPIC systems carried out in the first stage of the AROMAT - 2 campaign on 28.08.2016. The determinations were performed in a clear sky during 6:45 - 10:30 UTC. It can be observed that both systems recorded high values (between  $5.08 - 6.47 \times 10^{16}$  molecules/cm<sup>2</sup>) in the areas near the power plants at Turceni and Rovinari. Inaccuracies between the two DOAS systems arise due to the integration time used by the MPIC system (5 min) and 10 to 30 seconds used by the ZSL - DOAS UGAL system.

On the same day, observations of NO<sub>2</sub> VCD was performed with DOAS instruments mounted on a plane SWING - BIRA (Merlaud et al., 2014) and on a motodeltaplan ULM DOAS - UGAL (Merlaud et al., Constantin et al., 2017). Technical details on these DOAS systems can be consulted at <http://uv-vis.aeronomie.be/aromat/> or in the final report AROMAT 2 (Constantin et al., 2016). By comparing the DOAS observations on the ground with those from the air (Figure 4.25) and the wind direction (Northwest), we can observe similar NO<sub>2</sub> pollution values in the region near power plants located in the Jiu Valley.



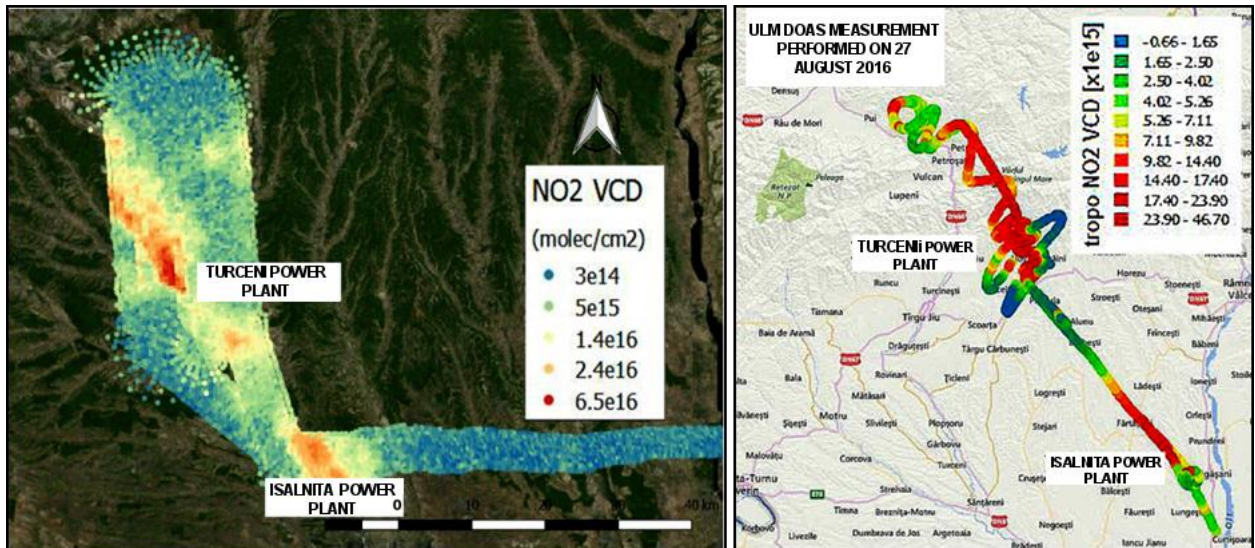


**Figure 4.25:** Airborne observations of the NO<sub>2</sub> made from ULM UGAL systems (right image) and SWING (left image) of 28.08.2015 09: 00-10: 00 UTC (adapted from Constantin et al., 2016)

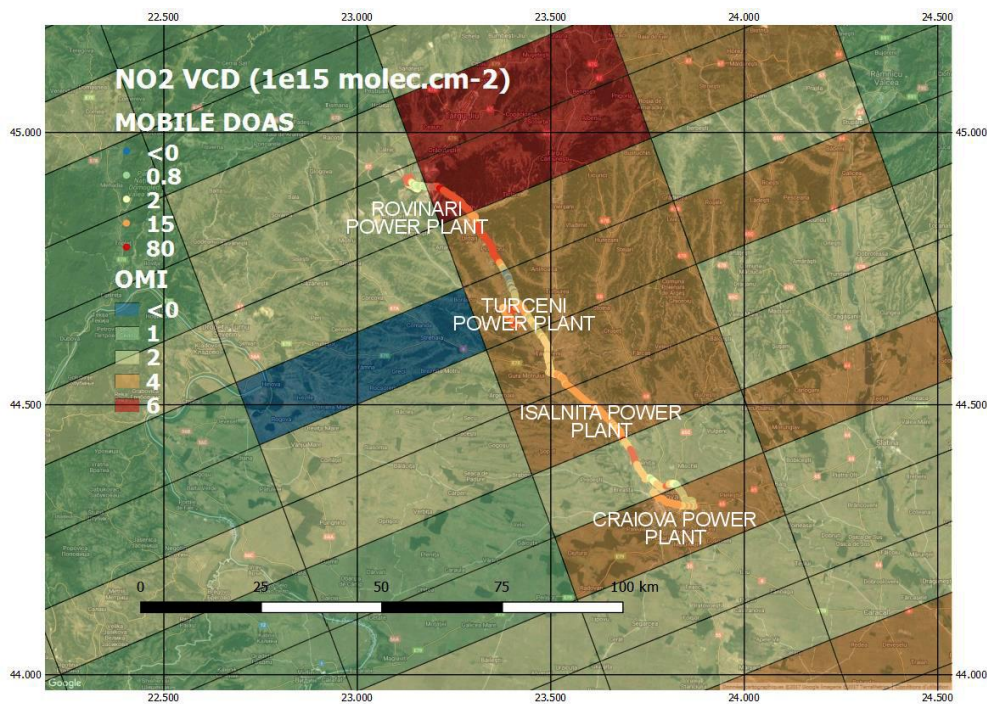


**Figure 4.26:** Comparison of NO<sub>2</sub> VCD extracted from observations of ZSL - DOAS UGAL and OMI systems on 27.08.2015 Craiova - Rovinari (adapted from Constantin et al., 2016)

In Figure 4.26 we can see the comparison in color codes between the satellite observations and the ZSL - DOAS UGAL system in the Jiu Valley region of 27 August 2015. It can be noticed that the values recorded by the satellite instrument are described by the dilution effect given by the extended resolution of detection of the OMI instrument. By comparing the average observations of the total NO<sub>2</sub> column recorded by the OMI satellite instrument on 27 August 2016, we can say that DOAS ground determinations have values comparable to those recorded from space.

The three mobile DOAS systems were operational for determining the tropospheric NO<sub>2</sub> content in Bucharest on 31 August 2016. Figure 4.27 illustrates the routes of the three DOAS mobile systems (left) together with the VCD<sub>tropo</sub> NO<sub>2</sub> values detected (right) for the 08:00 to 14:00 UTC. High values of NO<sub>2</sub> pollution were recorded by the three DOAS systems in the center of Bucharest and on the belt road in the West and North - West directions.



## UTILIZATION OF THE DIFFERENTIAL OPTICAL ABSORPTION SPECTROSCOPY IN QUANTIFICATION OF ATMOSPHERIC POLLUTION WITH NITROGEN DIOXIDE



**Figura 4.27:** Comparison between  $VCD_{\text{tropo}} \text{NO}_2$  detected by the MAX - DOAS MPIC system and the ZSL - DOAS UGAL and BIRA systems on 31.08.2015 in the 09:00: 14:00 UTC (left). Route of the three DOAS systems (right).

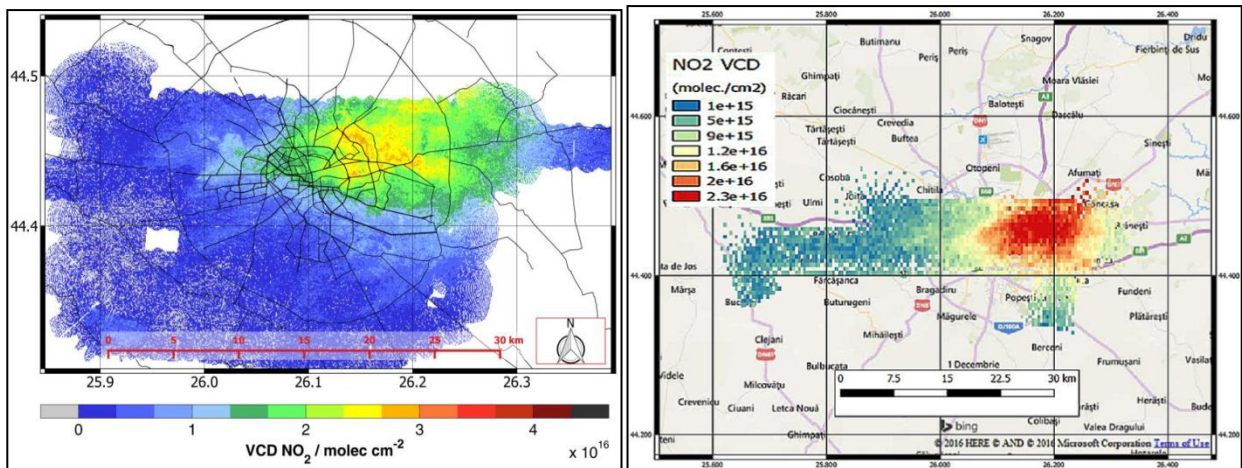


Figure 4.28 : Observations of the  $\text{NO}_2$  VCD's from DOAS systems: SWING (right image), AirMap (left image) on 28.08.2015 UTC 12:30 - 13:45 UTC (adapted from Constantin et al., 2016)).

Vertical  $\text{NO}_2$  column values detected by DOAS airborne instruments show similarities between 12:30 and 13:45 that are shown in Figure 4.28. Maximum values were recorded in the central part of Bucharest, the SWING instrument recording a maximum of  $2.3 \times 10^{16}$  molecules/cm<sup>2</sup> and the AirMap recording a maximum value of  $\text{NO}_2$   $VCD_{\text{tropo}}$  of  $2.8 \times 10^{16}$  molecules/cm<sup>2</sup>.

As a result of the AROMAT-1 and 2-zone campaigns near Bucharest, Rovinari and Turceni became world-interest areas for studying  $\text{NO}_2$  due to specific conditions. The conditions refer to the fact that values of the  $\text{NO}_2$  tropospheric densities in the order of  $1 \times 10^{17}$  molecules/cm<sup>2</sup> (in Turceni and Rovinari) and  $1 \times 10^{16}$  molecules/cm<sup>2</sup> (Bucharest) are recorded in these areas.

### 4.6.2 CINDI 2 measurement campaign

The CINDI-2 Measurement Campaign (Cabauw Intercomparison of Nitrogen Dioxide Measuring Instruments 2) was organized at the KNMI in Cabauw / CESAR in September 2016. The campaign was dedicated to the determination of  $\text{NO}_2$  in the troposphere by: making DOAS observations prior to the validation campaign the new TROPOMI instrument mounted on board the Sentinel 5P satellite (launched in October 2017), using MAX - DOAS observations to determine the suite of capabilities required for the tools to be used within the European MAX -

UTILIZATION OF THE DIFFERENTIAL OPTICAL ABSORPTION SPECTROSCOPY IN QUANTIFICATION OF  
ATMOSPHERIC POLLUTION WITH NITROGEN DIOXIDE

DOAS FRM4DOAS (Fiducial Reference Measurements for Ground - Based DOAS Air-Quality). In addition to MAX - DOAS observations, ZSL - DOAS mobile observations were made.

**Table 4.9:** Characteristics of DOAS mobile systems (adaptation after Apituley et al. 2018, Merlaud et al., 2018)

Team	Platform	Observation geometry	Spectral resolution (nm)	Internal temperature (° C)
BIRA	vehicle	zenit and 30°	200 - 750	Ambientală
BIRA	bycicle	zenit	280 - 550	Ambientală
BOKU	vehicle	zenit	300 - 550	Ambientală
UGAL	vehicel	zenit	280 - 550	Ambientală
MPIC	mini-van	1D scans	299 - 454	-5°

At this campaign 22 teams of researchers from around the world participated. In this section only teams that have conducted DOAS mobile observations around the KNMI research center in Cabauw will be mentioned wich are shown in Figure 4.29 and Table 4.9.

We performed observations with ZSL-DOAS UGAL system during this measurement campaign between September 14-25, 2016. The tracks of each DOAS mobile system for the determination of  $VCD_{\text{tropo}} \text{NO}_2$  are shown in Figure 4.29.

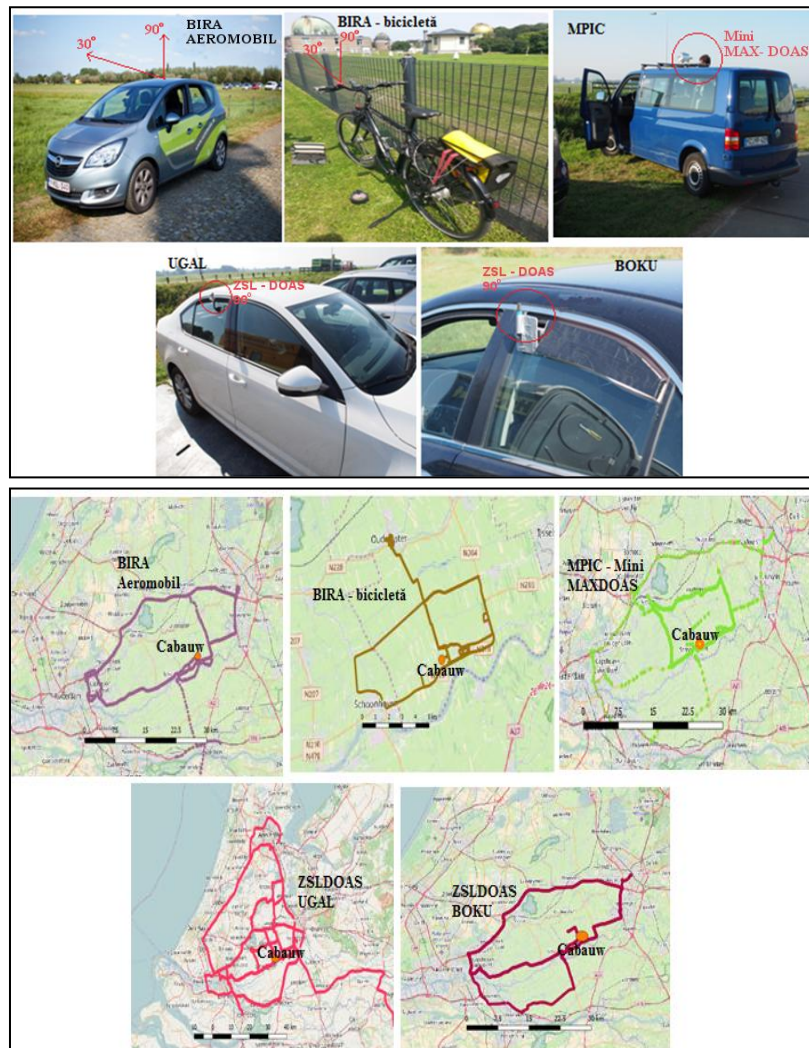


**Figure 4.29:** The DOAS mobile systems used to make observations during the CINDI-2 campaign. Routes performed by each DOAS mobile system (adaptation after Apituley et al. 2018, Merlaud et al., 2018)



DOAS mobile observations were made daily, but ideal weather conditions were recorded between September 13 - 15, 2016. Figure 4.30. shows the variations of the tropospheric vertical columns of nitrogen dioxide observed by the 5 mobile systems between 9 - 14 UTC. High levels can be seen between  $1.2 - 1.5 \times 10^{16}$  molecules/cm<sup>2</sup> recorded in the Southwest near Rotterdam. Similar values have been recorded by all DOAS mobile systems in the adjacent area of south-east of Rotterdam. According to meteorological data from the KNMI Institute, the average wind direction recorded during this period was North East. Comparison with weather data indicates that the high NO<sub>2</sub> values recorded by the DOAS systems are anthropic, most likely coming from the Rotterdam area.

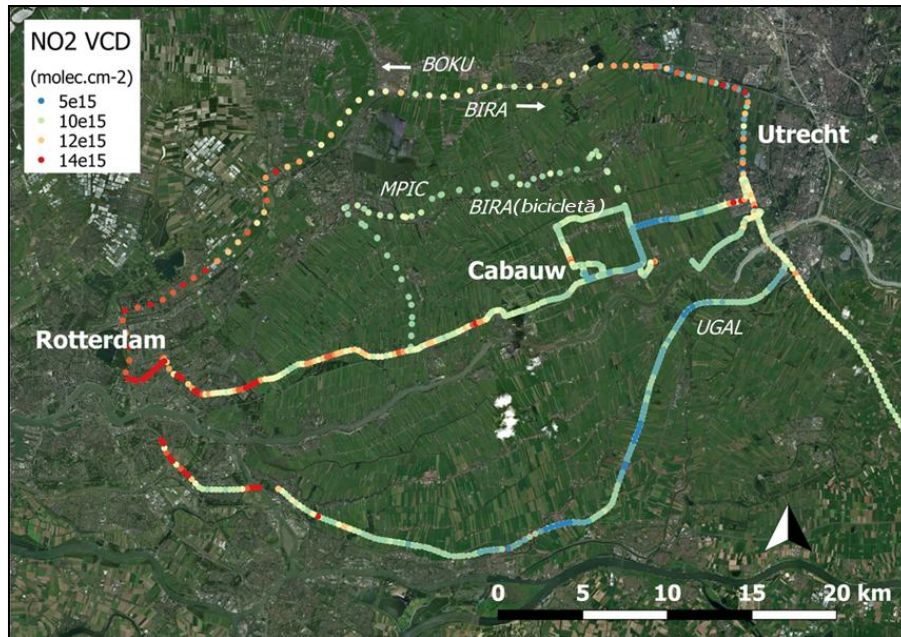


**Figure 4.30** : The NO<sub>2</sub> VCD variation recorded by the DOAS mobile systems during 13 - 15 September (adaptation after Apituley et al., 2018, Merlaud et al., 2018)

### 4.6.3 Conclusions

In this chapter we have presented studies of DOAS observations made from the ground, air and from space. These observations aimed at determining the densities of NO<sub>2</sub> molecules in the lower layers of the atmosphere, especially in the troposphere. Pollution studies using DOAS mobile systems on the ground and in the air were primarily aiming at testing these instruments for their use into validation of satellite observations. We underline that a first step in validating the DOAS determinations made from space is identifying similarities between the values recorded by airborne and ground DOAS systems.

The results of these researches have demonstrated that by using complementary or synergistic ground, airborne and spatial DOAS observations, it is possible to quantify, identify and understand mechanisms that produce variations in NO<sub>2</sub> content at continental, regional and even local level (small towns, locations).

During the AROMAT 2 campaign we participated with ZSL - DOAS mobile observations in the cities of Bucharest, Craiova, Rovinari and Turceni in August 2016.

In the CINDI - 2 campaign conducted in Cabauw (the Netherlands), we made NO<sub>2</sub> observations from the ZSLDOAS UGAL system along with other DOAS mobile systems on routes including urban agglomerations such as Rotterdam and Utrecht (Apituley et al., 2018).

## CHAPTER 5

# Development and use of an innovative MAX - DOAS „UGAL 2D – DOAS” system in NO<sub>2</sub> detection

### 5.1 Characteristics of the UGAL 2D - DOAS instrument

The UGAL 2D - DOAS instrument was developed by me in 2017 at the Faculty of Science and Environment at the "Dunarea de Jos" University in Galati. This instrument is the first prototype of MAX – DOAS system developed in Romania. The development of a MAX - DOAS system in Galati started by studying similar systems used during CINDI - 2 campaign (Cabauw, The Netherlands). The construction of the UGAL 2D - DOAS instrument makes possible the determination of NO<sub>2</sub> at different elevation angles or at different positions depending on the cardinal points (horizontal scan).

The composition of the UGAL 2D - DOAS system is shown in Figure 5.1. It consists of a tripod, the body (in which the electronic components are located) and the mobile arm. The movement of the UGAL 2D - DOAS instrument telescope to different angles was accomplished by programming automatic positioning cycles in the Arduino IDE programming language (Integrated development environment). These logic schemes are implemented into the Arduino UNO board which sends a signal to the driver board. The driver board translates the binary signal so that the stepper motor is actuated following a certain angle value.

The optical assembly and spectral acquisition instrument (spectrophotometer) used is identical to the one used in the mobile ZSL - DOAS applications made in Galati and in Europe for determination of tropospheric NO<sub>2</sub>.

Several logic schemes were performed for experiments with this instrument, each specific to the scanning mode used.

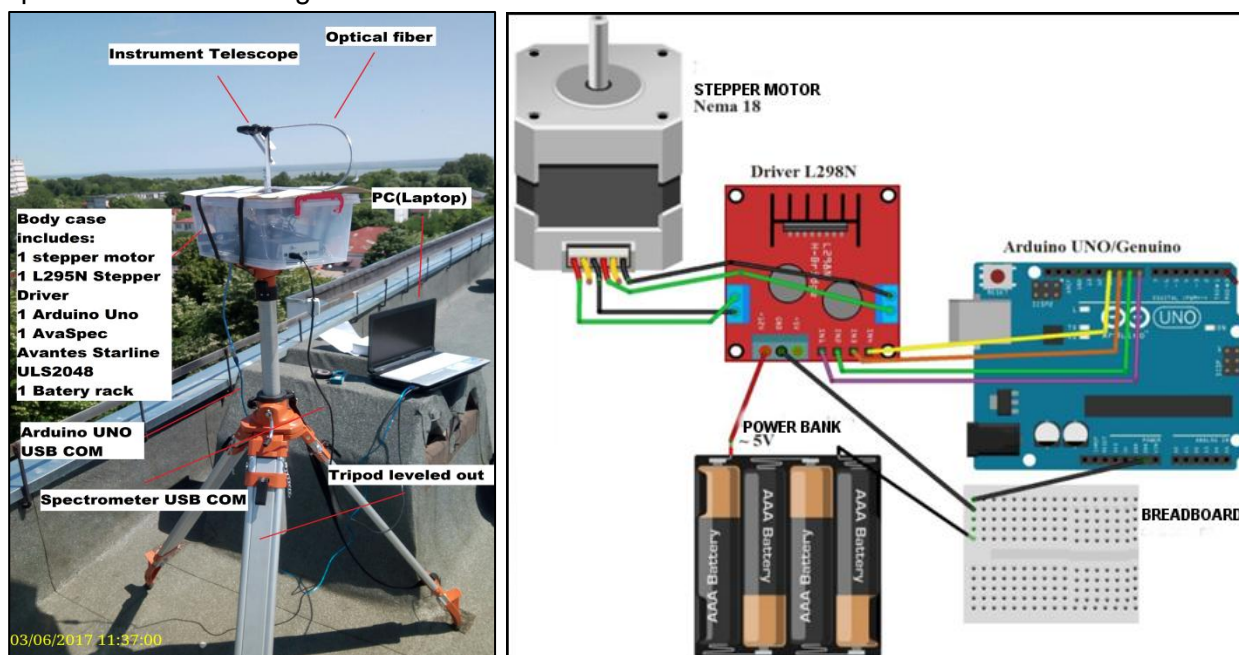


**Figure 5.1:** The components of the UGAL 2D - DOAS system (left). Schematic of the electronic component of the UGAL 2D - DOAS instrument (right).

## 5.2 Experimental methodology used for NO<sub>2</sub> detection

Experiments were performed on 10.04.2017 and 21.06 .2017 using the MAX-DOAS technique for determining the amount of NO<sub>2</sub> from the top of the building of the Faculty of Science and Environment (45 ° 26'59 "N 28 ° 03'00" E presented in Figure 5.2). All experiments were performed in conditions of maximum visibility (10 km) and clear sky.



**Figure 5.2:** Location of experiments made using UGAL 2D - DOAS system (download from [www.google.com/maps](http://www.google.com/maps))

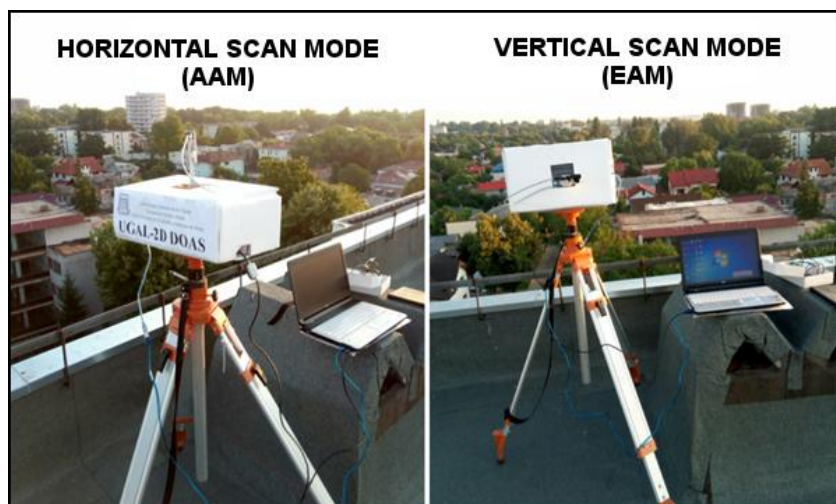


**Figure 5.3:** Scanning modes of UGAL 2D – DOAS instrument

For the first observations, Arduino IDE scripts were developed to perform vertical scanning called Elevation Angle Mode (EAM) and horizontal scans at 360 ° Azimut Angle Mode(AAM). Characteristics of scan modes are shown in Figure 5.3 and Table 5.1.

Spectral analysis was performed for all spectra recorded from the complete sequence of the two scan modes using QDOAS software. The results are expressed in differential slant density columns of nitrogen dioxide (NO<sub>2</sub> DSCD). These apparent columns provide information on NO<sub>2</sub> distribution both horizontally and vertically. The uncertainties of the determination of NO<sub>2</sub> DSCD are deduced from the spectral analysis performed with the QDOAS software between 25 - 30% with a mean value of  $\pm 0.78 \times 10^{15}$  molecules/cm<sup>2</sup>.

**Table 5.1:** Scanning modes of UGAL 2D - DOAS

Scanning mode	Date	Time	Integration time (ms)	Uncertainty NO <sub>2</sub> DSCD	Step time	Time of a complete scan
AAM_DSCD1	10/04/17	11:28-11:36	50	4- 21 %	12 s	≈ 8min
AAM_DSCD2	10/04/17	11:56-12:04	50	5 - 21 %	12 s	≈ 8min
EAM_DSCD1	10/04/17	12:21-12:25	30	6- 25.5 %	12 s	≈ 4min
EAM_DSCD2	10/04/17	12:40-12:44	30	10 - 28 %	12 s	≈ 4min



### 5.3 Experimental results and discussions

On 10 April 2017, the first experiments were performed in the two scan modes using the UGAL 2D - DOAS system

Figure 5.5 shows the NO<sub>2</sub> DSCD variations observed by the UGAL 2D - DOAS instrument performing EAM scans. The 0 degree position is equivalent to the parallel to the horizontal and 90 ° to the parallel to the zenith. Between 0 - 90 ° observation angles for both scan directions, an exponential decrease in NO<sub>2</sub> content is observed. This is mainly due to the longer radiation path recorded at elevation angles close to the horizontal positions. These observations made in the vertical plane represent relative NO<sub>2</sub> profiles.

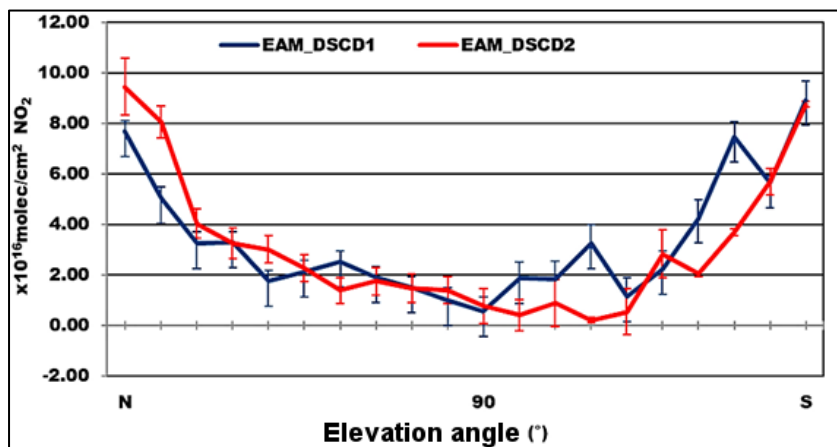


**Figure 5.2:** Result of the first EAM experiment represents the NO<sub>2</sub> DSCD for each elevation angles ranging from 0 ° (N) -180 ° (S) - performed on April 10, 2017, at 12:21 - 12:44 (local time).

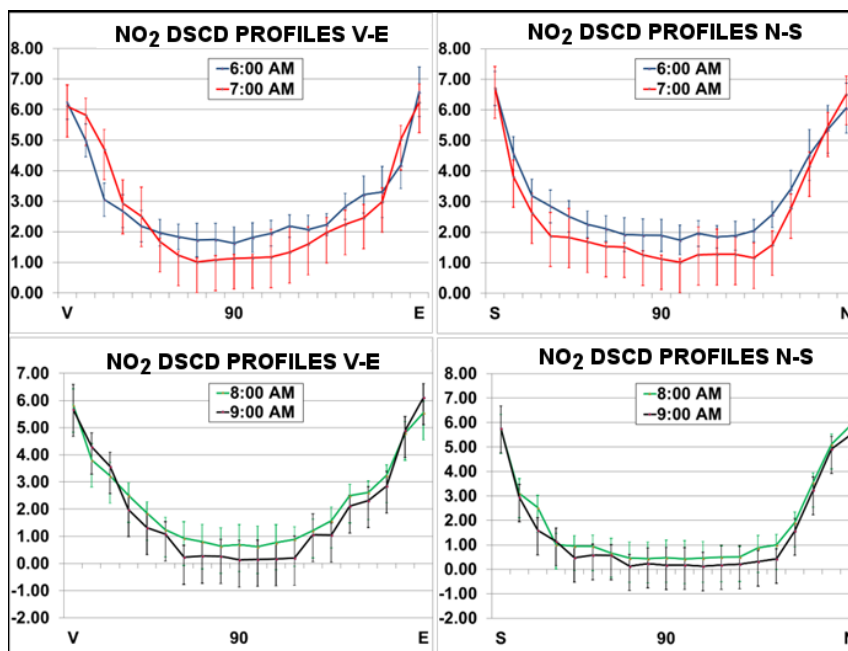


**Figure 5.3:** Apparent NO<sub>2</sub> DSCD profiles observed in EAM mode with the UGAL 2D - DOAS instrument on June 21, 2017, time range 06:00 - 09:00 (local time).

On July 21, 2017, MAX - DOAS observations of the apparent NO<sub>2</sub> profiles were made between 06:00 and 09:00 in the direction of the main cardinal points (N - S, E - V) shown in Figure 5.6. Variations in hourly mean of apparent NO<sub>2</sub> profiles can be observed. Within this timeframe, the radiation path is longer and the MAX - DOAS observations are susceptible to detecting the NO<sub>2</sub> variation in the stratosphere.

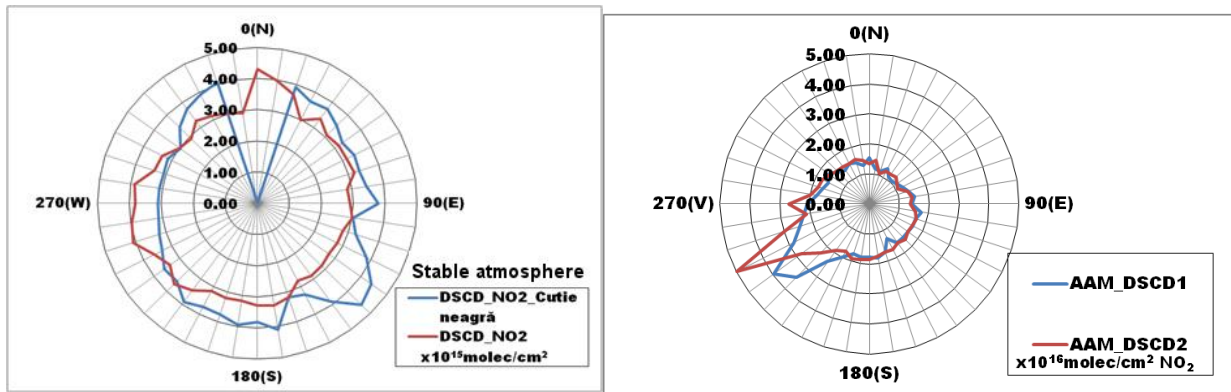


**Figure 5.4:** Results of DSCD NO<sub>2</sub> from AAM scans performed on April 10, 2017 between 10:20 - 10:38. The results of the black box experiment (image from left). Result of NO<sub>2</sub> DSCD recorded between 12:21 - 12:44 in windy conditions (image from right).

The scanning sequence of the instrument was validated by inserting a black box in the northern part of the instrument's field of view. This experiment included two 360 ° scans performed from 10:20 am to 10:38 pm in stable atmosphere (no wind). The first AAM scan was performed with blocking the visual field of the instrument, the second without the black box. Figure 5.7 (left image) shows the NO<sub>2</sub> DSCD values recorded during the "black box" experiment. The results of the experiment showed a decrease in the NO<sub>2</sub> detection signal in the direction of the North where the box was placed. The second scan was performed immediately after removing the box the instrument detected a uniform dispersion of the recorded NO<sub>2</sub> content. The highest value being recorded in the direction North 4.31 (± 0.51)x10<sup>15</sup> molecules/cm<sup>2</sup>. On the same day, another set of two AAM scans was performed, this time under relatively strong wind towards Southwest. The results of spectral analysis of both scans have showed an increase in NO<sub>2</sub> DSCD values in the Southwest direction. The maximum value was 4.97 (± 0.46)x10<sup>16</sup> molecules/cm<sup>2</sup>. High values was recorded in the South West direction possible caused by displacement and concentration of NO<sub>2</sub> emissions from different sources: road traffic, burning of fossil fuels, etc. Another possible cause is the detection of emissions from other major sources such as the Arcelor Mittal Steel Factory, located in the same direction.

#### 5.4 Comparison between MAX - DOAS observations and ZSL - DOAS mobile observations

On 21.06.2017 a comparative experiment was performed using observations of the 2D - UGALDOAS system in AAM mode and the observations of the ZSL - DOAS UGAL mobile system.

Both DOAS systems have identified high values in the South East of the city. The maximum value of DSCD NO<sub>2</sub> observed by the MAX - DOAS system 3.82(±0.25)x10<sup>16</sup> molecules/cm<sup>2</sup> was recorded in the time interval 13:01 - 13:05 (Figure 5.11 d). The maximum value of 3.68(± 0.32)x10<sup>16</sup> molecules/cm<sup>2</sup> was recorded by the ZSL-DOAS mobile system in the same time interval near the Prut oil factory (Figure 5.8 red circle). High values recorded by the MAX - DOAS instrument can also be caused by the NO<sub>2</sub> emissions of the intense road traffic , emissions that were also detected by the ZSL - DOAS system near the intersection of two main roads in Galati. Similar values of both systems were detected in the same region in all time intervals where AAM scans were performed with the MAX - DOAS system. High values were recorded sporadically by the two systems in North-West (Figure 5.8, orange circle and Figure 5.11, a and b) and Southwest (Figure 5.8, blue circle and Figure 5.11, g and h). These

quantities of NO<sub>2</sub> DSCD are probably produced by agglomerations of road traffic or other fixed sources resulting from population activity.

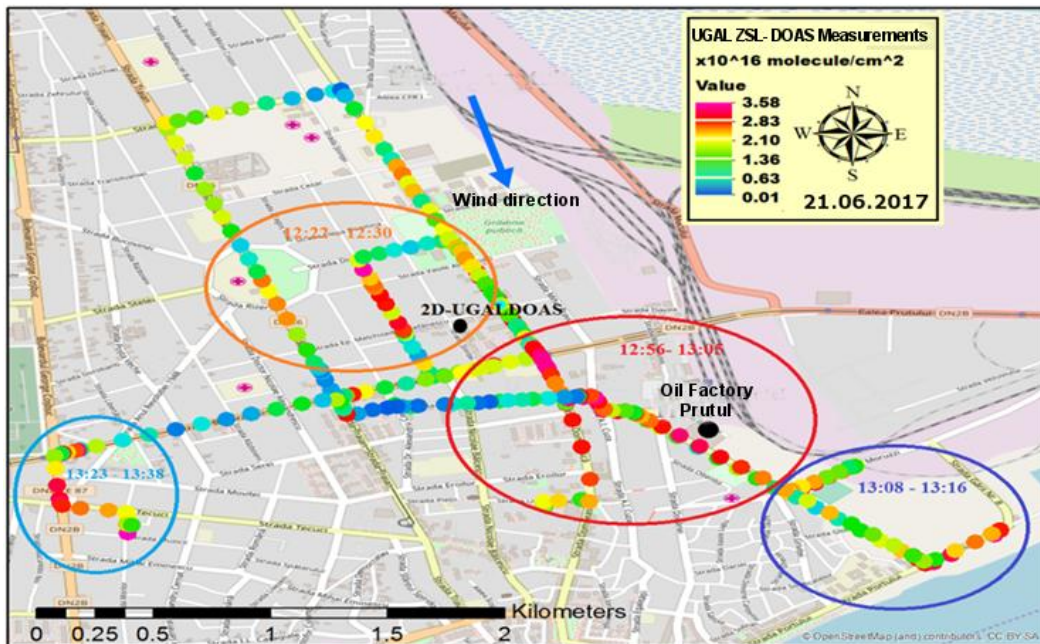


Figure 5.5: NO<sub>2</sub> DSCD variations observed by the ZSL - DOAS UGAL mobile system on 21 June 2017

By observing similar values of DSCD NO<sub>2</sub> recorded by the two DOAS systems in the same direction we can assume that AAM scans performed using the UGAL 2D - DOAS instrument have been validated. Taking into account that the MAX - DOAS instrument was positioned at about 30 m altitude and the DOAS system made ground observations in zenith geometry, we can assume that a two - dimensional scan of NO<sub>2</sub> pollution has been performed. The UGAL 2D - DOAS proven to be able to detect the direction in which high NO<sub>2</sub> pollution values are present. The instrument detected the pollution emitted from the oil factory Prutul that can be seen in Figure 5.10.



Figure 5.6: Picture of NO<sub>2</sub> pollution (red circle) emitted by the Prutul Oil Factory at 13:06 on 21.06.2017.



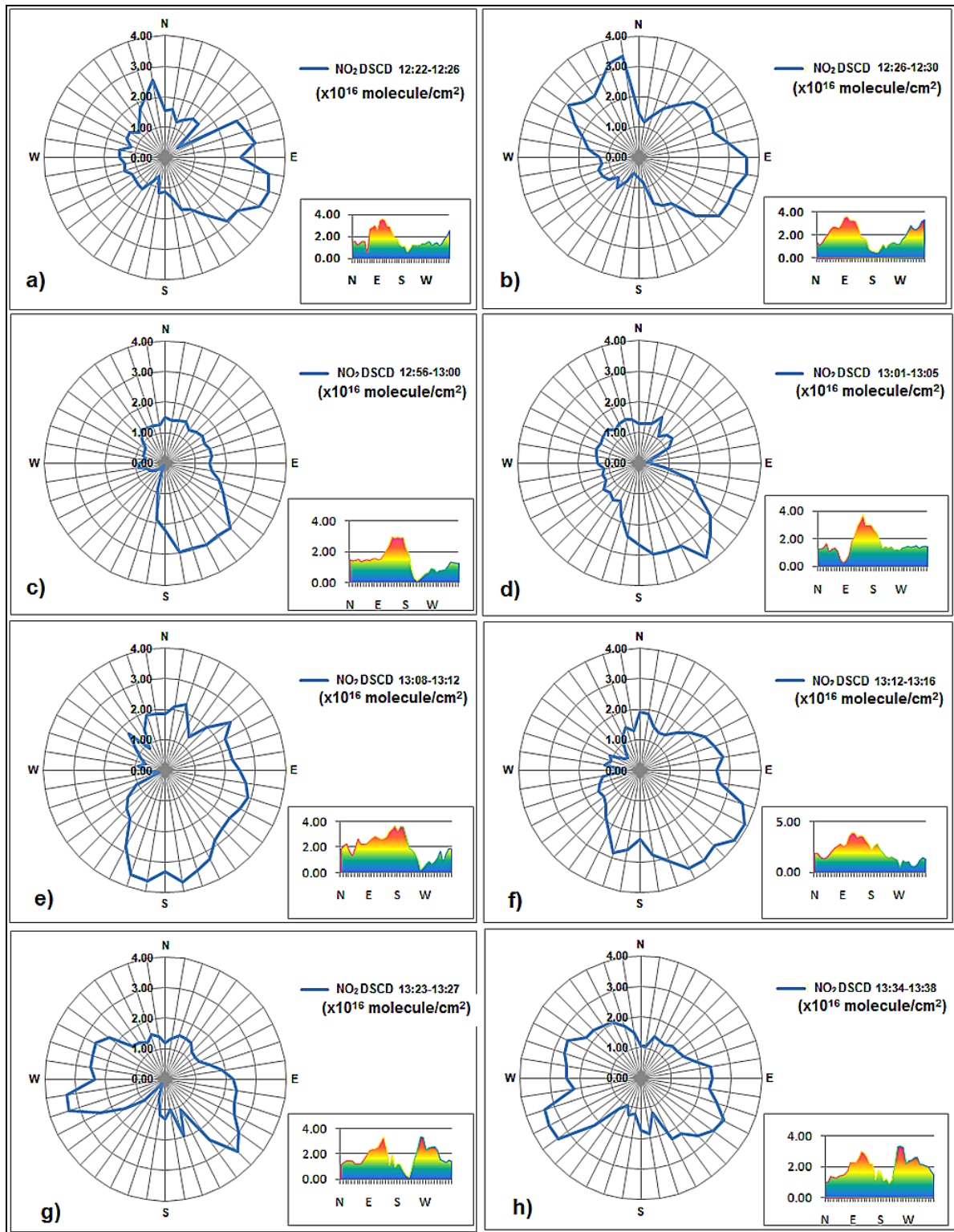


**Figure 5.7:** Variations for NO<sub>2</sub> DSCD observed in AAM mode using the UGAL 2D - DOAS system on June 21, 2017 in the time intervals: a) 12:22 - 12:26 b) 12:26 - 12:30 c) 12:56 - 13 : 30 d) 13:01 - 13:05 e) 13:08 - 13:12 f) 13:12 - 13:16 g) 13:23 - 13:27 h) 13:34 - 13:38.

## 5.5 Conclusions

In this chapter are presented for the first time the experiments performed in Galati Municipality on 10 April and 21 June 2016 of the first MAX - DOAS instrument developed in

Romania. The instrument is my personal contribution to the development of new instruments and methods for detecting atmospheric pollution. The development of the instrument is based on the knowledge gained in the ESA-funded CINDI-2 international campaign based on determining atmospheric pollution with NO<sub>2</sub> using ZSL-DOAS, MAX-DOAS and other instruments.

Experiments conducted in Galati focused on detecting NO<sub>2</sub> content using a UGAL 2D - DOAS instrument prototype. This instrument is capable of detecting spatial variation of NO<sub>2</sub> through horizontal scans in AAM mode and relative NO<sub>2</sub> DSCD profiles through EAM scanning mode. To perform evaluation of pollution using atmosphere scans a number of scanning algorithms and sequences were developed using component capabilities (Nema 17 "stepper motor, Arduino UNO board, L295N driver card) and coding scripts made in the programming language Arduino IDE.

The azimuth angle scanning module (AAM) was validated by the "black box" experiment in which the field of view of the instrument was obstructed in the North direction. Through the observations of the MAX - DOAS instrument, the effects of atmospheric conditions on the distribution of NO<sub>2</sub> pollution were detected on the same day. Observations made in the EAM mode provide information on the vertical distribution of NO<sub>2</sub> pollution.

Experiments on June 21 were conducted simultaneously with ZSL - DOAS mobile observations. The instrument scanning sequences was validated by detecting similar values of NO<sub>2</sub> by the two DOAS systems, the instrument's ability to detect areas in Galati Municipality where relatively large amounts of nitrogen dioxide were recorded. The experiments carried out have demonstrated the capabilities of detecting NO<sub>2</sub> variations produced by industrial sources (the ArcelorMittal steel plant and Prutul oil factory) and sporadic sources (road traffic). These variations of NO<sub>2</sub> DSCD were detected using both scanning modes implemented with the UGAL 2D - DOAS system.

By combining synergistically the two methods of DOAS technique, is possible to realize accurate mapping of atmospheric pollution with NO<sub>2</sub>. The results of these experiments support the idea that using this new atmospheric scanning instrument, important information is obtained about the dispersion of NO<sub>2</sub> pollution in the vertical and horizontal plane. Depending on the height at which AAM scanning is performed, it is possible to estimate the height at which the pollutant gas studied has the highest density. Such application can be implemented to find out the concentration of the pollutant gas for different heights. This can be achieved by coupling with an RTM to ensure the calculation of the light path length which is recorded by the instrument's telescope. This method also requires the instrument to be mounted on a mobile UAV platform or a vertically movable balloon. The main disadvantage of this technique is the need for a barrier-free visual field.



## CHAPTER 6

### Personal contributions and research directions

The studies and experiments performed in this thesis focused on the quantification of the NO<sub>2</sub> content in the lower layers of the atmosphere by means of differential optical absorption spectrometry technique. For the DOAS applications performed was used observations made from ground, air and from space. DOAS method is a actual tehniqe of determining the amount of NO<sub>2</sub> in vertical columns of the troposphere by means of remote sensing using solar radiation. The analysis method allows the determination of spatial and temporal variations of NO<sub>2</sub> via mobile platforms. The systems used are in continuous development.

The complementary or synergistic determinations carried out using DOAS mobile instruments from the ground, in the air and from space, present the spatial and temporal distribution of NO<sub>2</sub> recorded locally (in Galati Municipality), regional (observation in Eastern Europe) and continental (observations made in Europe).

The main results and future research directions of the studies conducted in this thesis are presented below:

- 1. Studies have been carried out to assess the atmospheric pollution at European level in Chapter 3. The objective of the research carried out is to determine the current situation of air pollution through the information provided by EU-validated databases. These studies have been carried out for the preparation of NO<sub>2</sub> determination campaigns using the DOAS technique in Europe. (L1 Roşu et al., 2016, B5, Roşu, A. et al., 2016)**

*Future research directions will include comparing the national annual NO<sub>2</sub> concentration with tropospheric NO<sub>2</sub> values extracted from observations made by DOAS satellite instruments across Europe for the same period or for a longer period.*

- 2. A series of studies have been carried out to determine the tropospheric content of NO<sub>2</sub> in Romania and Europe using DOAS observations from the ground, air and space onboard mobile platforms. These studies are concentrated in Chapter 4 of this thesys. Within this chapter, there are a number of research directions that include intercomparations and the determination of similarities between DOAS satellite observations and ground observations. So:**

- a) The role of NO<sub>2</sub> in O<sub>3</sub> formation in industrial areas was evaluated using complementary DOAS observations in space and soil determinations (B2, Red, A. et al., 2016);**

*Future studies will include the study of the variation and evolution of O<sub>3</sub> formation in NO<sub>2</sub> at the level of the troposphere through DOAS satellite observations. This study will focus on studying cities whose annual NO<sub>2</sub> emissions are detected by current satellite instruments (GOME-2, OMI, TROPOMI).*

- b) The similarity between NO<sub>2</sub> content extracted from DOAS observations and ground-based NO<sub>2</sub> concentrations for 5 major European cities (B3 Roşu et al., 2016) was**

**evaluated identifying OMI instrument as most accurate satellite instrument in detecting NO<sub>2</sub> pollution level above big cities;**

*Future research directions will include comparing the national NO<sub>2</sub> content and major European cities observed by advanced satellite instruments (OMI, TROPOMI) to those recorded by European air quality monitoring networks to date.*

- c) The tropospheric NO<sub>2</sub> content was quantified from the DOAS mobile observations performed locally using a simplified algorithm for the extraction of the tropospheric density columns. The first prediction maps of the NO<sub>2</sub> distribution were made by using DOAS mobile observations (B1 Roşu et al., 2016);**

*Future research will include conducting studies using mobile DOAS observations over a longer period of time. The dimension of the ideal determination grid will be determined to simulate city prediction maps. The results will show dispersion maps in which simulated or measured profiles of NO<sub>2</sub> and vectors of tropospheric transport (wind direction and wind speed) will be implemented.*

- d) The longest DOAS mobile observation tracks for determination of NO<sub>2</sub> VCD<sub>tropo</sub> were performed for the first time across the entire Europe. The algorithm for quantification of verticality column and errors was presented. Methods for determination with precision of SCD<sub>ref</sub> and AMF, parameters used for the extraction of tropospheric NO<sub>2</sub> content have been developed and applied. Comparisons were made between the satellite observations of the OMI instrument with the ZSL - DOAS UGAL conducted at the regional level (Eastern Europe - L2. Constantin et al., 2017) and the premiere throughout Europe (work under development);**

*Subsequent research using the DOAS technique on a vehicle includes: applying an off axis algorithm or dual channel technique (at 30 ° and zenith) for instantaneous determination of tropospheric columns, making comparisons with observations of the new satellite sensor TROPOMI (lunched in October 2017); developing a automation for ZSL - DOAS UGAL system in order to obtain real-time evaluation of tropospheric NO<sub>2</sub> columns.*

- 3. The first MAX - DOAS (UGAL 2D - DOAS) system in Romania has been developed. The first synergic observations were made between a MAX-DOAS system and a ZSL-DOAS system at the local level. Through these experiments, the scanning modes of the UGAL 2D - DOAS instrument were validated, identifying the major NO<sub>2</sub> pollution sources in the city of Galati (local industry and road traffic).**

The research directions will continue with the development of the UGAL 2D - DOAS instrument and bringing it to a level where it will ensure participation in the MAX - DOAS observation campaigns such as CINDI - 2. Subsequent developments will include system miniaturization and mountings on vertically mobile airborne platforms UAVs (optocopter) for the determination of NO<sub>2</sub> profiles for different altitudes. Another direction will be to use the BePro model to extract real tropospheric NO<sub>2</sub> profiles from UGAL 2D - DOAS system scans performed in EAM mode.

## References

1. \*\*\* <http://www.eea.europa.eu>.
2. \*\*\*<http://www.tropomi.eu>.
3. \*\*\*<https://www.slideshare.net/Themadagen/benno-oderkerk-avantes>
4. Agenția Pentru Protecția Mediului Galați (ANMP Galați): *Raport lunar asupra calității factorilor de mediu la nivelul Județului Galați*, Februarie 2017.
5. Apituley A., Hendrick, F., vanRoosendael, M., Richter A., Wagner, T., Friess, U., Kreher, K., den Hoed, M., Stein-Zweers, D., Eskes, H., Scheele, R., PETERS, A., Allaart, M., Jain, S., Bloch, A., Frumau, A., Merlaud, A., Tack, F., Lampel, J., Vonk, J., Berkhout, S., van der Hoff, R., Swart, D.: *Second Cabauw Intercomparison of Nitrogen Dioxide Measuring Instruments (CINDI-2) – Campaign Overview*, draft received on 12.01.2018 from BIRA (under editing for publication), 2018
6. Arpaç, K.H., Johnston, P.V., Miller, H.L., Sanders, R.W., and Solomon, S.: *Observations of the stratospheric BrO column over Colorado, 40° N*, J. of Geophys. Res., 99, D4, 8175–8181, 1994.
7. Bobrowski, N., Honninger, G., Galle, B., Platt, U.: *Detection of bromine monoxide in a volcanic plume*. Nature 423, 273–276, 2003.
8. Boersma, K. F., Eskes, H. J., Dirksen, R. J., Veefkind, J. P., Stammes, P., Huijnen, V., Richter, A.: *An improved tropospheric NO<sub>2</sub> column retrieval algorithm for the Ozone Monitoring Instrument*. Atmospheric Measurement Techniques, 4(9), 1905-1928, 2011.
9. Boersma, K. F., Eskes, H. J., Veefkind, J. P., Brinksma, E. J., Van Der A, R. J., Sneep, M., Bucsela, E. J.: *Near-real time retrieval of tropospheric NO<sub>2</sub> from OMI*. Atmospheric Chemistry and Physics, 7(8), 2103-2118, 2007.
10. Bogumil, K., Orphal, J., Burrows, J.P.: *Temperature dependent absorption cross sections of O<sub>3</sub>, NO<sub>2</sub>, and other atmospheric trace gases measured with the SCIAMACHY spectrometer*. In Proceedings of the ERS-Envisat-Symposium, Goteborg, Sweden, 2000.
11. Brasseur, G., and Solomon S.: *Aeronomy of the middle atmosphere*. Dordrecht, Boston, Lancaster, Tokyo: D. Reidel Publ, 1986.
12. Castell, N., Dauge, F. R., Schneider, P., Vogt, M., Lerner, U., Fishbain, B., Bartonova, A.: *Can commercial low-cost sensor platforms contribute to air quality monitoring and exposure estimates?*. Environment international, 99, 293-302, 2017.
13. Chance, K.V., and Spurr, R.J.D.: *Ring effect studies: Rayleigh scattering, including molecular parameters for rotational Raman scattering, and the Fraunhofer spectrum*, Appl. Optics, 36, 5224– 5230, 1997.
14. Constantin D., Merlaud, A. and AROMAT II team, ESA Study: “*Airborne Romanian Measurements of Aerosols and Trace gases*”, AROMAT-II Final Report, ESA Contract No.4000113511/NL/FF/gp, 21-11-2016.
15. Danckaert, T., Fayt, C., Van Roosendael, M., De Smedt, I., Letocart, V., Merlaud, A., Pinardi, G.: *QDOAS Software user manual*. Belgian Institute for Space Aeronomy (BIRA-IASB), version 3.2, 2017.
16. Davies, J.: *Correlation Spectroscopy*, Analytical Chemistry, 42, 101–112, 1970.
17. Dobson, G.M., Harrison, D.N.: *Measurements of the amount of ozone in the earth's atmosphere and its relation to other geophysical conditions*. Proceedings of the Royal Society of London. Series A, Containing Papers of a Mathematical and Physical Character, 110(756), 660-693, 1926.
18. Eisinger, M., Richter, A., Ladstatter-Weissenmayer, A., and Burrows, J. P.: *DOAS Zenith sky observations: 1. BrO measurements over Bremen (53° N) 1993–1994*, J. Atmos. Chem. 26, 93–108, 1997.
19. European Union: *Directive 2008/50/EC of the European Parliament and the Council on Ambient Air Quality and Cleaner Air for Europe*, 21 May 2008.
20. Fayt, C. and Van Roosendael M.: *Windoas 2.1, Software User Manual, BIRA-IASB*, 2011.
21. Fiedler, M.H., Frank, T., Gomer, M., Hausmann, K., Pfeilsticker, K., and Platt, U.: *Groundbased spectroscopic measurements of stratospheric NO<sub>2</sub> and OCIO in the arctic winter 1989/1990*, Geophys. Res. Lett., 20, 10, 963–966, 1993.
22. Friess, U., Hollwedel, J., König-Langlo, G., Wagner, T., and Platt, U.: *Dynamics and chemistry of tropospheric bromine explosion events in the Antarctic*, J. Geophys. Res., in press, 2004.
23. Friess, U., Wagner, T., Pundt, I., Pfeilsticker, K., and Platt, U.: *Spectroscopic Measurements of Tropospheric Iodine Oxide at Neumayer Station, Antarctica*, Geophys. Res. Lett., 28, 1941– 1944, 2001.
24. Gugiuman, I., Cotrău, M.: *Elemente de climatologie urbană: cu exemple din România*. Editura Academiei Republicii Socialiste România, 1975.
25. Harrison, A.W.: *Midsummer stratospheric NO<sub>2</sub> at latitude 40° S*, Can. J. Phys., 57, 1110–1116, 1979
26. Heckel, A.: *Messungen troposphärischer Spurengase mit einem MAX-DOAS-Instrument Nachweis von troposphärischem Formaldehyd in Norditalien während der Format Kampagne*, Diploma Thesis, University of Bremen, 2003.

UTILIZATION OF THE DIFFERENTIAL OPTICAL ABSORPTION SPECTROSCOPY IN QUANTIFICATION OF  
ATMOSPHERIC POLLUTION WITH NITROGEN DIOXIDE

---

27. Hendrick, F., Müller, J.F., Clémer, K., Wang, P., De Mazière, M., Fayt, C., Gielen, C., Hermans, C., Ma, J. Z., Pinardi, G., Stavrakou, T., Vlemmix, T., Van Roozendael, M.: *Four years of ground-based MAX-DOAS observations of HONO and NO<sub>2</sub> in the Beijing area*, Atmos. Chem. Phys., 14, 765-781, 2014.
28. Heue, K.P., Bruns, M., Burrows, J., Lee, W.D., Platt, U., Pundt, I., Richter, A., Schulz, B., Wagner, T., and Wang, P.: *Airborne Multi Axis DOAS Measurements During the SCIAVALUES and FORMAT Campaigns*, Geophysical Research Abstracts, 5, 12 405, 2003.
29. Hoff, R.M.: *Differential SO<sub>2</sub> Column Measurements of the Mt. Pinatubo Volcanic Plume*, Geophys. Res. Lett., 19, 175–178, 1992.
30. Honninger, G. and Platt, U.: *Observations of BrO and its vertical distribution during surface ozone depletion at Alert*, Atmos. Environ., 36, 2481–2489, 2002.
31. Honninger, G., Bobrowski, N., Palenque, E.R., Torrez, R., and Platt, U.: *Bromine and sulfur emissions from Salar de Uyuni, Bolivia*, Geophys. Res. Lett., accepted, DOI:10.1029/2003GL018818, 2004a.
32. Honninger, G., Friedeburg, C.V., Platt, U.: *Multi axis differential optical absorption spectroscopy (MAX-DOAS)*. Atmospheric Chemistry and Physics, 4(1), 231-254, 2004b.
33. Honninger, G., Leser, H., Sebastian, O., and Platt, U.: *Ground-based Measurements of Halogen Oxides at the Hudson Bay by Active Longpath DOAS and Passive MAX-DOAS*, Geophys. Res. Lett., accepted, doi:10.1029/2003GL018982, 2004c.
34. Intergovernmental Panel on Climate Change (IPCC) editors: Solomon, S., D. Qin, M. Manning, Z. Chen, M. Marquis, K.B. Averyt, M. Tignor and H.L. Miller: *Climate Change 2007: The Physical Science Basis. Contribution of Working Group I to the Fourth Assessment Report of the Intergovernmental Panel on Climate Change*, Cambridge University Press, Cambridge, United Kingdom and New York, NY, USA, 996 pp., 2007.
35. Johnston, P.V., and McKenzie, R.L.: NO<sub>2</sub> observations at 45°S during the decreasing phase of solar cycle 21, from 1980 to 1987, J. Geophys. Res., D94, 3473–348, 1989.
36. Kaiser, N.: *Off-axis-Messungen von tropospharischem NO<sub>3</sub>*, Diplomarbeit, Universität Heidelberg, 1997.
37. Kreher, K., Johnston, P.V., Wood, S.W., and Platt, U.: *Groundbased measurements of tropospheric and stratospheric BrO at Arrival Heights (78° S), Antarctica*. Geophys. Res. Lett., 24, 3021– 3024, 1997.
38. Leser, H., Honninger, G., Platt, U.: *MAX-DOAS measurements of BrO and NO<sub>2</sub> in the marine boundary layer*. Geophys. Res. Lett. 30(10), 1537, 2003. doi:10.1029/2002GL015811
39. Leue, C., Wenig, M., Wagner, T., Klimm, O., Platt, U., Jähne, B.: *Quantitative analysis of NO<sub>x</sub> emissions from Global Ozone Monitoring Experiment satellite image sequences*. Journal of Geophysical Research: Atmospheres, 106(D6), 5493-5505, 2001.
40. Lowe, A.G., Adukpo, D., Fietkau, S., Heckel, A., Ladstatter-Weißmayer, A., Medeke, T., Oetjen, H., Richter, A., Wittrock, F., and Burrows, J.P.: *Multi-Axis-DOAS observations of atmospheric trace gases at different latitudes by the global instrument network BREDOM*, Proc. 10th Sci. Conf. of IAMAS, CACGP and 7th Sci. Conf. of IGAC, Sept., Crete, 2002.
41. McElroy, C., McLinden, C., and McConnell, J.: *Evidence for bromine monoxide in the free troposphere during the Arctic polar sunrise*, Nature, 397, 338–341, 1999.
42. McKenzie, R.L. and Johnston, P.V.: *Seasonal variations in stratospheric NO<sub>2</sub> at 45° S*, Geophys. Res. Lett. 9, 1255–1258, 1982.
43. McKenzie, R.L., Johnston, P.V., McElroy, C.T., Kerr, J.B., and Solomon, S.: *Altitude distributions of stratospheric constituents from ground-based measurements at twilight*, J. Geophys. Res. 96, 15 499–15 512, 1991.
44. Merlaud, A., Constantin, D., Fayt, C., Maes, J., Mingireanu, F., Mocanu, I., Georgescu, L. Roozendael M. V.: *Small whiskbroom imager for atmospheric composition monitoring (swing) from an unmanned areal vehicle (UAV)*, In proceeding of 21st ESA Symposium on European Rocket and Balloon Programmes and related Research, pp 1-7, 2014.
45. Merlaud, A., Tack, F., Van Roozendael, M., Constantin, D., Rosu, A., Riffel, K., Donner, S., Wagner, T., Schreier, S., Richter, A., Eskes, H., Douros, J.: *Synergetic use of the Mobile-DOAS measurements during Cindi-2*, AS3.14/GI2.14, EGU2018-18038, 2018
46. Merlaud, A., van Roozendael, M., van Gent, J., Fayt, C., Maes, J., Toledo-Fuentes, X., Ronveaux, O., de Mazière, M.: *DOAS measurements of NO<sub>2</sub> from an ultralight aircraft during the Earth Challenge expedition*. Atmos. Meas. Tech., 5, 2057–2068, 2012.
47. Merlaud, A.: *Development and use of compact instruments for tropospheric investigations based on optical spectroscopy from mobile platforms* (Vol. 307). Presses univ. de Louvain, 2013.
48. Millan, M., Townsend, S., and Davies, J.: *Study of the Barringer refractor plate correlation spectrometer as a remote sensing instrument*, Utiat rpt. 146, m.a.sc. thesis, University of Toronto, Toronto, Ontario, Canada, 1969.
49. Millan, M., Townsend, S., and Davies, J.: *Study of the Barringer refractor plate correlation spectrometer as a remote sensing instrument*, Utiat rpt. 146, m.a.sc. thesis, University of Toronto, Toronto, Ontario, Canada, 1969.
50. Miller, H.L., Weaver, A., Sanders, R.W., Arpag, K., and Solomon, S.: *Measurements of arctic sunrise surface ozone depletion events at Kangerlussuaq, Greenland (67° N, 51° W)*, Tellus, 49B, 496–509, 1997.

UTILIZATION OF THE DIFFERENTIAL OPTICAL ABSORPTION SPECTROSCOPY IN QUANTIFICATION OF  
ATMOSPHERIC POLLUTION WITH NITROGEN DIOXIDE

---

51. Noxon, J.F., Norton, R. B., and Henderson, W. R.: *Observation of atmospheric NO<sub>3</sub>*, Geophys. Res. Lett., 5, 675–678, 1978.
52. Noxon, J.F.: *Nitrogen dioxide in the stratosphere and troposphere measured by ground-based absorption spectroscopy*, Science, 189, 547–549, 1975.
53. Oetjen, H.: *Messung atmosphärischer Spurengase in Ny Aalesund, Aufbau und Inbetriebnahme einer neuen DOAS-Meßsystems*, Diploma Thesis, University of Bremen, 2002.
54. Parlamentul României: „*Legea nr. 278/2013 privind emisiile industriale*”, publicată în Monitorul Oficial, Partea I nr. 671 din 01/11/2013
55. Petritoli, A., Ravegnani, F., Giovanelli, G., Bortoli, D., Bonafe, U., Kostadinov, I., Oulanovsky, A.: *Off-Axis Measurements of Atmospheric Trace Gases by Use of an Airborne Ultraviolet-Visible Spectrometer*, Applied Optics-LP, 41, 27, 5593–5599, 2002.
56. Petty, G. W.: *A first course in atmospheric radiation*, second edition, Sundog Publishing, Madison, Wisconsin, 2006.
57. Platt, U., Stutz, J.: *Differential absorption spectroscopy. Differential Optical Absorption Spectroscopy*. 135-174, ISBN 978-3-540-75776-4, 2008.
58. Pommereau, J. P. and Piquard, J.: *Observations of the vertical distribution of stratospheric OCIO*, Geophys. Res. Lett., 21, 1231– 1234, 1994.
59. Richter, A., Burrows, J. P., Nüß, H., Granier, C., Niemeier, U. *Increase in tropospheric nitrogen dioxide over China observed from space*. Nature, 437(7055), 129, 2005.
60. Richter, A., Burrows, J. P., Nüß, H., Granier, C., Niemeier, U. *Increase in tropospheric nitrogen dioxide over China observed from space*. Nature, 437(7055), 129, 2005.
61. Richter, A., Eisinger, M., Ladstätter-Weißenmayer, A., and Burrows, J. P.: *DOAS zenith sky observations. 2. Seasonal variation of BrO over Bremen (53° N) 1994–1995*, J. Atm. Chem., 32, 83– 99, 1999.
62. Rothman, L.S., Gordon, I.E., Barber, R.J., Dothe, H., Gamache, R.R., Goldman, A., Tennyson, J.: *HITEMP, the high-temperature molecular spectroscopic database*. Journal of Quantitative Spectroscopy and Radiative Transfer, 111(15), 2139-2150, 2010
63. Sanders, R.W., Solomon, S., Smith, J.P., Perliski, L., Miller, H.L., Mount, G.H., Keys, J.G., and Schmeltekopf, A.L.: *Visible and Near-Ultraviolet Spectroscopy at McMurdo Station Antarctica*, 9. Observations of OCIO from April to October 1991, J. Geophys. Res., 98, D4, 7219–7228, 1993.
64. Sanders, R.W., Solomon, S., Smith, J.P., Perliski, L., Miller, H.L., Mount, G.H., Keys, J.G., and Schmeltekopf, A.L.: *Visible and Near-Ultraviolet Spectroscopy at McMurdo Station Antarctica*, 9. Observations of OCIO from April to October 1991, J. Geophys. Res., 98, D4, 7219–7228, 1993.
65. Seinfeld, J. H., Pandis, S. N.: *Atmospheric chemistry and physics: from air pollution to climate change*. John Wiley Sons, 2016.
66. Sluis, W.W., Allaart, M.A., Piders, A.J., Gast, L.F.L.: *The development of a nitrogen dioxide sonde*. Atmospheric Measurement Techniques, 3(6), 1753, 2010
67. Smith, J. and Solomon, S.: *Atmospheric NO<sub>3</sub>: 3. Sunrise Disappearance and the Stratospheric Profile*, J. Geophys. Res., 95, D9, 13 819–13 827, 1990.
68. Smith, J., Solomon, S., Sanders, R., Miller, H., Perliski, J., Keys, J., and Schmeltekopf, A.: *Atmospheric NO<sub>3</sub>: 4. Vertical Profiles at Middle and Polar Latitudes at Sunrise*, J. Geophys. Res., 98, D5, 8983-8989, 1993
69. Solomon, S., Miller, H.L., Smith, J.P., Sanders, R.W., Mount, G.H., Schmeltekopf, A.L., Noxon, J.F.: *Atmospheric NO<sub>3</sub>, 1. Measurement technique and the annual cycle at 40°N*. J. Geophys. Res. 94, 11041–11048, 1989a.
70. Solomon, S., Mount, G., Sanders, R.W., Schmeltekopf, A.: *Visible spectroscopy at McMurdo station, Antarctica: 2. Observation of OCIO*. J. Geophys. Res. 92, 8329–8338 , 1987b.
71. Solomon, S., Mount, G.H., Sanders, R.W., Jakoubek, R.O., Schmeltekopf, A.L.: *Observations of the nighttime abundance of OCIO in the winter stratosphere above Thule*, Greenland. Science 242, 550–555, 13 Literature 557, 1988.
72. Solomon, S., Sanders, R.W., Carroll, M.A., Schmeltekopf, A.L.: *Visible and nearultraviolet spectroscopy at McMurdo Station, Antarctica*, 5. Observations of the diurnal variations of BrO and OCIO. J. Geophys. Res. 94, 11393–11403, 1989b.
73. Solomon, S., Sanders, R.W., Carroll, M.A., Schmeltekopf, A.L.: *Visible and nearultraviolet spectroscopy at McMurdo Station, Antarctica*, 6. Observations of the diurnal variations of BrO and OCIO. J. Geophys. Res. 94(D9), 11393–11403, 1989d. 10.1029/88JD03127.
74. Solomon, S., Sanders, R.W., Mount, G.H., Carroll, M.A., Jakoubek, R.O., Schmeltekopf, A.L.: *Atmospheric NO<sub>3</sub>, 2. Observations in polar regions*. J. Geophys. Res. 94(D13), 16423–16427, 1989c.
75. Solomon, S., Schmeltekopf, A. L., and Sanders, R. W.: *On the interpretation of zenith sky measurements*, J. Geophys. Res., 92, D7, 8311–8319, 1987.

UTILIZATION OF THE DIFFERENTIAL OPTICAL ABSORPTION SPECTROSCOPY IN QUANTIFICATION OF  
ATMOSPHERIC POLLUTION WITH NITROGEN DIOXIDE

---

76. Solomon, S., Smith, J.P., Sanders, R.W., Perliski, L., Miller, H.L., Mount, G.H., Keys, J.G., and Schmeltekopf, A.L.: *Visible and near-ultraviolet spectroscopy at McMurdo station, Antarctica, 8, Observations of nighttime NO<sub>2</sub> and NO<sub>3</sub> from April to October 1991*, J. Geophys. Res., 98, 993–1000, 1993.
77. Stamnes, K., Tsay, S. C., Wiscombe, W., Laszlo, I.: *DISORT, a general-purpose Fortran program for discrete-ordinate-method radiative transfer in scattering and emitting layered media: documentation of methodology* (p. 112). Tech. rep., Dept. of Physics and Engineering Physics, Stevens Institute of Technology, Hoboken, NJ 07030, 2000.
78. Stoiber, R. and Jepsen, A.: *Sulfur dioxide contribution to the atmosphere by volcanoes*, Science, 182, 577–578, 1973.
79. Thalman, R., Zarzana, K. J., Tolbert, M. A., Volkamer, R.: *Rayleigh scattering cross-section measurements of nitrogen, argon, oxygen and air*. Journal of Quantitative Spectroscopy and Radiative Transfer, 147, 171-177, 2013.
80. Valks, P., Pinardi, G., Richter, A., Lambert, J. C., Hao, N., Loyola, D., Emmadi, S.: *Operational total and tropospheric NO<sub>2</sub> column retrieval for GOME-2*. Atmospheric Measurement Techniques, 4(7), 1491, 2011.
81. van J.H.G.M., Geffen, K.F., Boersma, H.J., Eskes, J.D., Maasackers and Veeckind, J.P.: *TROPOMI ATBD of the total and tropospheric NO<sub>2</sub> data products document*, S5P-KNMI-L2-0005-RP, 2017.
82. Van Roozendaal, M., Hermans, C., DeMaziere, M., and Simon, P. C.: *Stratospheric NO<sub>2</sub> observations at the Jungfraujoch Station between June 1990 and May 1992*, Geophys. Res. Lett., 21, 1383–1386, 1994.
83. Van Roozendaal, M., T. Wagner, A. Richter, et al.: *Intercomparison of BrO measurements from ERS-2 GOME, ground-based and balloon platforms*, Adv. Space Res., 29, 1661-1666, 2002.
84. Vandaele, A. C., Hermans, C., Simon, P. C., Carleer, M., Colin, R., Fally, S., Coquart, B.: *Measurements of the NO<sub>2</sub> absorption cross-section from 42 000 cm<sup>-1</sup> to 10 000 cm<sup>-1</sup> (238–1000 nm) at 220 K and 294 K*. Journal of Quantitative Spectroscopy and Radiative Transfer, 59(3-5), 171-184, 1998.
85. von Friedeburg, C., Wagner, T., Geyer, A., Kaiser, N., Vogel, B., Vogel, H., and Platt, U.: *Derivation of Tropospheric NO<sub>3</sub> Profiles Using Off-axis-DOAS Measurements During Sunrise and Comparison with Simulations*, J. Geophys. Res., 107, D13, doi:10.1029/2001JD000481, 2002.
86. von Friedeburg, C.: *Derivation of Trace Gas Information combining Differential Optical Absorption Spectroscopy with Radiative Transfer Modelling*, PhD thesis, University of Heidelberg, 2003.
87. von Friedeburg, C.: *Derivation of Trace Gas Information combining Differential Optical Absorption Spectroscopy with Radiative Transfer Modelling*, PhD thesis, University of Heidelberg, 2003.
88. Wagner, T., Beirle, S., Brauers, T., Deutschmann, T., Frieß, U., Hak, C., Platt, U.: *Inversion of tropospheric profiles of aerosol extinction and HCHO and NO<sub>2</sub> mixing ratios from MAX-DOAS observations in Milano during the summer of 2003 and comparison with independent data sets*. Atmospheric Measurement Techniques, 4(12), 2685-2715. 2011.
89. Wagner, T., Bruns, M., Burrows, J.P., Fietkau, S., Finocchi, F., Heue, K.P., Honninger, G., Platt, U., Pundt, I., Richter, A., Rollenbeck, R., von Friedeburg, C., Wittrock, F., and Xie, P.: *The AMAX-DOAS Instrument and its Application for SCIAMACHY Validation*, Report, 2002.
90. Wagner, T., Ibrahim, O., Shaiganfar, R., & Platt, U.: *Mobile MAX-DOAS observations of tropospheric trace gases*, Atmospheric Measurement Techniques, 3(1), 129-140, 2010.
91. Wahner, A., Jakoubek, R. O., Mount, G. H., Ravishankara, A. R. and Schmeltekopf, A. L.: *Remote sensing observations of daytime column NO<sub>2</sub> during the airborne antarctic ozone experiment, August 22 to October 2, 1987*, J. Geophys. Res., 94, 16 619–16 632, 1989.
92. Wang, P., Bruns, M., Richter, A., Burrows, J.P., Heue, K.P., Pundt, I., Wagner, T., Platt, U.: *Validation of SCIAMACHY with AMAX-DOAS Measurements from the DLR Falcon*, Geophysical Research Abstracts, 5, 09 341, 2003.
93. Weaver, A., Solomon, S., Sanders, R.W., Arpag, K., and Miller, H.L.: *Atmospheric NO<sub>3</sub> 5. Off-axis measurements at sunrise: Estimates of tropospheric NO<sub>3</sub> at 40° N*, J. Geophys. Res., 101, D13, 18 605–18 612, 1996.
94. WHO, *Nitrogen oxides*. Geneva, (Environmental Health Criteria, No. 188), 1997.
95. Wittrock, F., Muller, R., Richter, A., Bovensmann, H., and Burrows, J. P.: *Measurements of iodine monoxide (IO) above Spitsbergen*, Geophys. Res. Lett., 27, 1471–1474, 2000.
96. Wittrock, F., Oetjen, H., Richter, A., Fietkau, S., Medeke, T., Rozanov, A., and Burrows, J. P.: *MAX-DOAS Measurements of atmospheric trace gases in Ny-Ålesund*, Atm. Chem. Phys. ° Discuss. 3, 6109–6145, 2003.
97. Wittrock, F., Oetjen, H., Richter, A., Fietkau, S., Medeke, T., Rozanov, A., Burrows, J. P.: *MAX-DOAS measurements of atmospheric trace gases in Ny-Ålesund-Radiative transfer studies and their application*. Atmospheric Chemistry and Physics, 4(4), 955-966, 2004.